PhD degree in Systems Medicine (curriculum in Molecular Oncology)

European School of Molecular Medicine (SEMM),

University of Milan and University of Naples "Federico II"

Settore Disciplinare: MED/04

Role of p21 in the immune response against breast cancer

Federica Predolini

European Institute of Oncology (IEO), Milan

*Supervisor:*Prof. Pier Giuseppe Pelicci, MD,PhD
European Institute of Oncology (IEO), Milan

Co-*Supervisor:*Dott.ssa. Alessandra Insinga,PhD
European Institute of Oncology (IEO), Milan

PhD Coordinator: Prof. Giuseppe Viale

Anno accademico 2019-2020

Table of contents

List of Abbreviations

Abs = Antibodies

ACT = Adoptive cell transfer

AI = Autoimmunity

AID = Autoimmune disorders

AML = Acute myeloid leukaemia

APC = Antigen-presenting cell

BC = B cell

BM = Bone Marrow

CD = Cluster of differentiation

CDK = Cyclin-dependent kinase

CDP = Common dendritic progenitors

CIP/Kip = CDK interacting protein/Kinase inhibitory protein

CFSE = Carboxy fluorescein succinimidyl ester

CKI = Cyclin-dependent kinase inhibitor

CLP = Common lymphoid progenitors

CMP = Common myeloid progenitors

CSC = Cancer stem cell

CTLs = Citotoxic T cells

CTLA-4 = Cytotoxic T-lymphocyte associated protein 4

DC = Dendritic cell

DD = DNA damage

DDR = DNA damage response

DSBs = double=strand breaks

ECM = Extracellular matrix

ErbB2 = Receptor tyrosin-protein kinase erbB2

FACS Fluorescence activated cell sorting

HLA = human leucocyte antigen

HP = Homeostatic proliferation

HSC = Hematopoietic stem cell

IC = Immune complex

ICI = Immune checkpoint inhibitor

IFN = Interferon

IL = Interleukin

ILC = Innate lymphoid cells

IFN Interferon

iNOS = Inducible nitric oxide synthase

i.p. Intraperitoneal

iPS = induced pluripotent stem cells

i.v. = Intravenous

KI = Knock-in

KO = Knock-out

Lin = Lineage

LN = lymph node

LSC = Leukaemia stem cell

LT-HSC = Long-term hematopoietic stem cell

Ly = Lymphoid antigen

MC = Monocyte

MDSC = Myeloid-derived suppressor cells

MFP = Mammary fat pad

MHC = Major histocompatibility complex

MMM = marginal-zone metallophilic macrophages

MØ = Macrophage

MZM = marginal-zone macrophages

NK = Natural killer cell

PALS = Periarteriolar sheat

PCNA = Proliferating cell nuclear antigen

PD = Programmed death-1 receptor

PD-L1 = Programmed death-ligand-1

PB = Peripheral blood

PCR = Polymerase chain reaction

Rb = Retinoblastoma

ROS = Reactive oxygen species

RT = Room Temperature

Sags = Superantigens

SC = Stem cell

scRNAseq = Single Cell RNA sequencing

SLE = Systemic lupus erythematosus

TAM = tumor associated macrophages

TC = T cell

Tgd = Gamma delta T cells

Th = T helper cells

TIL = Tumor infiltrated Lymphocyte

TNM = Tumor, Nodes, Metastases

T-reg = Regulatory T cell

TCR = T cell receptor

TGF-β = Transforming growth factor beta

TIL = Tumor-infiltrating lymphocyte

TLR = Toll-like receptor

TME = Tumor microenvironment

TNF = Tumor necrosis factor

UMAP = Uniform Manifold Approximation and Projection for Dimension Reduction

WAF1 = Wildtype activating factor-1

WT = Wild-type

List of Figures

List of Tables

Abstract

The immune system plays a major role in the surveillance against tumors. Tumor cells develop different strategies to escape immune surveillance, while immune therapies are designed to overcome mechanisms that mediate tolerance to tumor cells.The cell-cycle inhibitor p21 regulates immune tolerance, as revealed by the susceptibility of p21-deficient (p21-/-) mice to develop mild autoimmune diseases. My host-lab has reported that p21-/- myeloid leukemias are unable to transplant into syngeneic mice. I demonstrated that the same phenotype applies to p21-/- breast cancers, and that p21-/- tumors reacquire transplantability when injected into immunodeficient mice. Thus, I investigated cellular and molecular mechanisms underlying the effect of p21 in evading the immune surveillance against breast cancer. I showed that depletion of p21 selectively in CD11b+c+ antigen presenting cells (APCs) induces a robust MHCII-dependent and antigen-independent proliferation of CD4+ lymphocytes endowed with effector/memory phenotype and potent anti-tumor activities, mimicking homeostatic proliferation of T cells. Single-cell RNA sequencing of WT and p21-/- CD11b+c+ APCs showed differential expression of genes encoding antigen-processing and -presentation membrane proteins. Notably, I showed that p21-/- CD11b+ APC cells (comprising ~50% of the CD11b+c+ subpopulation) can be used *in vitro* to generate T cells with potent anti-cancer effect *in vivo*, thus paving the way to novel anti-cancer immunotherapeutic approaches in humans.

1. Introduction

1.1 The cell-cycle inhibitor p21

1.1.1 Functions of p21 in cell-cycle inhibition

Cell-cycle checkpoints are crucial for genome integrity following exposure to DNA-damaging agents and, more in general, stress signals[1,71]. Their deregulation is involved in cancer progression [2] and negatively influences anticancer treatment strategies[3]. Cyclins and cyclin-dependent kinases (CDKs) control cell cycle progression and their sequential activation triggers initiation and transition between the various phases of the cell cycle[5]. When cyclin/CDK complexes are activated, the members of retinoblastoma (Rb) protein family are phosphorylated and inactivated, promoting progression through G1 phase and the entrance into the cell cycle[5,71].

First identified in 1993[22;23], the p21 protein is encoded by the gene CDKN1A, and is also known as wildtype activating factor-1 (WAF1) or cyclin-dependent kinase inhibitory protein-1 (CIP1). p21 is a universal inhibitor of CDKs (CDK1, CDK2, CDK4/6) and a critical regulator of cell cycle progression[6,71]. To inhibit CDKs, p21 must bind simultaneously to both cyclin (cyclins D/E/A and B) and CDKs[183]. The function of p21 in the cell-cycle was first described as part of the cellular response to DNA damage. Treatment of non-transformed cells with DNA-damaging agents, such as γ irradiation or chemotherapy, causes DNA double-strand breaks (DSBs) and other types of DNA lesions, leading to activation of the DNA Damage Response (DDR)[8]. DDR-induced phosphorylation p53 leads to destabilization of the p53-Mdm-2 complex, accumulation of p53 and activation of p53-transcriptional targets, including p21[4] (p21 possesses two strong p53-responsive elements within its promoter)[4]. Increased p21, on its turn, inhibits CDK4,6/cyclin-D and cell cycle progression during G1/S phases (G1 arrest)[7,8]. Notably, levels of p21 in the G1 phase of the cell cycle correlate with the length of

the G1 phase [184]. It has been proposed that the arrest in G1 generates the time required to repair damaged DNA[185], suggesting that p21 plays a critical role also in DNA repair. Consistently, p21 enhances DNA repair after chemotherapy in glioma cells[186] and limits DNA damage accumulation in hematopietic and mammary stem cells[187].

p21 upregulation can also cause cell growth arrest in the G2 phase[9], by inhibiting CDK2/cyclin-E, and is required, together with p53, to support G2-arrest following DNA damage[10,71]. Notably, p21 is activated by p53 also in non-transformed cycling cells in the absence of exogenously-induced DNA damage. In such unperturbed conditions, DNA damage accumulates spontaneously during S-phase and activates p53 and p21 at levels, however, which are not sufficient to induce a G1 arrest, yet they are competent to prevent premature S-phase exit.

Finally, p21 promotes cellular senescence, a cellular status of irreversible proliferative arrest that occurs during normal embryonic development, upon damage in adult tissues, to initiate tissue remodelling, andin normal cells after a limited number of cell divisions[188]. Initially described in fibroblasts, growth arrest of senescent cells is initiated p53 activation and transcriptional activation of p21. P53 and p21 activation in senescent cells, however, is only transient, and is followed by up-regulation of another CDK inhibitor, $p16^{Ink4A}$, which is responsible for the maintenance of the senescence[189,190];. p21, however, can mediate cellular senescence via p53- independent pathways and through different mechanisms, including gene expression regulation[12] and ROS accumulation, as shown in normal fibroblasts and in p53-negative cancer cells[8,71].

1.1.2 Positive Regulation of cell-cycle by p21

Depending on the cellular context and its expression levels, p21 may also function as an activator of the cell cycle.In vitro experiments suggest that at low concentrations p21 can stabilize and activate CDK complexes. In particular, while two molecules of p21 are required to inhibit cyclin D/cdk4 and cyclin D/cdk6; at equimolar concentrations p21 stimulates the assembly of cyclin D/cdk4 or cyclin D/cdk6 activity and triggers the nuclear targeting of these complexes[11]. Consistently, cyclin D/Cdk4 complexes fail to form in fibroblasts lacking p21 and the other CDK inhibitor p27[191].

1.1.3 Other functions of p21

In parallel to its cell cycle regulation function, p21 has been found to be involved in the regulation of a variety of other cellular functions, which will be briefly described. i) **DNA replication.** Regulation of DNA replication was one of the first functions of p21 independent of CDK-inhibition[192]. This function depends on the ability of p21 to bind PCNA, a nuclear protein that envelops DNA and provides an anchor point for DNA polymerases. Notably, regardless of the induction of p21 following DNA damage, the levels of p21 in the S phase of the cell cycle remain consistently low, as a result of the activity of various E3 ligases, including SCFSkp2, CRL4Cdt2, HDM2, CRL2LRR1, and APC / CCdc20[14]. Consistently, small changes in p21 levels during the S phase affect DNA replication speed and origin firing, probably by regulating the interaction of PCNA with other partner. For example, down-regulation of p21 induces alteration of DNA elongation[193] . ii) **Apoptosis.** p21 has been implicated both as an apoptosis inhibitor and as a pro-apoptosis factor[14]. The cytoplasmic form of p21 inhibits multiple caspases and other effectors of apoptosis, including pro-caspase-3, caspase-8, caspase-10, apoptosis signal-regulating kinase 1 and stress-activated protein kinase[194]. However, in specific cellular and experimental contexts, p21 promotes apoptosis, as described in glioma or ovary-carcinoma cells, upon treatment with cisplatin, in hepatocytes,

following bile acid-induced MAPK-activation or in thymocytes, upon Fas-ligand treatment. iii) **Differentiation.** In different tissues, terminal differentiation is associated with the up-regulation of p21 and the permanent exit from the cell cycle[195]. Consistently, p21 expression is regulated by lineage-determining transcriptionfactors, such as MyoD, a transcription factor that induces the exit of myocytes from the cell cycle and their fusion into myotubes [196]. Notably, the p21 promoter contains a binding sites for MyoD. A direct effect of p21 in the induction of terminal differentiation has been demonstrated in the case of oligodendrocytes, monocytes, megakaryocytes, erythroid progenitors and adipocytes[197]. Multiple evidences suggest that the activity of promoting differentiation of p21 is linked to its cytoplasmic form[14, 212,213,214,215,216.] For example, cytoplasmic p21 in rat neurons promotes[213] neurite outgrowth and differentiation through loss of stress fiber formation[212,213].Moreover, cytoplasmic p21 is associated with rat pancreatic differentiation from myofibroblast to fibroblast conversion and protects against apoptosis[214]. During murine C2C12 myoblast differentiation, the appearance of the apoptosis-resistant phenotype is correlated with p21 induction[215] and its cytoplasmic localization in mature myofibrils through phosphorylation at Ser-153[216]. Together, these data highlight the role of the cytoplasmic p21 in normal cell differentiation.The role of cytoplasmic p21 in cell differentiation is influenced by a number of factors including its expression level, postmodification, cell type, differentiation stage and cell microenvironment[14].Iv) **Stem cells.** p21 has been proposed as an inhibitor of the process of cellular reprogramming, in particular of the reprogramming of adult somatic cells into pluripotent stem cells (iPS)[19]. In mouse embryo fibroblasts, for example, down-regulation of p53 or p21 increases the efficiency of reprogramming[198]. On the other hand, the expression of p21 is essential for maintaining the self-renewal of stem cells of adult tissues, as demonstrated for hematopoietic stem cells, keratinocyte stem cells and neuronal stem cells[197]. The apparent contradictory effect of p21 on the maintenance of stem cell fate and induction of terminal differentiation is probably

explained by the opposing effects of p21 levels. At low/basal levels, p21 protects stem cells from their exhaustion, by protecting them from damage accumulation, while at high levels it might favor cell-cycle exit and terminal differentiation[127,217,218,219,220,221]. v) **Cell migration.**P21 has been reported to favor cell migration[8]. This function of p21 is ascribed to its cytoplasmic form[8] and its ability to bind members of the Rho family of GTPases, which are critical regulators of cytoskeletal dynamics (actin stress fiber formation, focal adhesion assembly, actin-myosin contractility) and cell migration[197]. P21 could also contribute to cell migration through its proliferation inhibitor function. Cell migration, in fact, is favored when cells are induced to halt cell proliferation.

1.1.4. Multiple binding-properties of p21

As mentioned above, the first p21 interactorsidentified were Cyclin / CDKs and PCNA. The binding activities are independent and located in different regions of the molecule. Amino-terminal aminoacid residues 17-24 and 74-79 bind cyclins and CDKs, respectively, while amino acids carboxy-terminal 143-160 bind PCNA. Of note, each of the two binding-domains is sufficient to mediate inhibition of, respectively, CDK2 and PCNA. P21, however, is capable of forming complexes with numerous other proteins and the list of interactors of p21 is constantly expanding (**see figure 1**). The marked ability of p21 to come into contact with other proteins is probably due to the lack of a defined tertiary structure of p21. It is believed that p21 can bind other relatively low affinity proteins, with a folding mechanism on the target that allows the acquisition of a defined tertiary structure upon binding[199].

Table 1 **Summary of the main cellular p21 interacting proteins**

Binding Protein	Region of p21 Bound	Nuclear/ Cytoplasmic	Function	References
Cyclins	17–24 and 155–7	Both	}assembly of D/B cyclin/cdks, nuclear	}
Cdks	53–8 and 74–9	Both	}localization, cyclin/cdk inhibition	} reviewed in 6–8
PCNA	143–60	Nuclear	Blocks DNA replication	}
ASK1	1–140	Cytoplasmic	ASK1 inhibition	14
C8 α-subunit	140–64	ND	Recruitment of p21 to the proteasome	55
Calmodulin	145–64	Nuclear	Nuclear import of complex	57, 61
CARB	ND	Nuclear	Competes with p21 for cyclin B1 binding	92
CK2	46–65	ND	CK2 inhibition	93–95
c-Myc	139–64	Nuclear	Inhibition of c-myc-dependent transcription	96
E2F-1	1–90	Nuclear	Suppression of E2F-dependent transcription	64
GADD45	139–64	Nuclear	Enhanced cell cycle arrest	97, 98
MDM2	87–164	Nuclear	Reduces p21 stability	52
Procaspase 3	1–33	Cytoplasmic	Blocks procaspase activation	12, 13
SAPK	1–84	ND	SAPK inhibition	65
SET	140–4 and 156–64	Nuclear	p21/SET complex inhibits cyclin B/cdk1	99
STAT3	ND	Nuclear	Inhibition of STAT3-dependent transcription	100
TOK1	149–64	Nuclear	Increased cdk2 inhibition	101
TSG101	1–86	ND	Increased cyclin/cdk inhibition	66
WISp39	28–56	Nuclear	Stabilization of p21	102

ND, not determined.

Fig.1.Summary of the main cellular p21 interacting proteins.Cell Cycle 5:12, 1313-1319, 15 June 2006]; ©2006 Landes Bioscience [200]

1.1.5. Regulation of p21 Expression and Activity

The expression of p21 is regulated at various levels (transcriptional, post-transcriptional, post-translational) and is subject to tight control by various signaling pathways. Apart from p53, p21 transcription can be activated by various other transcription factors, oncogenes, tumor suppressors, inflammatory cytokines and nutrients, including TGFβ (transforming growth factor beta), TNFα (tumor necrosis factor alpha), IFNγ (interferon gamma), or APC (adenomatosis polyposis coli)[201]. Notably, transcription of p21 is inhibited by Myc[202,20] an oncogene frequently over-expressed in a variety of different cancers[203]. At the post-transcriptional level, the half-life of the p21 transcript is regulated by several miRNAs and some proteins that bind to AU-rich elements in its 3′-UTR[19]. At the posttranslational level, the stability of p21 protein is regulated via phosphorylation, by various kinases (Akt, GSK3, p38, JNK, ASK1, PKA, PKC, Pim-1, Mirk and cyclinE / cdk2), degradation through the ubiquitin / proteasome pathway and cleavage by caspases[19]. Reversible protein phosphorylation also regulates its subcellular localization and ability to interact with its targets.

1.2. Role of p21 in tumor growth

P21 has different effects on tumorigenesis, acting as a tumor suppressor or oncogene, based on its intracellular localization, specific cellular contexts and genetic backgrounds.

1.2.1 p21 as tumor suppressor

P21 expression levels are frequently decreased in human cancer, as a consequence of p53 inactivation and Myc overexpression[13,14]. In this context, low p21 levels have been correlated with poor prognosis in patients with colorectal cancer, non-small-cell lung carcinoma, breast, gastric, ovarian and pancreatic cancer[14]. Structural alterations of p21 are extremely rare in cancer, with the exception of mutations in Burkitt's Lymphoma[15], melanomas[16], breast cancer[18]and bladder cancer[204], and deletions in thyroid carcinomas [17]. More frequently, the expression of p21 is downregulated by epigenetic mechanisms, such as hypermethylation, as documented in non-small cell lung, prostate, high grade breast cancer and acute lymphoblastic leukemia[205]. Some single nucleotide polymorphisms of p21 associated with an increased risk of developing esophageal, colorectal and estrogen-related cancer have also been described[197]. As far as mouse model systems are concerned, the p21 deletion is associated with an increased incidence of late in life tumors, although with a much lower frequency than that which occurs in mice with p53 deletion[21].

1.2.2 p21 as oncogene

Elevated levels of p21 expression have been documented in different cancer types (breast, prostate, cervical, renal cell, testicular, esophageal squamous cell and hepatocellular carcinomas, and multiple myelomas, gliomas, acute myeloid leukemias and soft tissue sarcomas) and frequently correlated with bad prognosis[206,207]. High levels of cytoplasmic p21 have been associated with advanced TNM and shorter survival in a large series of patients with

gastric cancer[208]. In addition, most of the structural abnormalities of the p21 gene mentioned above were not assigned as loss-of-function mutations.

1.2.3.Role of nuclear and cytoplasmic p21 in tumor growth

Based on the localization within different subcellular compartments, p21 exerts different effects on tumorigenesis. In the nucleus p21 behaves like a tumor suppressor while, when it is localized in the cytoplasm, p21 acts as an oncogene[14,24] and it is associated with cell growth and survival by promoting the assembly of the D-type cyclins with CDK4 and CDK6 and inhibiting apoptosis, respectively[14]; moreover, p21 may also act as a chaperone for cyclin E in order to initiate G1/S progression. It is suggested that, when p53 is damaged or lost, cytoplasmic p21 may exert the above-mentioned oncogenic effects, in addition to facilitating cell migration[8]. When p21 is localized in the nucleus it favors its tumor suppressive activities by inhibiting cell division and growth and it can also downregulate some DNA repair pathways and induce senescence[8,14,25]. The relation between p53 status and p21 subcellular localization is not fully understood and so far two studies have shown different results: in the first, the high cytoplasmic levels of p21 were linked to an high p53 levels in breast cancer[26]; in the second one, p21 nuclear localization was linked to p53 detection and PCNA expression in multiple myeloma[27,71].

1.3. Role of p21 in immunity

1.3.1 Role of p21in the innate immune system

CKIs (negative regulators of CDKs) have been classified into two families: Cip/Kip family and INK4 family[28,29,72]. Cip/Kip family comprises $p21^{CIP1}$, $p27^{KIP1}$, and $p57^{KIP2}$ which are all also involved in the regulation of the immune system[30]. Cell cycle regulators behave in the

Innate immune response as immune facilitators. CDKs and CKIs in particular play direct roles in ensuring expansion of the cells (Monocyte/Macrophages and Dendritic cells) in the innate immune system and maintaining balanced innate immune activities[30]. Innate immunity is the first line host defense and has an essential role in preventing infections and it is nowadays regarded as a multicomponent system essential for maintaining immediate defence against pathogens, for the recruitment of the adaptive immune system and maintenance of self-tolerance. The innate immunity is not just linked to adaptive responses, but it works by itself and also together with the adaptive immune system. For a long time, dysregulated innate immune responses were considered lethal and innate-related therapies were considered irrelevant for diseases that appear during childhood and adulthood. Today you know that these diseases are linked with malfunctions of innate immunity and many of them have been defined. The scientific discoveries and the knowledge accumulated throughout the years has enabled the development of targeted therapies (e.g. IL-1 inhibitors for autoinflammatory diseases)[209].The cellular components of the innate immune system include neutrophils, monocytes/macrophages, dendritic cells, and innate lymphoid cells. CDKs and CKIs (in particular CKI1, 2, 4) have a non-cell-cycle function in the innate immune response. CDK1, 2, and 4 were shown to be essential for the translation of type I IFN mRNA[31] and they cover an important role during viral infection when monocytes need to produce type I interferon. The absence of CDK activity, as caused by a pan-CDK inhibitor (including CDK1, 2 inhibitor), leads to removal of IFN-β mRNA from the translating polysome complex, while global translation is not affected, suggesting that CDK activity is required for IFN-β production[31], which in turn initiates immune system activation. CKI, such as $p21^{CIP1}$, $p27^{KIP1}$, and $p16^{INK4A}$ directly regulate macrophage differentiation and activity[32,33,34]; in fact, p21-/- macrophages overreact when stimulated. Mice deficient in p21appear to be more susceptible to lipopolysaccharide- induced septic shock, which is associated with increased serum levels of

the inflammatory factor IL-1β[36,37]. Furthermore, p21deficiency leads to autoinflammatory diseases, such as lupus erythematosus[35,72]. IL-1β released from macrophages is essential for activation of macrophagesand ofother immune cells, including neutrophils and monocytes; p21suppresses IL-1β at both the transcription and pro-protein levels(IL-6 and TNFα synthesis areincreased in $p21^{-/-}$ macrophages as compared to WT cells and the secretion of IL-1β requires cleavage of the pro-protein by caspase-1 which is activated by the inflammasome[36)], suggesting a role for p21in limiting excessive macrophage activation[36,37]. Moreover, the transcription factor NF-κB mediates macrophages activation and p21-deficiency in macrophages correlates with increased NF-κB activity[37,72] (**Fig.2**).

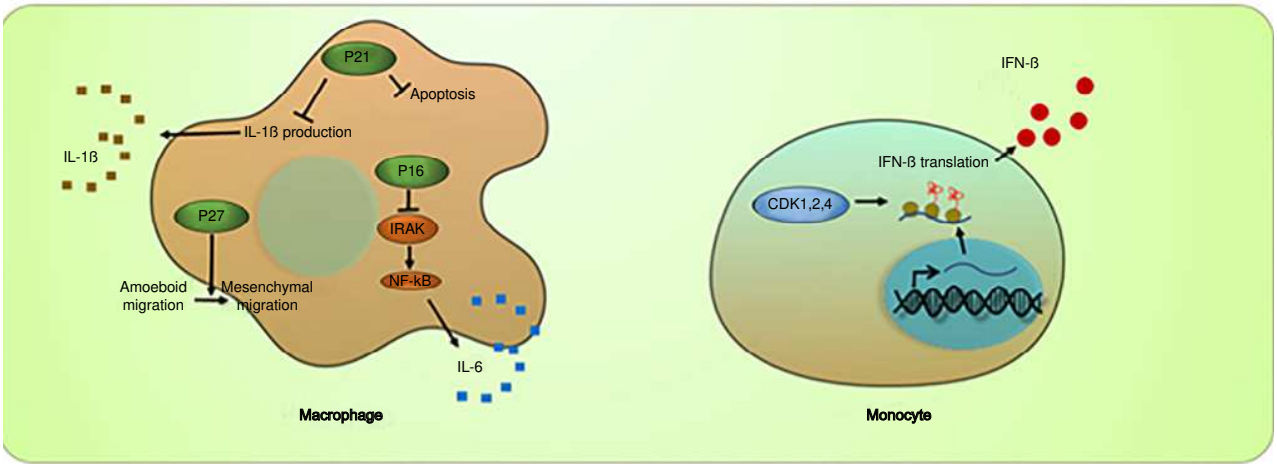

Fig.2. Roles of cell cycle regulators in innate immune response. CDKs play a positive role in IFN-β translation. CDK inhibition leads to reduction of IFN-β mRNA in the polysome complex. CDK inhibitor $p21^{CIP1}$ is also required to suppress overproduction of IL-1β, and $p16^{INK4A}$ is required to suppress IL-6, in macrophages. $p27^{KIP1}$ has the role to promote mesenchymal migration in order to facilitate the tumor infiltration of macrophage *(Laphanuwat P et al. Frontiersin. 2019)*[72]

1.3.2 Role of p21 in autoimmunity

p21 may affect multiple processes of the immune system. De- regulation of cell-cycle was shown to cause break of self-tolerance and associated autoimmune disorders[147]. In humans, it has been demonstrated that mutations in p21 and other genes such as HLA class I and II are associated with the development of systemic lupus erythematosus (SLE) [150,151]. Nutrophils

modified functional properties were associated with SLE, among them: decreased clearance of apoptotic material and increased synthesis of different proteins including oxidants, hydrolytic enzymes, and inflammatory cytokines that contribute to tissue damage through the expansion of inflammatory cells that attack multiple organ systems, leading to disease and eventually death[222] Studies in mice also demonstrated a role of p21 as a suppressor of autoimmunity[154,152]. It has been shown that in mice of mixed genetic background, deletion of p21 led to the development of severe and lethal lupus-like autoimmunity[152]. Characteristics of lupus, such as splenomegaly, lymphadenopathy, glomerulonephritis, T-cell accumulation and high levels of anti-DNA antibodies were observed in these mice[152]. The extreme disease outcome was associated to the mixed genetic background of these mice that enhanced the effect of p21 deletion[152].Actually,p21-deficient mice of pure genetic C57BL/6 background develop normally and over time show a mild loss of tolerance to DNA and a moderate, yet not lethal, lupus-like phenotype[154].

My thesis project aimed at the characterization of molecular and cellular mechanisms underlying the lack of transplantability of p21-/- mammary tumors into syngeneic hosts. As I will describe in the Results sections, I demonstrated that the lack of transplantability of p21-/- tumors is the consequence of the presence, in the tumor microenvoronment of the injected tumors, of a specific subpopulation of antigen presenting cells (APCs), which activated a potent anti-tumoral CD4+ response. Thus, I will briefly summarize in this introduction some background information related to T-cell responses (classic, to super-antigens and homeostatic) and the tumor micro-environment, with particular emphasis on APCs.

1.4 T-cell proliferation mechanisms

The immune system is persistently exposed to foreign antigens deriving from microbes (harmless or pathogenic) and from self-antigens (normal or transformed) and its main goal is to achieve two outcomes: to eliminate dangerous pathogens and transformed cells while preserving harmless commensal microbes and normal cells[47,48]. Among the cells involved in the Immune system are T cells. A T cell is a type of lymphocyte, which develops in the thymus gland and plays a central role in the immune response; it differs from other lymphocytes by the presence of a T-cell receptor on its surface. TCR (T Cell Receptor) includes two peptide chains, either α/β or γ/δ, non-covalently associated with CD3γδε and ζ chains[47,48]. 90% percent of peripheral blood T cells have α/β peptide chain, while γ/δ chain is present on 4% (range 1-10%) of peripheral blood and lymph node lymphocytes and 1% of thymocytes.The three regions V (variable), J (junctional) and C (constant) are contained in the α *peptide*, while the β *peptide* chain has an additional fourth region D (diversity). The constant region (α/β chain) of the TCR complex interacts with the CD3γδε and ζ chains and is characterized by an immunoglobulin like domain, a connecting peptide, a transmembrane and cytoplasmic domain.When T cells are activated, they -depending on the type of stimulus- can displaythree types of responses: classical response, superantigen response and homeostatic response.

1.4.1 T cell classical response

During a classical response, an APC (antigen presenting cell) processes a given antigen and an epitope from a protein antigen acts as a bridge between the MHC complex (or HLA, Human Leukocyte Antigen,in humans), the APC and the TCR[47,48]. In a classical response 0.0001-0.001% of the body's T-cells are activated and T cells need two signals in order to became activated. The first signal is the binding of the T cell receptor to its cognate peptide presented by the MHC on an APCs. MHCI presents peptides of 8-13 amino acids in length to CD8+ T

cells while MHCII presents 12-25 amino acid peptides to CD4+ T cells[63]. The second signal derives from co-stimulation. The only co-stimulatory receptor constitutively expressed by naïve T cells is CD28 that binds the proteins CD80 and CD86 (together constituting the B7 protein) on the APCs. T cells need both signals in order to be activated, otherwise they become anergic; this mechanism avoids inappropriate response to self-peptides because self-peptides are not presented with an appropriate co-stimulation[63].

1.4.2 T cell superantigen response

T cell superantigens (Sags) are microbial proteins thattrigger excessive and aberrant activation of T-cells *in vitro* and *in vivo*[49,50]. A common feature of these T-cell activation is massive systemic immune activation, as reflected by high serum levels of TNFα, IL-1, IL-6 and IFNγ; the associated toxic shock is likely to be due to excessive release of cytokines. Compared to a normal antigen-induced T-cell response where only few clones of T-lymphocytes proliferate (0.0001-0.001% of the body's T-cells are activated), these SAgs short-circuit the immune system and result in massive and polyclonal activation of T-cells (up to 20% of the body's T-cells are activated).Sags bind to the TCR and MHC-II receptors outside ofthe classical antigen-binding site, bypassing the feature of conventional antigen processing[49,50]. SAgs bind to the V_β domain of the TCR and different SAgs have specificity for one or a limited set of V_β domains and can stimulate all T cells bearing the particular V_β designation. SAg-induced T-cell activation requires MHC-II positive cells but it is not MHC-II restrictive, and binding of MHC-II receptor determines the susceptibility of an individual to the particular SAg.Besides V_β-specific T-cell activation, certain SAgs, for example Staphylococcal Enterotoxin H, induce V_α-specific T-cell activation[49,50] (**Fig.3**).

Autoimmune reaction may be favored by breakdown of tolerance caused by immunostimulatory properties of SAgs. In a number of autoimmune diseases,

including rheumatoid arthritis, multiple sclerosis, Sjögren's syndrome, autoimmune thyroiditis and psoriasis, a skewed pattern of Vβ usage has been observed [50].

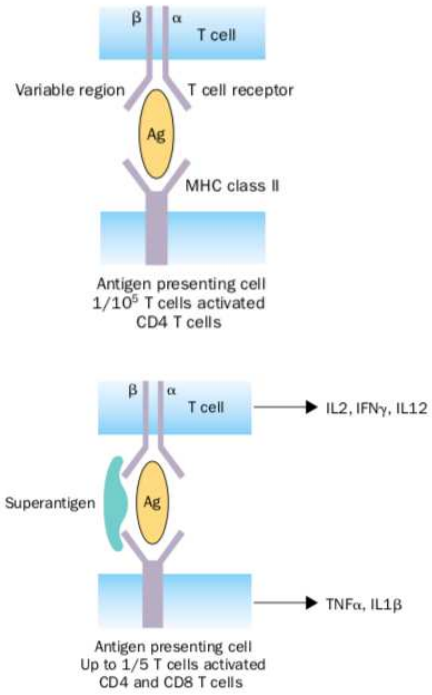

Fig.3. Contrasting mechanisms of conventional antigen (upper panel) and superantigen (lower panel) presentation (lower panel) (*Martin Liewelyn et al. Lancet infectious disease 2002*)[50].

1.4.3 Homeostatic CD4+ T cell proliferation

Throughout life, T cells in the periphery are tightly kept at a relatively constant level in terms of number and composition, suggesting the existence of a homeostatic mechanism(s)[42,73]. Alterations in the homeostasis generate a series of compensatory mechanisms that reinstate the homeostatic equilibrium. Lymphopenia may be caused by physiological processes during the neonatal period or by pathogenic conditions (such as viral infection)[38-39]. Booki Min et al.[39] demonstrated that a physiologic lymphopenic environment exists in neonatal mice and supports CD4+ T cell proliferation. Proliferating naive CD4+ T cells within neonates acquire memory phenotype and their homeostatic proliferation is inhibited by the presence of both memory and naive CD4+ T cells while it is enhanced by 3-day thymectomy and is independent

of IL-7; moreover this proliferation requires a class II MHC-TCR interaction and a CD28-mediated signal.Viral infections cause clonal expansion of antigen-specific CD8+ T cells with a massive expansion of their peripheral component and up to ~90% of the total CD8+ T cells may become antigen specific in case of lymphocytic choriomeningitis viral infection[64]. When the infection is cleared, homeostasis come back to the normal level and the most part of the effector cells are eliminated, leaving newly generated virus-specific memory T cells[64]. Overall, T cell homeostasis is a fundamental process that needs a precise balance between proliferation and apoptosis. A plethora of evidences indicate that dysregulations in T cell homeostasis can lead to inflammatory disorders, including autoimmune diseases[40,41,73]. Mild and severe lymphopenic models were used to investigate proliferative T cell responses, initially and generally called homeostatic proliferation (or lymphopenia- induced proliferation), and revealed that T cell proliferation within lymphopenic settings is highly heterogeneous. Indeed, there are at least two mechanistically distinct proliferation modes referred to as spontaneous/fast proliferation and homeostatic/slow proliferation[42,73].

1.4.3.1 Slow Homeostatic proliferation

Slow homeostatic proliferation (HP) is a slow response that arises within mild lymphopenic state following sublethal irradiation or T cell ablation and in the presence of functionally intact thymus[42,43]. During slow HP, CD4+ T cells undergo a cell division every 3–4 days[42]. The interaction of the TCR with the MHC-peptide complex contributes to the responses as blocking the interaction inhibits proliferation[44,45]. The TCR engagement alone, however, is not enough for proliferation and the presence of antibodies against IL-7 (homeostatic cytokine) inhibits slow HP of T cells[42], demonstrating that signals generated from both TCR and cytokine receptors must be integrated to trigger proliferation. The nature of the antigens involved in slow HP remains uncertain but it is likely low affinity self-antigens because slow HP is not impaired in germ-free lymphopenic recipients[46,73].

1.4.3.2 Fast Homeostatic Proliferation

Fast homeostatic proliferation is a strong proliferation characteristics of severe lymphopenic hosts, comprinsing mice with mutation in genes involved in lymphocyte generation. Spontaneously proliferating cells divide more than a cell division per day even in the absence of homeostatic cytokines[42,46]. In case of CD4+ T cells, the requirement for spontaneous proliferation is rather unique, because MHC II molecules are required for proliferation[43]. As to CD8+ T cell spontaneous proliferation the requirement is less rigorous: either MHC I or MHC II are sufficient to induce proliferation[43]. Another important feature of fast HP is that the proliferating cells turn into phenotypically different populations. They rapidly differentiate into memory/effector phenotype cells, acquiring memory/effector cell markers and an ability to produce inflammatory cytokines upon stimulation[46,73]. Spontaneously proliferating T cells show CD44 upregulation and CD62L downregulation; CD44 is a cell-surface glycoprotein involved in cell–cell interactions, cell adhesion and migration while CD62L (also known as L-selectin) belongs to adhesion/homing-receptors family and play important roles in lymphocyte-endothelial cell interactions. Unlike T cells activated by cognate antigens, do not express early activation markers (CD69 and CD25); in this way they are allowed to preferentially migrate into non-lymphoid tissues as antigen- stimulated effector/memory T cells do.

1.5 Autoimmunity and Cancer

As described above, under lymphopenic conditions, lymphocytes undergo HP, a general mechanism that maintains T cell numbers through controlled expansion. In addition to its role in normal immune function, HP might lead to autoimmune disease and yet might also be beneficial in tumor immunotherapy, as has been shown in both animal models and humans[73]. The HP occuring in response to the available lymphoid space favor the proliferation of

autoreactive T cells and autoimmunity. Likewise, the available lymphoid space provides an environment for the proliferation of tumor-specific T cells, thus promoting tumor immunity[153]. Cancer and autoimmune disorders (AID) are bidirectional associated; infact in one hand an increased risk of malignancies (both hematological and non-hematological) has been observed in different autoimmune disorders while on the other hand, some malignancies can increase the risk of autoimmune disorder development. Autoimmunity (AI) results from the progressive and continuous breakdown of immune check and balance mechanisms protecting host tissues from destruction[121,122]. As a preexisting condition, the autoimmune process starts 2–4 years before diagnosis. Most AIDs progress either as an organ-specific disease, as in multiple sclerosis and type 1 diabetes or as a multiorgan disease, as in systemic lupus erythematous (SLE) or rheumatoid arthritis. Patients with autoimmune disorders, such as SLE, rheumatoid arthritis and inflammatory bowel disease have an increased risk of developing cancers (hematological disorders and solid tumors)[123]. Several reports showed that cancer survival decreases significantly in patients with preexisting AID or chronic inflammatory diseases[124,125,126] and this decrease in survival has been largely associated with a higher risk of developing immune-related adverse events (unwanted inflammatory events) in response to anticancer therapy than in the overall population.

Autoimmune diseases and immune-suppressive treatments may allow for tumor development[155,156,157]. For example, it has been observed that patients with rheumatoid arthritis have increased risk of lymphomas and lung cancer[158]. On the other side, immune-therapies against different types of cancer often correlate with the break of immune-tolerance and consequent autoimmune responses[155,159,160]. Indeed, emerging evidence suggests that development of autoimmunity during cancer treatment correlates with inhibition of tumor growth. It has been reported that patients with metastatic melanoma treated with antibodies against immune- checkpoint inhibitors (anti-CTLA-4 antibodies) develop severe autoimmune

diseases[161], which correlates with tumor regression. Another study also reported positive correlation between severe autoimmunity and immune response against metastatic melanoma, ovarian and renal cell carcinoma[162].

In conclusion, multiple factors play a role in determining the outcome of the aberrant inflammatory process, including the type of inflicted tissue or organ, the degree of tissue injury sustained, the type of cells activated, the amounts of protein and lipid mediators that are locally and systemically secreted by Immune cells, and the extent to which immune regulatory checkpoints are activated. Collectively, these comprise the microenvironment and more specifically the Tumor Micro Environment (TME).

1.6 Role of T cells in tumorigenesis

T cells are components of the adaptive immune system that act as effectors of immunity by acquiring functional and effector phenotypes whose activity has inflammatory or anti-inflammatory consequences[51,74]. During the early stages of tumor initiation, in the presence of enough immunogenic antigens, naïve T cells are primed in the draining lymph nodes, followed by their activation and migration to the TME (Tumor Microenvironment), after which they start to mount a protective effector immune response eliminating immunogenic cancer cells. A high level of T-cell infiltration in tumors is associated with a favorable prognosis in different types of tumors like Melanoma[52] and breast cancer[53]. CD8+T cells are the most important anti-tumor cells. After priming and activation by APCs, the CD8+T cells differentiate into cytotoxic T lymphocytes (CTLs) and exert an anti-tumoral attack consisting in the direct destruction of target cells through the exocytosis of perforin and granzyme-containing granules[54,55,74]. CD4+ T helper 1 (Th-1) cells mediate an anti-tumoral response through secretion of high amounts of proinflammatory cytokines such as IL-2, TNF-α, and IFN-γ, promote T-cell priming and activation and CTL cytotoxicity; they also control the anti-tumoral activity of macrophages and NK cells and an overall increase in the presentation of tumor

antigens[56,57,58]. The presence of tumor-infiltrating CD8+ T cells and Th-1 cytokines in tumors correlates with a favorable prognosis in terms of overall survival and a disease-free survival in many malignancies[59]. However, cancer cells have learned to exploit the immunosuppressive properties of T cells while impairing the effector functions of antitumor T cells[60,74]. When tumors grow and the TME changes, new antigens are produced and consequently also the ability of the immune system to prime new repertoires of T cells and direct them toward the tumor changes, altering the efficacy of tumor containment. If the immune system works to preventing tumor growth, cancer cells together with the TME suppress the anti-tumor function by engaging immune checkpoints and the recruitment of CD4+ Tregs. Tregs are responsible for the suppression of the priming, activation, and cytotoxicity of other effector immune cells, such as Th1 CD4+ T cells, CTLs, macrophages, NK cells, and neutrophils[62]. Thus, the antitumor T-cell immune response depends on both the ability of the tumor antigen(s) to induce an immune response and the presence / absence of inhibitory signals that can impair the T cells' functions[51]. The two most characterized checkpoint molecules are CTLA-4 and PD-1. These proteins act as negative regulators of T-cell function, ensuring peripheral tolerance during immune regulation, and have been associated with immune evasion in cancer[61,74]. Several research groups have successfully targeted CTLA4 and PD1 as treatments for different recalcitrant cancers, research that earned James P. Allison and Tasuku Honjo Nobel Prize in 2018. These evidences highlight the importance of the immunotherapies.

1.6.1 Cancer Immunotherapy

Immunotherapy is deeply changing the landscape of cancer treatment. Cancer immunotherapies are designed to activate/boost the immune system to attack cancer cells through natural mechanisms, thus resulting, in principle, in fewer off-target effects than chemotherapies or other agents that directly kill tumor cells[65]. The development of immune checkpoint inhibitors (ICI), compounds that target molecules with immune-response inhibiting

functions, represents a revolutionary milestone in the field of immune-oncology[65]. The two most common ICI strategies involve PD-1/PD-L1 blockade and CTLA4 inhibition, which act, respectively, by inhibiting the interaction between PD1 (expressed on activated T cells) and PD-L1 (expressed by tumor cells), or blocking the activity of CTLA4 (a co-inhibitory molecule that regulates the extent of T cell activation). Recent reports show that treatment with ICI induce durable responses in a large fraction of patients with various types of metastatic tumors, thus unraveling the high potential of cancer immunotherapy[65]. Despite their unquestionable success, ICI still have two important limitations: i) a significant portion of patients does not respond (40-90%, depending on the tumor type); and ii) they are associated with substantial immune-related toxicity. Immunotherapy, however, encompasses more than ICI alone. Dendritic cell (DC) vaccination, for instance, makes use of autologous DCs to generate an immune response against specific tumor-associated antigens[66,67]. Despite its highly favorable toxicity profile, DC vaccination showed so far only poor clinical benefit (only 10-20% of the patients responded to treatment, with no long-term responses). Recent data, however, suggest that a synergistic approach with other agents might improve DC vaccines' efficacy[70]. Adoptive cell transfer (ACT), instead, has achieved more exciting results in cancer clinical trials. T-cell-based ACT comprises the use of both TILs (extracted from fresh tumor samples) or peripheral blood lymphocytes (they can be used either in their natural state or modified genetically) (CAR-T cells)[68,69]. Current ACT response rates with CAR-T cells are 80%-90% for hematological malignances and 30% for metastatic melanoma refractory to multiple lines of therapy[70]. In summary, although immunotherapy is revolutionizing cancer treatment, there is still much to be done to fulfill its therapeutic potential in terms of both efficacy and safety[68](**Fig.4**).

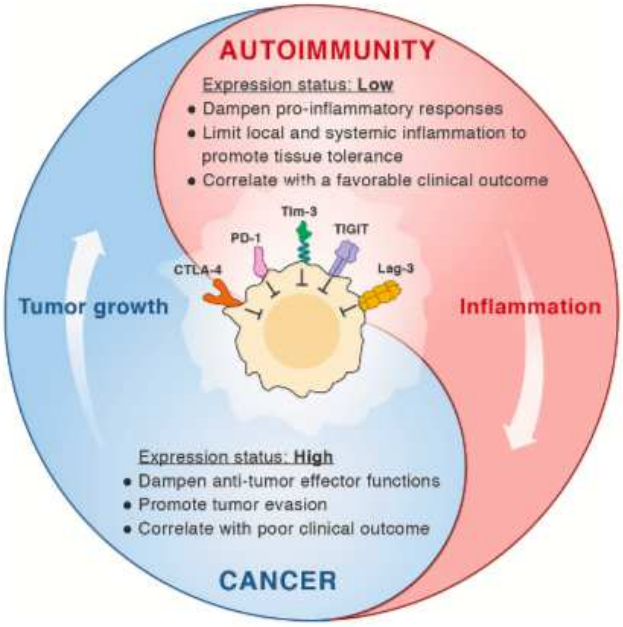

Fig.4 The Yin and Yang of co-inhibitory receptors. Representation of the co-inhibitory receptors' functional role in autoimmunity and cancer.. (*Alexandra Schnell et al. Cell Research 2020*)[75]

1.7 The Tumor Micro Environment (TME)

The Tumor micro environment (TME) is the cellular environment where tumors or cancer stem cells (cells in a tumor with the abilities to self-renew and drive tumorigenesis[60,109]) exist. The TME includes surrounding immune cells, blood vessels, extracellular matrix (ECM), fibroblasts, lymphocytes, bone marrow-derived inflammatory cells, and signaling molecules[110,111]. Cancer development and progression are affected by the interaction between malignant and cells of the TME[112,113,109]. While nonmalignant cells often play a pro-tumorigenic function at all phases of carcinogenesis by stimulating uncontrolled cell proliferation[114,60], malignant cells invade healthy tissues and spread to other body parts through the lymphatic or circulatory system. As I have already anticipated, the TME comprises different cellular components. First, endothelial cells which play a key role in tumor development and tumor cell protection from the immune system[114]; these cells offer nutritional

support for tumor growth and development. A further component is immune cells such as granulocytes, lymphocytes, and macrophages that are involved in various immune responses and activities, for example the inflammatory reactions orchestrated by the tumor to promote survival. The most represented immune cell type in the TME is the macrophage[114,115,109]; macrophages play different roles that are linked to cancer development and progression, for example they promote the escape of tumor cells into the circulatory system and can suppress antitumor immune mechanisms and responses[115]; moreover previous studies revealed that macrophages can help circulating cancer cells extravasate at distant sites, such as the lungs, which can lead to the persistent growth of metastatic colonies[60,111] **(Fig.5**). Plethora of studies have revealed that tumor-associated macrophages (TAMs) can augment, mediate, or antagonize the antitumor activity of irradiation, cytotoxic agents, and checkpoint inhibitors. The last cell type in the TME is the fibroblast[116,117]that allows cancer cells to migrate from the primary tumor location into the bloodstream for systemic metastasis and provides passage for endothelial cells undergoing angiogenesi.. Previous studies examined the role of the Extracellular matrix (ECM) in cancer development and progression. The ECM is a network of macromolecules (glycoproteins, collagens, and enzymes) that support biomechanical activities and functions in the body[114,60,109]. Notably, the ECM is composed of active tissue components that influence cell adhesion, proliferation, and communication[1118,116,117];the cellular growth factors in the ECM near other cell membranes, such as integrins, are implicated in the communication with the TME. Moreover, the ECM further influences the migration of cancer cells by altering its physical properties, composition, and topography[119,109].

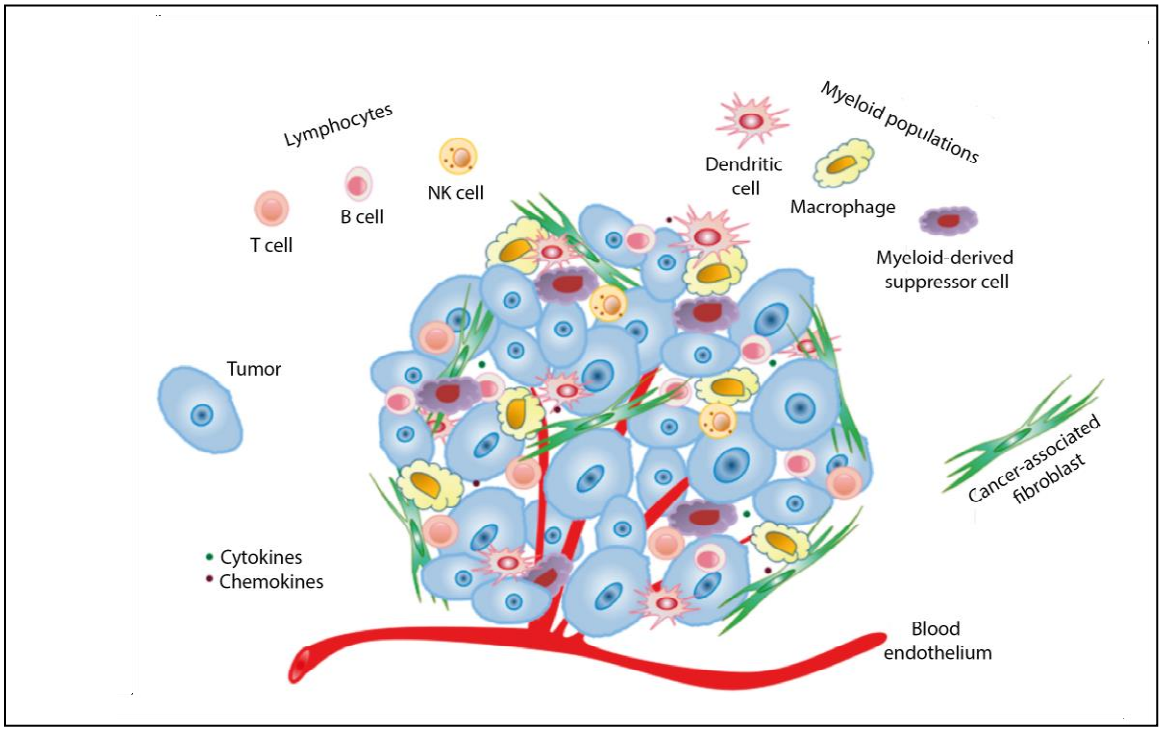

Fig.5 Cellular constituents of the tumor microenvironment that shape tumor immunological landscape. The tumor microenvironment consists of complex cellular and molecular constituents including immune cells of hematopoietic origin and stromal cells of non-hematopoietic origin. The immune cell compartment comprises populations of dendritic cells, macrophages, and myeloid-derived suppressor cells. The stromal compartment consists of cancer-associated fibroblast and endothelial cells of the lymphatic and blood vasculature(*Cui, Y et al. Int. J. Mol. Sci. 2016*)[120]

1.7.1 Immune cells in the TME

TME comprises of tumor stroma, blood vessels, infiltrating inflammatory cells and a variety of associated tissue cells. Both adaptive and innate immune cells, such as T cells, B cells, dendritic cells (DCs), macrophages, and natural killer (NK) cells can be found in TME. Most immune cells of the TME inhibit anti-tumor immunity and promote tumor growth and progression[163,164]. In other cases, specific tumor-infiltrating immune cells (i.e. cytotoxic T lymphocytes) exert anti-tumor effects, and can be regarded as an attempt of host's immune response to react to slow tumor progression ("immune-surveillance")[153,169]. However, the pro-tumoral effects of the TME exceed consistently its anti-tumoral effects, resulting in tumor

escape and progression. In a variety of tumors, the majority of infiltrating inflammatory cells are $CD4^+$ and $CD8^+$ tumor-infiltrating lymphocytes (TILs)[163,170].TILs can recognize specific tumor-associated antigens, however their effector function is often inhibited by other immune cells present in TME (such as regulatory T cells or Tumor Associated Macrophagess), rendering them defective in supressing tumor growth[163]. A crucial portion of $CD4^+$ T cells present in TME are $CD4^+CD25^+Foxp3^+$ cells known as regulatory Tcells (T-regs)[164,170].Under physiological conditions, T-regs have a critical role in maintaining homeostasis of cytotoxic lymphocytes. In cancer, T-regs have immune-suppressive role and they often block the proliferation of cytotoxic T cells in TME either by direct contact or secretion of specific inhibitory cytokines (such as IL-10 and TGF-β)[38,44]. These cells also interfere with tumor-associated antigen-presentation by downregulatingco-stimulatory molecules onDCs[168]. Anothertypeofcellswithimmune-suppressivefunctionfoundinTMEisMDSCs (Myeloid derived suppressor cells)[170,171].They originate from the common myeloid progenitor in the bone marrow and often have a direct inhibitory effect on cytotoxic lymphocytes[171]. They are also known to impede M1 macrophage polarization[172], antigen-presentation by DC[167], and NK cellcytotoxicity[173]. Solid tumors are also infiltrated with macrophages, known as TAMs. TAMs often perform suppressive functions in TME by releasing inhibitory cytokines such as IL-10, prostaglandins and ROS[163,164,165]. In response to diverse microenvironmental stimuli, macrophages can be polarized towards different functional phenotypes. Polarization of macrophagessignificantlyimpactstumorigenesis.Macrophagesactivated Inaclassicalfashion are polarized towards M1 phenotype and they may counteract tumor growth[174,175], while alternatively activated M2 macrophages often have a pro-tumoral role[166,176]. In fact, in avariety of human tumors, infiltrated macrophages are associated with M2 phenotype and their presence in TME negatively correlates with patient's survival[166]. It has been suggested that hypoxic TME in solid tumors is one of key factors that induces TAM polarization by up-

regulating M2-related genes[177,178,179]. Other than inhibiting lymphocyte effector function, TAMs are also shown to be responsible for tumor entry in the vasculature[180,181], allowing for tumor dissemination.

1.8 Immune cell subsets

Different immune cell subsets are distributed between primary and secondary lymphoid organs; primary lymphoid organs include the bone marrow and the thymus while secondary lymphoid organs include the lymph nodes, the spleen, the tonsils. I will briefly discuss the distribution of immune cell subsets in the spleen, which is of relevance for the experiments I will describe in the Results section of mythesis.

1.8.1 Immune cell subsets distribution in the mouse spleen

The spleen is a secondary lymphoid organ specialized in filtering blood-borne antigens and in removing/recycling of old or damaged erythrocytes[76,77]; the spleen is also important for myelopoiesis[76]. The spleen is composed by two distinct compartments: the red pulp and the white pulp. The Red pulp contains venous sinuses that act as filters to trap old or damagederythrocytes that are phagocytosed by red pulp macrophages[78], while the white pulp is involved in immune responses against blood-borne antigens and pathogens. The White pulp is divided in three regions: 1. T cell zone or periarteriolar sheath (PALS); inner PALS contain CD4+ and CD8+ T cells, interdigitating DC and migrating B cells while outer PALS contain macrophages[79]; 2. B cell follicles that are continuous with PALS and include B cells, CD4+ T cells and follicular DC[79]; 3. A marginal zone -situated between the red pulp and the PALS- with the function of screening the blood-borne antigens[79] . Common subsets of DC (located mainly within the white pulp)[76] and a number of distinct macrophages/monocytes cell types (located in red pulp) in the spleen have been well characterized and their functional importance in terms of their comparative roles in antigen presentation is still under investigation[77] (**Fig.6**).

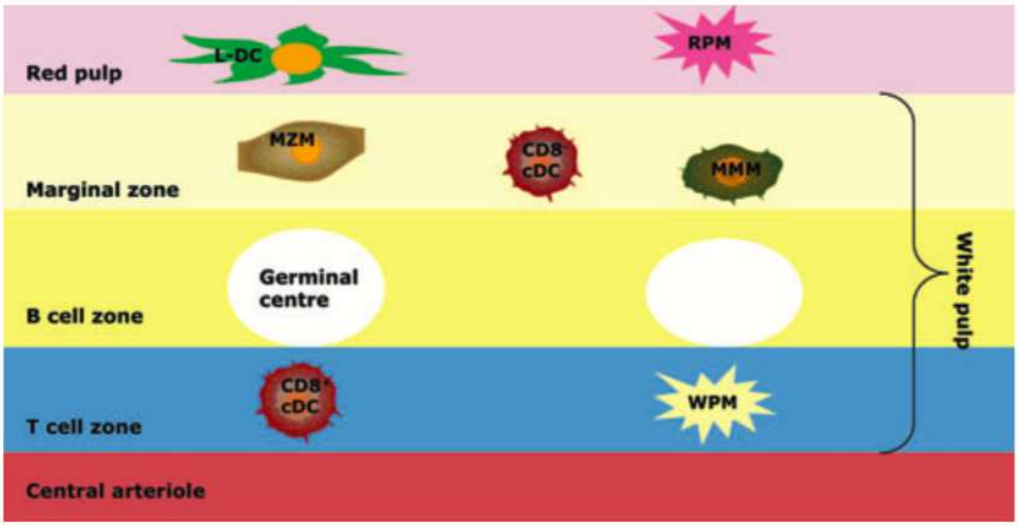

Fig.6. Compartimentalization of antigen presenting cells (APC) within splenic red and white pulp regions. Both $CD8^{+}$cDC and white pulp macrophages (WPM) lie in the T cell zone, whereas marginal-zone metallophilic macrophages (MMM), marginal-zone macrophages (MZM) and CD8cDC lie within the marginal zone. RMP are localized in the red pulp. The tentative location of L-DC within the red pulp region is based on experimental verification of high accessibility for blood-borne antigen compared with other DC subsets (*Ying Y. hey, et al. J.Cell.Mol.2012*)[77].

1.8.2 The myeloid subset

The myeloid subset in spleen includes granulocytes, monocytes and macrophages[76].

Granulocytes (neutrophils, eosinophils, basophils and mast cells) are $Ly6G^{+}$ cells present in the red pulp region[80]. Monocytes develop in the bone marrow (BM) from a common myeloid/dendritic cell progenitor[81,82] and migrate into the blood and spleen as mature cell[82] andthey terminally differentiate in the spleen to give macrophages.

1.8.2.1 Monocytes

The characterization of monocyte subsets in tissues is still ongoing, and recent investigations demonstrate that the early phenotypic descriptors do not exactly mirror the phenotype of similar subsets in the spleen[84]. Current thinking is that inflammatory monocytes, also referred to as "classical monocytes"[85], home to sites of infection where they induce an inflammatory

response, and may also differentiate to give TNF/iNOS-producing dendritic cells[86]. Resident monocytes are also known as “non-classical monocytes” and migrate in steady-state conditions as precursors of tissue-resident macrophages (for example in liver, spleen, lung and skin)[85,87]. Undifferentiated monocytes reservoir resident in the spleen was found to be similar to blood monocytes in terms of both phenotype and gene expression[88]. Monocytes were shown to mobilize from the spleen into sites of inflammation in the heart, with inflammatory monocytes clearing damaged tissues, and resident monocytes promoting wound healing[88,83].

1.8.2.2 Macrophages

The Spleen contains 4 different subsets of resident macrophages. Two subsets are located within the marginal zone: marginal-zone metallophilic macrophages (MMM) and marginal-zone macrophages (MZM)[79]. MMM are localized near the PALS and B cell follicles[89] andthey are thought to function in induction of cytotoxic T cell responses against blood-borne and self -antigens[89,90.] ; they can be visualized by staining with the MOMA-1 monoclonal antibody, and localize near the PALS and the B cell follicles[79]; MZM are located closer to the red pulp and express a number of Toll-like receptors (TLR), the MARCO scavenger receptor and the C-type lectin, SIGNR1, for clearance of microorganisms[79,91]. White pulp macrophages during germinal ceter reactions are involved in phagocytosis of apoptotic B and distinguishable as $CD11b^{-}F4/80^{-}CD68^{+}$ cells[92]. Red pulp macrophages clear old or damaged red blood cells and recycle of heme-groups and are characterized by F4/80 expression ($CD11b^{+}F4/80^{+}CD68^{+}$)[93]. Moreover, macrophages can be classified as pro-inflammatory (classical) or anti-inflammatory (non- classical) subsets of M1 and M2 macrophages on the basis of their functions, adding further functional diversification to the myeloid lineage[94.].

1.8.3 The dendritic subset

Dendritic cells (DCs) are the most efficient APCs in the immune system.They represent a heterogeneous class of cells with subtypes differing in tissue location, migratory pathway, cell surface marker expression, immunological function and dependence on infections or inflammatory stimuli for their generation[95]. They are widely distributed throughout the body and distinct subsets have been described in spleen, mucosa, intestine and epidermal tissue[95]. Some DC have been classified as migratory and these cells appear to survey the environment by constant uptake of tissue antigens. In the presence of pathogen-related 'danger signals', they mature and migrate to the lymph nodes (LN) to present antigens to the T cells[96]. In contrast, lymphoid tissue-resident DC do not migrate, but take up and present incoming antigens to T cells[96]. Multiple subsets of DCs have been identified in both humans and mice[95,97]. Conventional DCs (cDCs) represent the main DC subset in the spleen and have been further classified into $CD8a^+$ and $CD8a^-$subsets. $CD8a^+$ cDCs are phenotypically distinct as $CD11c^+CD11b^-CD8a^+MHCII^+B220$cells, whereas $CD8a^-$cDCs are $CD11c^+CD11b^+CD8^-MHCII^+B220$cells[98]. These subsets differ in immune function, including cytokine production and ability to cross-present antigen[99].It has been proposed that $CD8a^+$ cDCs play a role in the maintenance of tolerance to self-antigens, consistent with their close proximity to T cells in the resting state, and their notable capability for cross-presentation [100,101]. $CD8a^+$ cDCs are also the predominant producer of IL-12, important for $CD8^+$ T cell proliferation[95]. In addition, they have recently been described as a major producer of IFN-k in response Toll-like receptor (TLR) 3 stimulation with double-stranded RNA[102]. In contrast, $CD8a^-$cDCs have weaker cross-priming ability and are mainly localized in the marginal zone of spleen[100]. Upon stimulation with lipopolysaccharides, $CD8a^-$cDCs migrate to T cell areas and secrete inflammatory chemokines[100]. The primary role of $CD8a^-$cDCs, however, still remains

unclear[97]. Plasmacytoid DCs exist as a plasmacytoid pre-DC (p-pre-DC) in the steady-state. They are relatively long-lived, circulating cells, that produce high levels of type I interferon after stimulation with viral or other microbial agents[103]. Plasmacytoid DCs -like cDCs- have been described to arise from a common dendritic progenitor (CDP)[104]. Inflammatory stimuli initiate the conversion of p-pre-DC into pDC, and the production of type I interferons that enhance the function of NK cells, B cells, T cells and DC during antiviral responses. Subsequently, pDCs differentiate to give the $CD8^{+}CD205$-DC subset, distinct from $CD8^{+}$ cDCs that also regulate T cell function[105]. Plasmacytoid DCs are mainly distinguished by their $CD11c^{lo}CD11b^{-}B220^{+}$ phenotype and production of type I interferons in response to TLR7 and TLR9 signalling [96,106]. Dendritic-like cells (L-DCs) is a novel subset of dendritic cells that has been identified in both murine and human spleen[84,107,108]. Following comprehensive flow cytometric analysis of many splenic myeloid and dendritic subsets[84], L-DCs are now identifiable by their phenotype as $CD11b^{hi}CD11c^{lo}CD43^{lo}CX_3CR1^{lo}$ cells, also lacking expression of MHCII, Ly6C, Ly6G, and Siglec-F.

2. Materials and Methods

2.1 Mouse strains

Mouse colonies were maintained in a certified pathogen-free animal facility at the European Institute of Oncology. All experimental procedures including mice have been approved by the Italian Ministry of Health and have been performed in accordance with the Italian Legislation and with the international guidelines for the care and use of animals. All mice were euthanized by high concentrations of CO_2inhalation. FVB/Hsd (FVB) animals were purchased from Envigo Rms Srl. NOD.CB17/Prkdcscid/J (NOD-*scid)* mice were purchased from Charles River and $p21^{-/-}$ FVB mice were provided from breeding area of the mouse facility (Cogentech) at Campus European Institute of Oncology.

MMTV-ErbB2(FVB-Tg(MMTV-Erbb2)NK1Mul/J)mice were provided by Jackson Lab. P21-/- MMTV-ErbB2 were obtained from a cross between male MMTV-ErbB2 and female p21-/- FVB and generated in the breeding area of the mouse facility (Cogentech) at Research Campus of European Institute of Oncology.MMTV-ErbB2 mice express an activated form of ErbB2 Rat oncogene under control of LTR promoter of murine Mammary Tumor Virus (MMTV). The activated/transformed form of ErbB2 oncogene is characterize by an Amino Acid replacement at position 664 (Val^{664} to Glu^{664}). Murine ErbB2 tumor are multifocal and develops spontaneously in these mice with 100% penetrance at 3-6months of age (median 4 months) and resembles the human ErbB2 tumor.WNT1/FVB mice (FVB.Cg-Tg(Wnt1)Hev/J were provided by Jackson Lab. p21-/- WNT1/FVB were obtained from a cross between male WNT1/FVB and female p21-/- FVB and generated in the breeding area of the mouse facility (Cogentech) at Research Campus of European Institute of Oncology.These Wnt-1 mice express a transgene with MMTV LTR placed 5' to

the *Wnt1* (formerly *int-1*) gene in the opposite transcriptional orientation. Mammary glands of these mice are hyperplastic.

2.2 *In vivo* procedures

2.2.1 Primary ErbB2/Wnt tumor digestion and *in vivo* transplantation

WT and p21-/- ErbB2 or Wnt primary tumors were used as a source of tumor cells.

When primary tumors reached (maximum) an overall diameter of 1cm, WT and p21-/- MMTV-ErbB2 or WN1/FVB mice were sacrificed and tumor mass collected and digested in Digestion Media (DMEM, 5% Penicillin/Streptavidin, 5% L-Glutammine (L-Glut), 5% Ianuloridase, 5% Collagenase) at 37°C for at least 4 hours. At the end, digested tumor could be frozen in Freezing Media (Fetal Bovine Serum South America, 10% Dimethilsulfoxide) for future experiment or used immediately.

For *in vivo* ErbB2/Wnt transplantation, 300000 tumor cells were thawed, resuspended in 40µl PBS1X (Phospate Buffered Saline) and injected in mammary fat pad of anesthetized (Intraperitoneal injection of Avertin sigma at 0.5ug Avertin/1g mouse) 7-12 weeks old WT andp21-/- FVB, NOD-*scid* or Sub-lethally irradiated FVB recipients (5.5 Gray). Upon transplantation, tumor mass takes on average 60 days to become palpable and mice were followed for the disease development by manual palpation and measure of tumor mass (measure was performed weekly). Mice have been also followed every 2-3 days to evaluate any sign of distress, such as hair loss and reluctance in motion. At the onset of the disease (tumor mass=0.8mm3), mice were euthanized (using CO_2).

2.2.2 Spleen or CD11b+ cell addition to ErbB2 tumor cells and*in vivo* transplantation

WT ErbB2 thawed tumor cells were used as a source of tumor cells; WT and p21-/- spleen cells were obtained respectively from the smashing of WT and p21-/- FVB mice spleens; WT and p21-/- CD11b+ cells were obtained respectively from the smashing of WT and p21-/- FVB spleens and isolated by sorting technique.

Spleen or CD11b+ cells were added to ErbB2 tumor cells at ratio 4:1 (1.2 millions spleen or CD11b+ cells : 300000 ErbB2 cells) in a volume of 45µl PBS 1X (Phosphate Buffered Saline) and injected into the mammary fat pad of anesthetized (intraperitoneal injection of

Avertin sigma at 0.5ug Avertin/1g mouse) 7-12 weeks old WT FVB syngeneic recipient mice.

Upon transplantation, mice were followed for the disease development by manual palpation and measure of tumor mass (measure was performed weekly). Mice have been also followed every 2-3 days to evaluate any sign of distress, such as hair loss and reluctance in motion. At the onset of the disease (tumor mass=0.8mm3), mice were euthanized (using CO_2).

2.2.3 MHCII+ or CD11b+ cell depletion from ErbB2 tumor cells

WT and p21-/- ErbB2 tumor cells were stained with antibodies anti-MHCII, anti-CD11b and depleted of MHCII+ or CD11b+cell populations by sorting technique or MACS® MicroBeads technology for column-based magnetic cell isolation using nano-sized beads coated with coated with anti-mouse MHCII or CD11b antibodies (Mylteni Biotec). Afterwhich, MHCII- or CD11b- ErbB2 tumor cells where injected in mammary fat pad of anesthetized (Intraperitoneal injection of Avertin sigma at 0.5ug Avertin/1g mouse) 7-12 weeks old WT FVB syngeneic recipient mice (300000 cells/mouse in 40µl PBS1X). Upon transplantation, mice were followed for the disease development by manual palpation and measure of tumor mass (measure was performed weekly). Mice have been also followed every 2-3 days to evaluate any sign of distress, such as hair loss and reluctance in motion. At the onset of the disease (tumor mass=0.8mm3), mice were euthanized (using CO_2).

2.3 *In vitro* assays

2.3.1 T cell proliferation and phenotype assay

CD11b+, CD11c+, CD11b+c+, CD11b+c- or CD11b-c+ cells were isolated by sorting technique from smashed p21-/- and WT FVB spleens, while CD3+CD4+ T or CD3+CD8+ T cells were isolated by sorting technique from smashed WT FVB spleens and stained with Cell Trace CFSE fluorescent dye (INVITROGEN) for characterization of their proliferation (T cells were incubated with 10μM CFSE solution in PBS 1%FBS for 6 minutes 37° C, dark). Cells were cultured together in 96-well plate in sterile complete RPMI-1640 medium (500ml RPMI-1640 Sigma Aldrich, 10% North America Fetal Bovine Serum, 2.5ml no essential aminoacids, 2.5ml Sodium Pyruvate, 5% Penicillin/Streptavidin 5% L-Glutamine, 200μl B-Mercaptoethanol) at 1:4 ratio (CD11b+: T cells). Cells were kept in the incubator at 37^{o} degrees with 5% CO_2 for 96 hours with the possibility to try different experimental conditions: with/without 3.75mg/ml anti-mouse MHCII (I-A/I-E) (Biocell), with/without tumor lysate (5ug) (Tumor lysate was obtained through heat shock treatment and resuspension with 22g needle of thawed WT ErbB2 tumor cells and quantified by BCA assay), with/without Interleukin 7 (PeproTech)(5 and 10 ng/ml) and anti-Interleukin 7 (PeproTech) (5 ng/ml). After 96 hours, primed CD3+$CD4^{+}$or CD3+CD8+ T cells were collected and stained with an antibodies' cocktail for identification of T cell population and characterization of their proliferation and phenotype at BD FACS Celesta.

2.3.1.1 Time points T cell proliferation assay

CD11b+ cells were isolated by sorting technique from smashed p21-/- and WT FVB spleens, while CD3+CD4+ T cells were isolated by sorting technique from smashed WT FVB spleens and stained with Cell Trace CFSE fluorescent dye (INVITROGEN) for characterization of their proliferation (T cells were incubated with 10μM CFSE solution in PBS 1%FBS for 6 minutes 37° C, dark). Cells were cultured together in 96-well plate in sterile complete RPMI-1640 medium (500ml RPMI-1640 Sigma Aldrich, 10% North America Fetal Bovine Serum, 2.5ml no essential aminoacids, 2.5ml

Sodium Pyruvate, 5% Pen/Strep, 5% L-Glutamine, 200µl B-Mercaptoethanol) at 1:4 ratio (CD11b+:CD3+CD4+). Cells were kept in the incubator at 37^{o} degrees with 5% CO_2 for different times (4 days, 10 days and 15 days) paying attention to add at each time point (starting from day4 incubation) fresh sorted CD11b+ cells maintaining the ratio 1:4 (CD11b+ : CD3+CD4+). At each time point, CD3+CD4+ T cells were collected and stained with an antibodies' cocktail for identification of T cell population and characterization of their proliferation at BD FACS Celesta.

2.3.1.2 Titration of CD11b+ cells in T cell proliferation assay

CD11b+ cells were isolated by sorting technique from smashed p21-/- and WT FVB spleens, while CD3+CD4+ T cells were isolated by sorting technique from smashed WT FVB spleens and stained with Cell Trace CFSE fluorescent dye (INVITROGEN) for characterization of their proliferation (T cells were incubated with 10µM CFSE solution in PBS 1%FBS for 6 minutes 37° C, dark). Cells were cultured together in 96-well plate in sterile complete RPMI-1640 medium (500ml RPMI-1640 Sigma Aldrich, 10% North America Fetal Bovine Serum, 2.5ml no essential aminoacids, 2.5ml Sodium Pyruvate, 5% Pen/Strep, 5% L-Glutamine, 200µl B-Mercaptoethanol) at different ratios 4:1, 4:0.1 and 4:0.05 (CD3+CD4+: CD11b+). Cells were kept in the incubator at 37^{o} degrees with 5% CO_2 for 96 hours. After 96 hours, primed CD3+CD4^{+} T cells were collected and stained with an antibodies' cocktail for identification of T cell population and characterization of their proliferation at BD FACS Celesta.

2.3.2 CBA assay

CD11b+ cells were isolated by sorting technique from smashed p21-/- and WT FVB spleens, while CD3+CD4+ T cells were isolated by sorting technique from smashed WT FVB spleens and stained with Cell Trace CFSE fluorescent dye (INVITROGEN) for characterization of their proliferation (T cells were incubated with 10µM CFSE solution in PBS 1%FBS for 6 minutes 37° C, dark). Cells were cultured together in 96-well plate in sterile complete RPMI-1640 medium (500ml RPMI-1640

Sigma Aldrich, 10% North America Fetal Bovine Serum, 2.5ml no essential aminoacids, 2.5ml Sodium Pyruvate, 5% Pen/Strep, 5% L-Glutamine, 200µl B-Mercaptoethanol) at 1:4 ratio (CD11b+:CD3+CD4+). Cells were kept in the incubator at 37^{o} degrees with 5% CO_2 for 96 hours. After 4 days of incubation, surnatant was collected and cytokines production was characterized and measured using the BD^{TM} Cytometric Beads Array System (CBA) by which you can simultaneously detect multiple (n=7) soluble cytokines in a sample.

2.4 *In vitro/in vivo* assays

2.4.1 *In vitro* priming ofCD4+ T cells and their injection in NOD-scid mice

CD11b+ cells were isolated by sorting technique from smashed p21-/- and WT FVB spleens, while CD3+CD4+ T cells were isolated by sorting technique from smashed WT FVB spleens. Cells were cultured together in 6-well plate in sterile complete RPMI-1640 medium (500ml RPMI-1640 Sigma Aldrich, 10% North America Fetal Bovine Serum, 2.5ml no essential aminoacids, 2.5ml Sodium Pyruvate, 5% Pen/Strep, 5% L-Glutamine, 200µl B-Mercaptoethanol) at 1:4 ratio (CD11b+:CD3+CD4+). Cells were kept in the incubator at 37^{o} degrees with 5% CO_2 for 96 hours. After 96 hours, primed CD3+CD4^{+} T cells were collected and injected in tail vein of NOD-*scid* mice (1200000 cells/mouse in 200ul PBS1X), while ErbB2 tumor cells were injected the day after (300000 cells/mouse in 40µl PBS1X) in Mammary Fat Pat after anesthesia (Intraperitoneal injection of Avertin sigma at 0.5ug Avertin/1g mouse).

2.5 Sequencing experiments

2.5.1 T cell receptor (TCR) Clonality

CD11b+ cells were isolated by sorting technique from smashed p21-/- and WT FVB spleens, while CD3+CD4+ T cells were isolated by sorting technique from smashed WT FVB spleens and stained

with Cell Trace CFSE fluorescent dye (INVITROGEN) for characterization of their proliferation (T cells were incubated with 10μM CFSE in PBS 1%FBS for 6 minutes 37° C, dark). Cells were cultured together in 96-well plate in sterile complete RPMI-1640 medium (500ml RPMI-1640 Sigma Aldrich, 10% North America Fetal Bovine Serum, 2.5ml no essential aminoacids, 2.5ml Sodium Pyruvate, 5% Pen/Strep, 5% L-Glutamine, 200μl B-Mercaptoethanol) at 1:4 ratio (CD11b+:CD3+CD4+). Cells were kept in the incubator at 37^{o} degrees with 5% CO_2 for 96 hours. After 4 days CFSE med/low signal CD3+CD4+ T cells were isolated by sorting technique. Once CFSE med/low T cells were isolated, DNA was extracted according to manufacturer'sprotocol (QIAmp DNA Micro QIAGEN)and PCR performed in order to create libraries for the VDJ recombination region of T cell receptors according to manufacturer'sprotocol (ImmunoSEQ mmTCRB Adaptive Biotechnology). At the end, libraries were sequenced using ImmunoSEQ KIT and MISEQ software (Adaptive Biotechnology) for data analysis by which it is possible to extrapolated automatically the productive clonality calculated using only the productive rearrangements in the sample (productive rearrangements is the sum of unique productive rearrangements in the sample) and the TCRVbeta enrichment based on percent(template) where template refer to the number of biological molecules put into the assay before PCR amplification and sequencing. Using the internal bias control of the immunoSEQ assay, it is possible to calculate the orginal number of templates of sample material sequenced.

2.5.2 RNA single cell sequencing

2.5.2.1 Sample isolation and preparation

CD11b+ cells were isolated by sorting technique from smashed p21-/- and WT FVB spleens and concentrated at~5,000 cells *per* sample (700cell/ul).

2.5.2.2 Sequencing technique

WT and p21-/- CD11b+ cells were processed for library preparation using the 10x Chromium technology and sequenced on NovaSeq 6000 Sequencing System (Illumina) with an asymmetric paired-end strategy with a coverage of about 75,000 reads/cell.Demultiplexing, barcode processing and single-cell 3' gene counting separately for each sample were obtained using Cell Ranger v3.0.2. Gene-by-cell matrices (also called, in bioinformatic jargon,'feature-barcode matrices") were obtained using confidently mapped, non-PCR duplicates with valid barcodes and unique molecular identifiers.

2.5.2.3 RNA single cell sequencing data analysis

Before proceeding with the analyzes we performed these steps:

1. We removed from our samples the cells that had more than 10% of the transcripts coming from mitochondrial genes.

2. To further exclude those cells that were outliers in terms of library complexity and that might possibly include multiple cells or doublets, we calculated the distribution of genes detected *per* cell *per* each sample and removed any cells in the top 2% quantile.

3. To exclude low-quality cells, we also removed cells that had fewer than 500 detected genes.

At the end we then normalized the raw data by the total expression of each cell and multiplied by a scale factor of 10,000.To identify cellular states characteristics of the p21-/- APCs, we first tried to deconvolve the heterogeneity of the WT and p21-/- CD11b+ subsets using a computational approach based on the assignment of cellular identity for single-cell transcriptomes through their comparison to reference-datasets of purified cell types.To this end, we compared our sc-RNAseq datasets with the Immunological Genome Project (ImmGen) database[143], using the SingleR (single cell recognition)computational tool [144].

Seurat R packagewas used for the Quality filtering, identification of highly variable genes, dimensionality reduction, standard unsupervised clustering algorithms and cluster markers identification.

2.6 Cell sorting and Flow Cytometry analysis

AllthecellsusedforFACSanalysiswerefirstincubatedinblockingsolution (PBS1X, 1% BSA)for30minutes at 4^{o}C, after which specific fluorochrome-conjugated antibodies were added to the staining solution in concentration 1:200, if not indicated diversely by the manufacturer. Cells were stained for 1h at 4^{o}C in dark and consecutively analyzed via FACS (FACSDiva Version 6.1.1software).

For *in vivo* experiments, MHCII+ or CD11b+ cell populations were isolated from ErbB2 tumor cellsvia FACS Sorting Strategy: anti-MHCII (Pe-Cy7-conjugated, eBioscience, Cat. No 25-5321-82), anti-CD11b (FITC-conjugated,eBioscience, Cat. No 11-0112-85) were used; or via MACS® Microbeads technology for column-based magnetic cell isolation using nano-sized beads coated with anti-mouse MHCII or CD11b antibodies (Mylteni Biotec).

For *in vivo* experiments, CD11b+ cell population was added to ErbB2 tumor cells -starting from spleen cells- usingFACS Sorting Strategy: anti-CD11b (FITC-conjugated,eBioscience, Cat. No 11-0112-85) were used.

For *in vitro* experiments, CD3+CD4+ T, CD3+CD8+ T cells and CD11b+ or CD11c+ cells and the 3subpopulations (b+c+, b+c-, b-c+) were isolated from smashed spleens via FACS sorting strategy: anti-CD11b (FITC- conjugated,eBioscience, Cat. No 11-0112-85), anti-CD4 (PE-conjugated, eBiosciences, Cat. No 12-004-82), anti-CD3 (PE-cy7-conjugated, BioLegend, Cat. No 100219), anti-CD8 (APC-conjugated, BioLegend, Cat. No 100712), anti-CD11c (percp-5.5-conjugated, Biolegend Cat. No.117325) were used.

For the identification, analysis of proliferation and effector function of T cells in the T cells proliferation and phenotype assay, following antibodies were used: anti-CD4 (PE-conjugated,

eBiosciences, Cat. No 12-004-82), anti-CD3 (PE-cy7-conjugated, BioLegend, Cat. No 100219), anti-CD8 (APC-conjugated, BioLegend, Cat. No 100712), anti-CD44 (APC-cy7- conjugated, BioLegend Cat. No 103027), anti-CD62L (Percp5.5-conjugated, BioLegend,Cat.No104431).

FACS analysis were performed using FlowJo software.

For *in vitro / in vivo* experiments, CD3+CD4+ T and CD11b+ cells were isolated from smashed spleens via FACS sorting strategy: anti-CD11b (FITC- conjugated,eBioscience, Cat. No 11-0112-85), anti-CD4 (PE-conjugated, eBiosciences, Cat. No 12-004-82), anti-CD3 (PE-cy7-conjugated, BioLegend, Cat. No 100219), were used.

For sequencing experiments, CD3+CD4+ T cells and CD11b+cell populations were isolated from smashed spleens via FACS sorting strategy: anti-CD11b (FITC-conjugated,eBioscience, Cat. No 11-0112-85) and anti-CD4 (PE-conjugated, eBiosciences, Cat. No 12-004-82) were used.

For FACS characterization of CD11b+ cell types, anti-CD11b (FITC-conjugated,eBioscience, Cat. No 11-0112-85), anti-CD11c(Percp-5.5-conjugated, BioLegend Cat. No 117325), anti-CD8 (PE-conjugated, BioLegend, Cat. No 100712), anti-MHCII (BV650-conjugated, BD Biosciences Cat. No. 563415), anti-Ly-6C (Percp5.5-conjugated, BioLegend,Cat.No128011), anti-Ly6G (APC-conjugated BioLegend Cat. No 127613) were used.

3. Aims of the project

My project stems from two key findings: i)primary p21-/- MMTV-ErbB2 breast tumors do not transplant in recipients with a functional immune system, but re-acquire the ability to grow in sub-lethally irradiated or immunedeficient mice; and ii) the same MMTV-ErbB2 breast cancers obtained in WT mice are not transplantable in non-irradiated p21-/- syngeneic recipients. Based on these observations, we hypothesizedthat a cellular component of the p21-/- microenvironment was responsible for the activation of a potent cell-extrinsic anti-tumor response. My goal was to test this hypothesis. In particular, I aimed at i) identifying the specific cell subpopulation responsible for the observed anti-tumor response; and ii) characterizing the molecular mechanism of the potent anti-cancer effect.

4. Results

4.1 Lack of p21 expression in immune-competent cells activates a potent anti-tumor response *in vivo*

4.1.1 p21-/- ErbB2 tumors do not grow in syngeneic mice but reacquire transplantability in irradiated or immunodeficient mice

Several years ago, my host-lab reported that myeloid leukemias do not develop in mice with genetic ablation of the p21 locus (p21-/- mice), as in the case of AMLs expressing the AML1-ETO fusion protein, or, if they develop, do not grow upon transplantation into syngeneic mice, as in the case of AML expressing the PML-RAR fusion protein[127]. To investigate if p21-/- mice were resistant to other tumor types, we analyzed mammary tumor development in the absence of p21, using transgenic mice overexpressing a mutated form of the breast cancer-associated ErbB2 oncogene under the control of the MMTV promoter (ErbB2 transgenic mice) [128]. ErbB2 mice were crossed with syngeneic p21-/- mice to generate ErbB2-p21-/- compound mice. ErbB2 and ErbB2-p21-/- mice developed mammary tumors with similar latencies (~3 months) **(Fig.7)**and penetrance (~100%). Cell suspensions from WT or p21-/- ErbB2 mammary tumors were then transplanted into the mammary fat pad of WT syngeneic mice, according to established procedures (see Methods 2.2.1). WT ErbB2 tumors grew in recipient mice leading to mouse death in 100% animals within 3 months. Strikingly, primary p21-/- ErbB2 tumors did not transplant, with all mice still alive after more than 1 year of observation ($p<0.0001$) (**Fig.8**). We obtained same results using transgenic mice expressing the Wnt[129] oncogene, which also develop breast cancers (**Fig.9**)

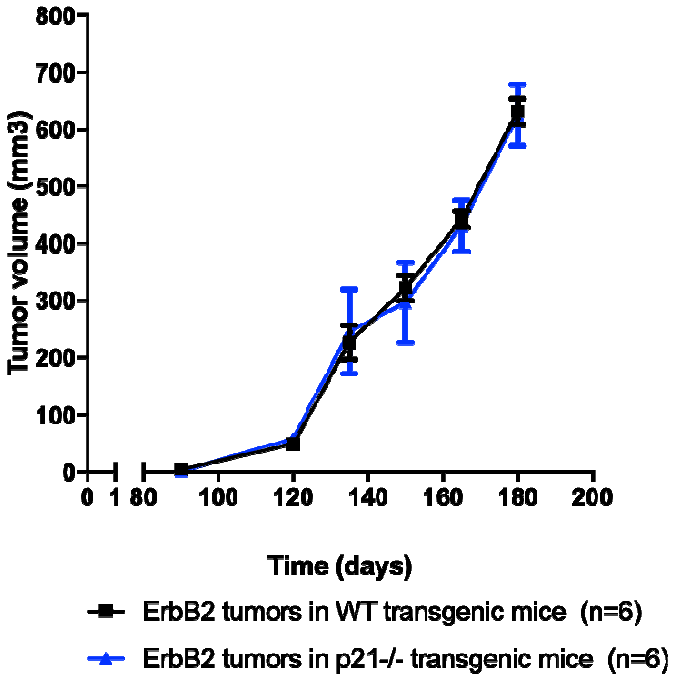

Fig.7 Tumor growth curve of ErbB2 tumors in WT and p21-/- transgenic mice.
Transgenic mice overexpressing a mutated form of the breast cancer-associated ErbB2 oncogene under the control of the MMTV promoter (ErbB2 transgenic mice). ErbB2 mice were crossed with syngeneic p21-/- mice to generate ErbB-p21-/- compound mice. ErbB2 and ErbB2-p21-/- mice developed mammary tumors with similar latencies (~3 months) and penetrance.

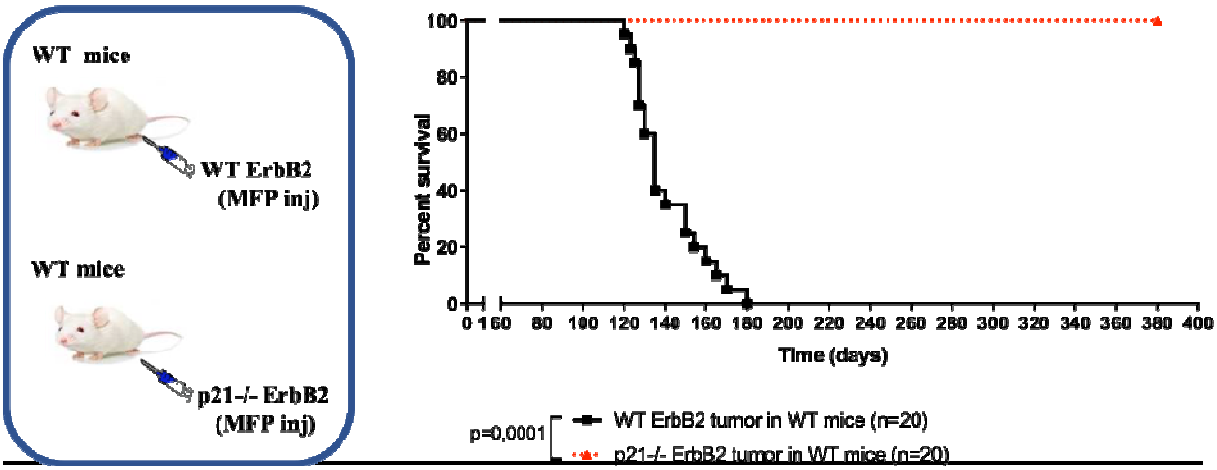

Fig.8 Survival curvesof syngeneic WT mice after transplantation of WT and p21-/- ErbB2 tumors.Cell suspensions from WT or p21-/- ErbB2 tumor cells (300,000/mouse) were transplanted into the mammary fat pad and mice were sacrificed when tumors reached an overall diameter of 1cm. The survival curves shown above are derived from three independent experiments that were analyzed together using the log-rank (Mantel-Cox) statistical test.

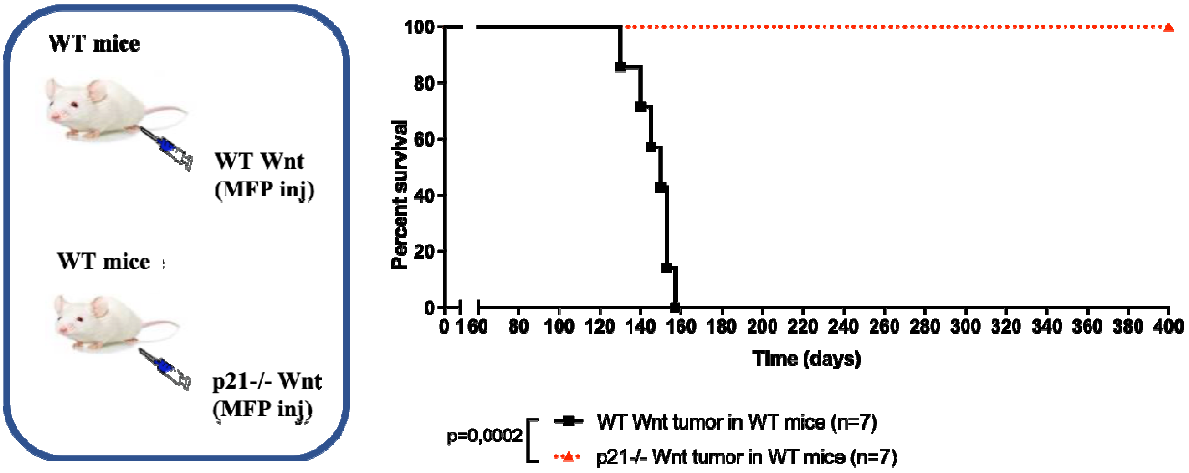

Fig.9 Survival curves syngeneic WT mice after transplantation of WT and p21-/- Wnt tumors.Cell suspensions from WT or p21-/- Wnt tumor cells (300,000/mouse) were transplanted into the mammary fat pad and mice were sacrificed when tumors reached an overall diameter of 1cm. The survival curves shown above are derived from two independent experiments that were analyzed together using the log-rank (Mantel-Cox) statistical test.

Surprisingly, when transplanted into sublethally γ-irradiated or immunodeficient(NOD-scid) mice, the p21-/- ErbB2 tumors "re-acquired" the capacity to grow, leading to death of all recipients within ~5months (p=0.0001) (**Fig.10**). These data demonstrate that p21-/- ErbB2 mammary tumors are unable to propagate into intact syngeneic mice and suggest that the absence of p21 in the tumor tissue activate a potent cell-extrinsic tumor-suppressor response in the immune-competent host.

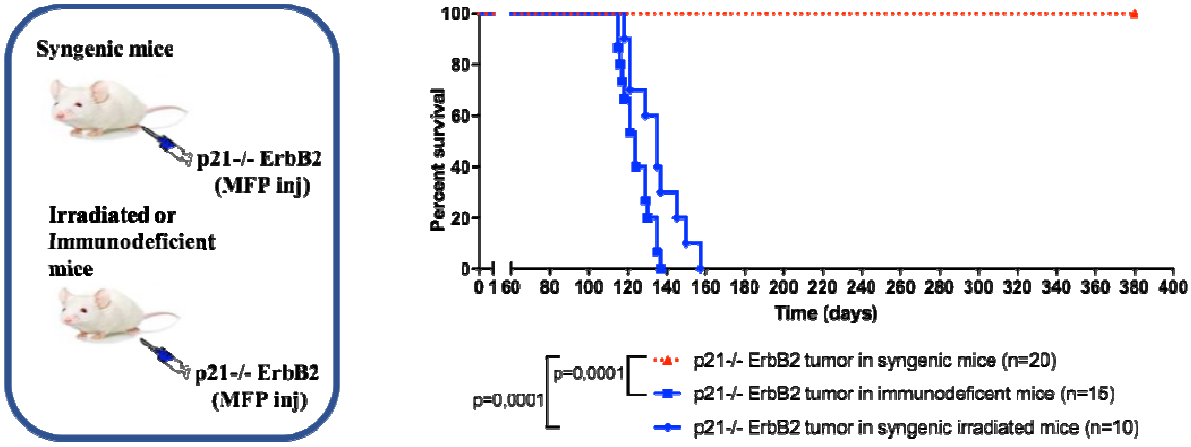

Fig.10 Survival curves of WT syngeneic, immunodeficient or irradiated mice after transplantation of p21-/- ErbB2 tumors.Cell suspensions from p21-/- ErbB2 tumor cells (300,000/mouse) were transplanted into the mammary fat pad of WT syngeneic, immunodeficient or irradiated mice. As immunodeficient mice we used NOD-scid mice or mice irradiated with 5.5 Gray. Mice were sacrificed when tumors reached an overall diameter of 1cm. The survival curves shown above are derived from three independent experiments that were analyzed together using the log-rank (Mantel-Cox) statistical test.

4.1.2 WT ErbB2 tumors do not grow in p21-/- mice

The ErbB2-tumor cells (WT or p21-/-) used for the transplantation experiments described above were derived from primary mammary tumors, and consist of tumor epithelial-cells and cells of the tumor microenvironment (TME). TME consists of a variety of resident and infiltrating host cells including immune cells, blood vessels, fibroblasts, signaling molecules and the extracellular matrix (ECM)[112]. Thus, we investigated whether activation of a tumor suppressor response to the p21-/- ErbB2 tumor tissue in the immune-competent host is mediated by the p21-/- epithelial tumor cells or the p21-/- TME cells. To this end, we transplanted WT ErbB2 tumors into syngeneic p21-/- hosts. Strikingly, WT ErbB2 tumors did not engraft in p21-/- recipients (p=0.0001) (**Fig.11**), thus suggesting that the p21-/- TME is indeed responsible for the anti-tumor immune response elicited by p21-/- ErbB2 tumors.

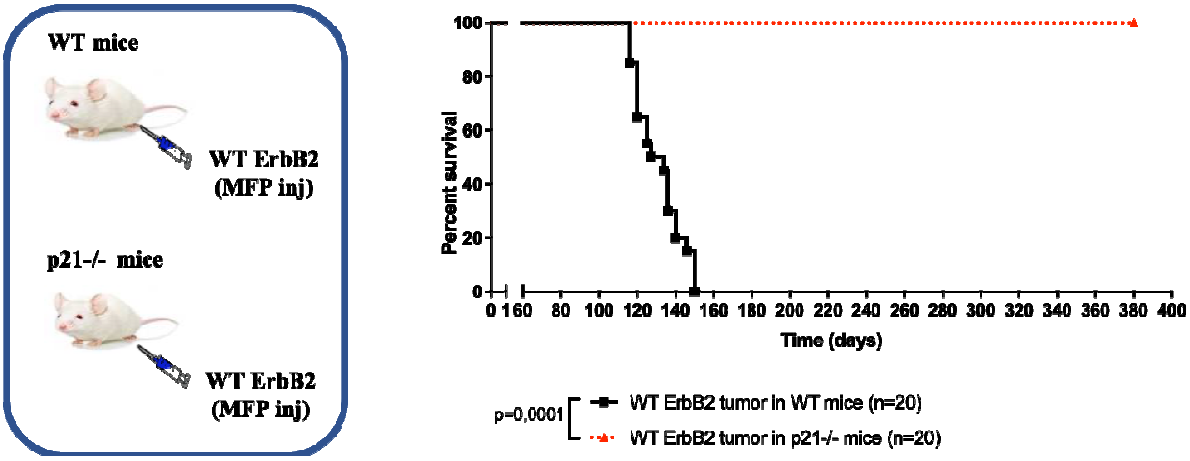

Fig.11 Survival curves of WT or p21-/- syngeneic mice after transplantation of WT ErbB2 tumors.WT ErbB2 tumor cells (300,000/mouse) were transplanted into the mammary fat pad of WT or p21-/- syngeneic hosts and mice were sacrificed when tumors reached an overall diameter of 1cm. The survival curves shown above are derived from four independent experiments that were analyzed together using the log-rank (Mantel-Cox) statistical test.

4.1.3 p21-/- spleen cells prevent growth of WT ErbB2-tumors in WT recipients

The spleen is the second most important lymphoid organ and plays a major role in the regulation of immunity[130]. It is involved in the production and storage of T and B lymphocytes, dendritic cells (DCs) and macrophages [130]. To provide direct evidence that the p21-/- immune system is responsible for the observed anti-tumor response, we tested the ability of WT or p21-/- spleen cells to halt growth of WT ErbB2 tumors. To this end, we co-transplanted cell suspensions from p21-/- spleens along with WT ErbB2 tumors into WT recipients, and monitored tumor growth. While WT spleen cells showed marginal effects, co-transplantation of p21-/- spleen cells markedly delayed tumor growth (p=0.0001) (**Fig.12**). These findings demonstrate that the anti-tumor immune response activated by the p21-/- TME can be recapitulated by p21-/- spleen cells.

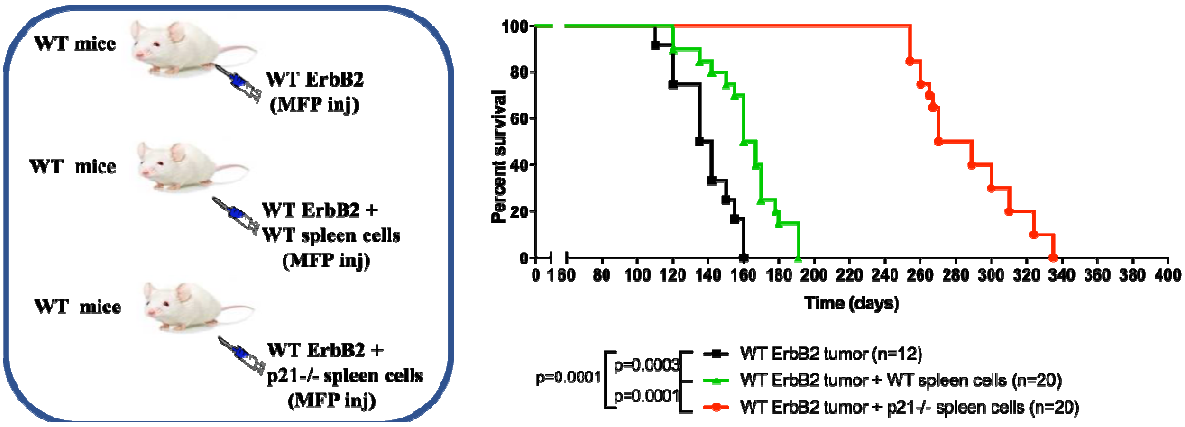

Fig.12 Survival curves of syngeneic mice after transplantation of WT ErbB2 tumorsin the presence of WT or p21-/- spleen cells.
WT ErbB2 tumor (300,000 cells/mouse) were mixed with cell suspensions from WT or p21-/- spleens (ratio 1:4) and co-transplanted into the mammary fat pad of WT syngeneic mice. WT ErbB2 tumor cells alone were used as positive control. Mice were sacrificed when tumors reached an overall diameter of 1cm. The survival curves shown above are derived from three independent experiments that were analyzed together using the log-rank (Mantel-Cox) statistical test.

4.2 p21-/- APCs induce an anti-tumor response *in vivo*

4.2.1 Depletion of MHCII+ cells or CD11b+ cells from p21-/- ErbB2 tumors restore their transplantability in syngeneic mice.

The spleen is the major reservoir of immunocompetent T and B lymphocytes and Antigen Presenting Cells (APCs) (dendritic cells, macrophages and B cells)[130]. To identify the p21-/- cellular component responsible for the anti-tumor response, we first focused on APCs. This choice was based on parallel experiments performed in my host-lab that demonstrated that T-cell depletion from p21-/- leukemias or transplantation of p21-/- leukemias in B-cell deficient JHT mice[131] did not revert their growth potential (data not shown), thus ruling out the involvement of T and B cells. MHC Class II (MHCII) are a class of major histocompatibility complex (MHC) molecules found mainly on APCs, including dendritic cells and macrophages[132]. CD11b is an integrin family member that is expressed on the surface of different immune-competent cells, including subpopulations of dendritic cells and monocyte/macrophages[133]. Therefore, we investigated whether depletion of cells expressing MHCII or CD11b molecules (MHCII+ or CD11b+ cells) from p21-/- ErbB2 tumors abrogates their ability to activate a tumor response upon injection into WT syngeneic mice.MHCII+ - depleted tumor-cell suspensions from WT or p21-/- ErbB2 primary tumors were then injected into the mammary fat pad of syngeneic WT mice and monitored for tumor growth. While depletion of MHCII+ cells from WT ErbB2 tumors had no effects on their ability to grow *in vivo*, depletion of MHCII+ cells partially rescued the growth potential of p21-/- ErbB2 breast cancers (5 out of 9, p=0.02) (**Fig.13).** Depletion of MHCII+ cells was performed using either MACS® MicroBead Technology for column-based magnetic cell isolation using nano-sized beads coated with anti-mouse MHCII antibodies (Mylteni Biotec) (2 of 3 experiments)(**Fig.14A**), or by FACS-sorting using anti-MHC antibodies (1 of 3 experiments). Efficiency of depletion of MHCII+ cells was ~50% when using microbeads or columns, while was >80% by sorting (**Fig.14B**). **Figure 13** represents the union of these three experiments.

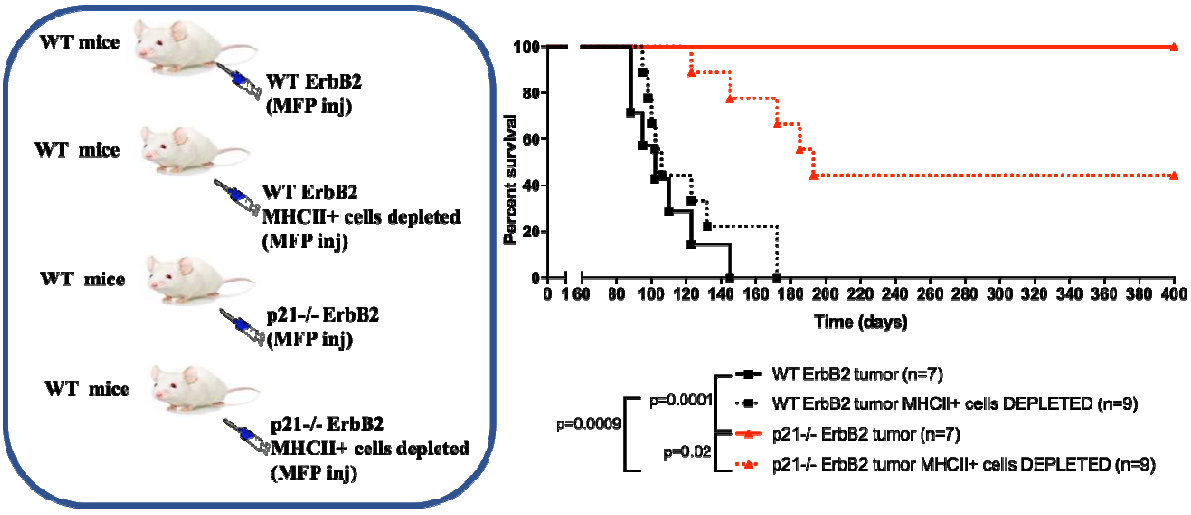

Fig.13 Survival curves of WT syngeneic mice after transplantation of WT or p21-/- ErbB2 tumors depleted of MHCII+ cells.

WT or p21-/- ErbB2 tumor cells (300,000/mouse) were subjected to MHC depletion and transplanted into the mammary fat pad of WT syngeneic mice. Mice were sacrificed when tumors reached an overall diameter of 1cm. In two out of the three experiments depletion of MHCII+ cells was performed using anti-MHCII MACS® MicroBead Technology for column-based magnetic cell isolation using nano-sized beads coated with anti-mouse MHCII antibody (Mylteni Biotec), obtaining a depletion of ~50%; in the third experiment depletion of MHCII+ cells was performed by FACS-sorting, with a depletion efficiency of >80%. The three experiments were analyzed together using the log-rank (Mantel-Cox) statistical test. The three mice with the longest survival in the Kaplan-Meier curve are from the cohort of mice injected with ErbB2 tumors after depletion of MHCII+ cells using FACS-sorting (see figure 14B).

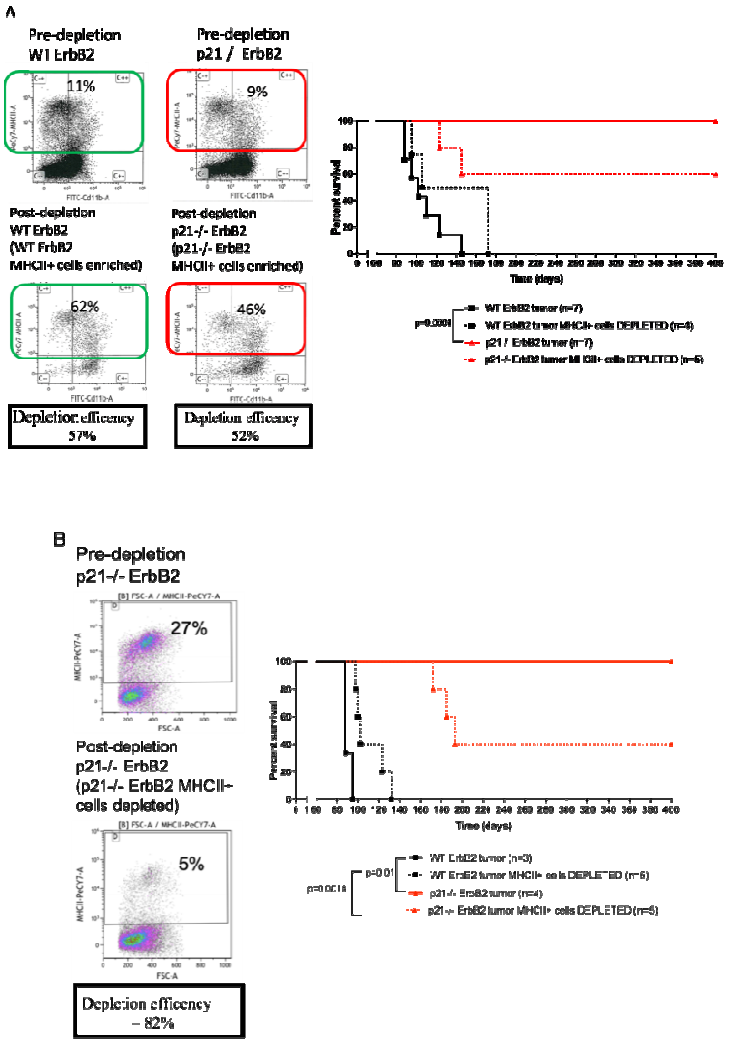

Fig.14 Survival curves of WT syngeneic mice after transplantation of WT or p21-/- ErbB2 tumors depleted of MHCII+ cells.WT or p21-/- ErbB2 tumor cells (300,000/mouse) were subjected to MHC depletion and transplanted into the mammary fat pad of WT syngeneic mice. Mice were sacrificed when tumors reached an overall diameter of 1cm. A. Kaplan-meier curves represents the two experiments where depletion of MHCII+ cells was performed using MACS® MicroBead Technology for column-based magnetic cell isolation using nano-sized beads coated with anti-mouse MHCII antibody (Mylteni Biotec); on the left the upper figures represent the pre-depletion percentage of MHCII+ in the WT and p21-/- ErbB2 cells while the lower squares represent the percentage of MHCII+ cells in the ErbB2 samples enriched of MHCII+ cells (samples not used for the injection), obtaining a depletion efficiency of ~50%; B. Kaplan-meier curves represent the experiment in which depletion of MHCII+ cells was performed by FACS-sorting; on the left the upper figure represents the pre-depletion percentage of MHCII+ in the p21-/- ErbB2 cells while the lower square represents the percentage of MHCII+ cells in the ErbB2 sample depleted of MHCII+ cells with a depletion efficiency of >80%.In order to calculate the depletion efficiency, B. I considered the pre-depletion percentage of MHCII+ cells = 100% (27%=100%); then I made a proportion in order to obtain the % of MHCII+ cells in post-depletion sample considering pre-depletion MHCII+cells=100% ((5/27)X100=18%); afterwhich I calculated the difference: 100%-18%=82%= Depletion efficency. A.Considering that (in case of WT ErbB2 sample) the theoretical % of MHCII+ cells in post-depletion sample should be =100%, I calculated the difference between the theoretical 100% post-depletion % and pre-depletion % (100%-11%=89%); then, considering that the difference between 11% (pre-depletion MHCII+) and 62% (post-depletion MHCII+) is 51%, this means that we had an efficiency of 57% (considering 89%=100%).A. and B. experiment were analyzed separately using the log-rank (Mantel-Cox) statistical test.

As for the MHCII+ cells, CD11b+ cells were depleted using either MACS® MicroBead Technology for column-based magnetic cell isolation using nano-sized beads coated with anti-mouse CD11b antibody (Mylteni Biotec) (2 experiments) (**Fig.15A),** and FACS-sorting (1 experiment), using anti-mouse CD11b antibody (**Fig.15B**). Efficiency of depletion was >50% when using microbead technology, and =100% by sorting tecnique. After depletion of CD11b+ cells, tumor cell suspensions were injected into the mammary fat pad of WT mice, which were then monitored for tumor growth. Notably, depletion of CD11b+ cells rescued completely the growth potential of p21-/- ErbB2-tumors in all of the transplanted mice (9 out of 9 mice succumbed within 5-6 months from the injection of CD11b+ - depleted p21-/- ErbB2-tumors), while it had no effects on the growth of WT ErbB2 tumors (**Figure 16**). Taken together, these data demonstrate a key role of p21-/- cells expressing MHCII and/or CD11b molecules in mediating an anti-tumor response *in vivo*, and strongly suggest the involvement of cells with APC function.

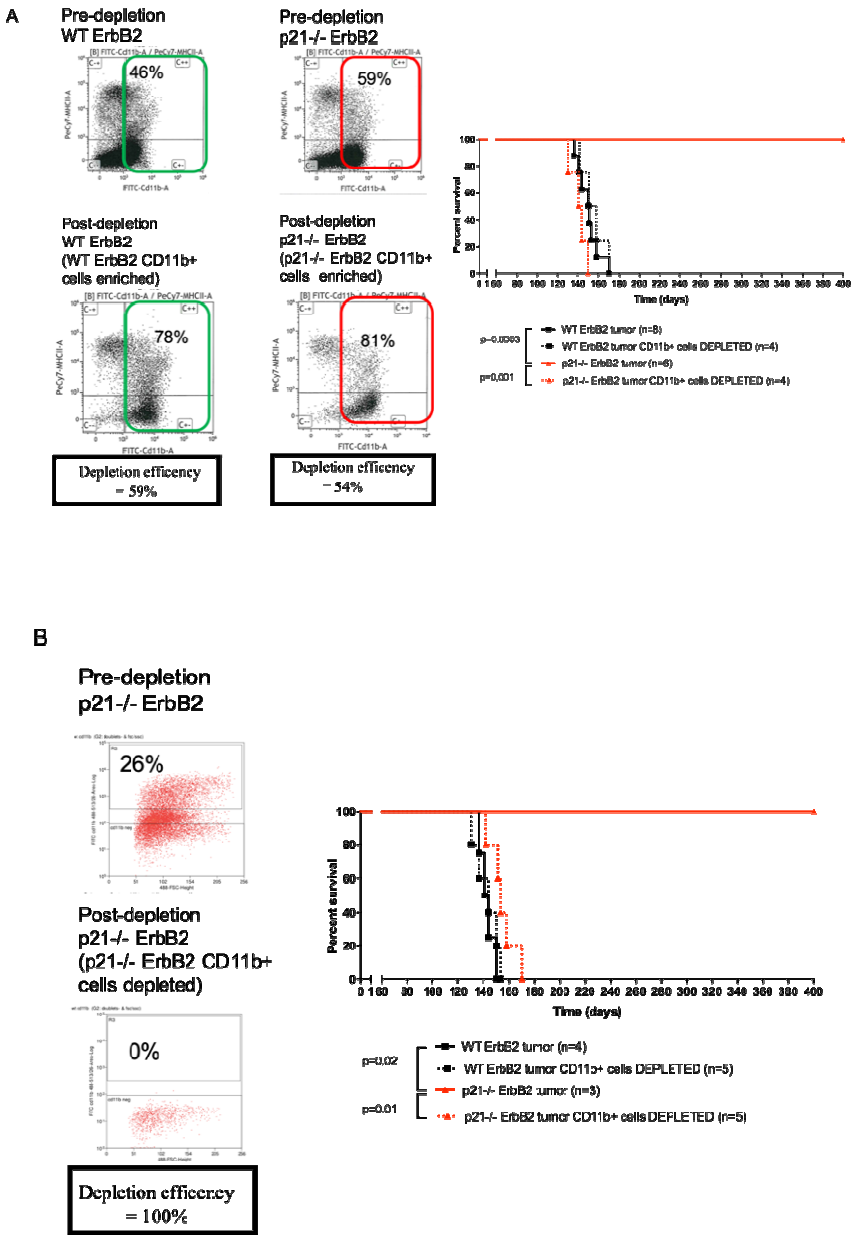

Fig.15 Survival curves of WT syngeneic mice after transplantation of WT or p21-/- ErbB2 tumors depleted of CD11b+ cells.

WT or p21-/- ErbB2 tumor cells (300,000/mouse) were subjected to CD11b depletion and transplanted into the mammary fat pad of WT syngeneic mice. Mice were sacrificed when tumors reached an overall diameter of 1cm. A. Kaplan-meier curves represent the two experiments where depletion of CD11b+ cells was performed using MACS® MicroBead Technology for column-based magnetic cell isolation using nano-sized beads coated with anti-mouse CD11b antibody (Mylteni Biotec);on the left the upper figures represent the pre-depletion percentage of CD11b+ in the WT and p21-/- ErbB2 cells while the lower squares represent the percentage of CD11b+ cells in the ErbB2 samples enriched of CD11b+ cells (samples not used for the injection) obtaining a depletion efficiency of >50%; B. Kaplan-meier curves represent the experiment in which depletion of CD11b+ cells was performed by FACS-sorting; on the left the upper figure represents the pre-depletion percentage of CD11b+ in the p21-/- ErbB2 cells while the lower square represents the percentage of CD11b+ cells in the ErbB2 sample depleted of CD11b+ cells with a depletion efficiency of =100%. A. and B. experiments were analyzed separately using the log-rank (Mantel-Cox) statistical test.

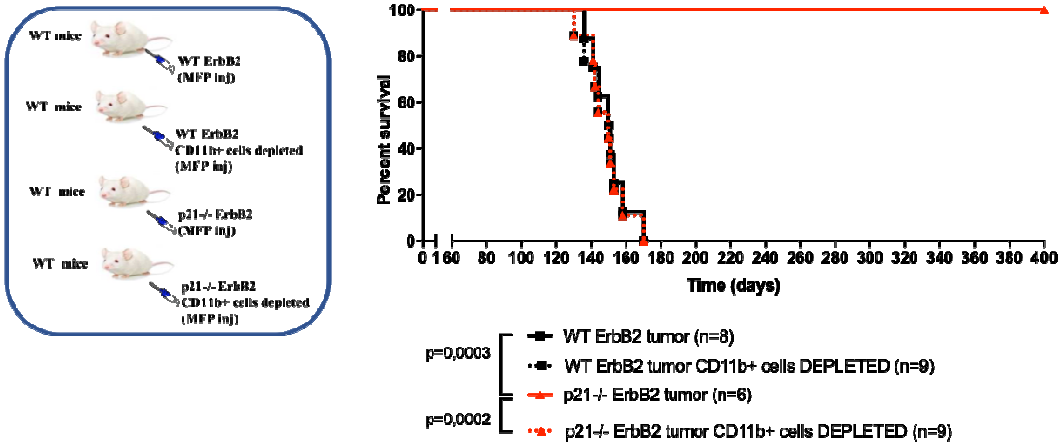

Fig.16 Survival curves of WT syngeneic mice after transplantation of WT or p21-/- ErbB2 tumors depleted of CD11b+ cells.
WT or p21-/- ErbB2 tumor cells (300,000 cells/mouse) were subjected to CD11b+ -cell depletion and transplanted into the mammary fat pad of WT mice. Mice were sacrificed when tumors reached an overall diameter of 1cm. In two out of three experiments ErbB2 tumors were depleted of CD11b+ by MACS® MicroBead Technology for column-based magnetic cell isolation using nano-sized beads coated with anti-mouse CD11b antibody (Mylteni Biotec) , with a depletion efficiency >50%; in one experiment ErbB2 tumors were instead depleted of CD11b+ cells by FACS-sorting with a depletion efficiency of =100%. The three experiments were analyzed together using the log-rank (Mantel-Cox) statistical test.

4.2.2 Addition of p21-/- CD11b+ cells significantly delays tumordevelopment of WT ErbB2-tumors in WT syngeneic mice

We next investigated whether p21-/- CD11b+ cells are sufficient to mediate the anti-tumor response activated by the p21-/- splenocytes. To this end, we co-transplanted WT or p21-/- CD11b+ cells and WT ErbB2-tumors in syngeneic WT mice, and then monitored tumor growth. CD11b+ cells were purified by FACS-sorting from suspensions of spleen cells with purity of >90% **(Fig.17).** As **Figure 18** shows, co-injection of WT CD11b+ cells had no effect on the growth of ErbB2 tumors, while p21-/- CD11b+ cells significantly delayed tumor growth, thus demonstrating that p21-/- CD11b+ cells are sufficient to induce a potent anti-tumor response *in vivo*.

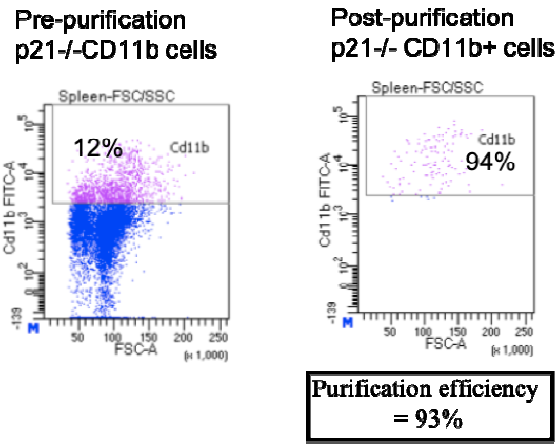

Fig.17 Purification efficiency of CD11b+ cell population isolated from p21-/- spleen by FACS-sorting.p21-/- Spleen cells were stained with anti-CD11b antibody and by FACS-sorting technique CD11b+ cell population was purified. The figures represent the percentage of CD11b+ cells in the p21-/- spleen cells and the percentage of CD11b+ cells in the sample after CD11b+ isolation/purification with a purification efficiency of =93%

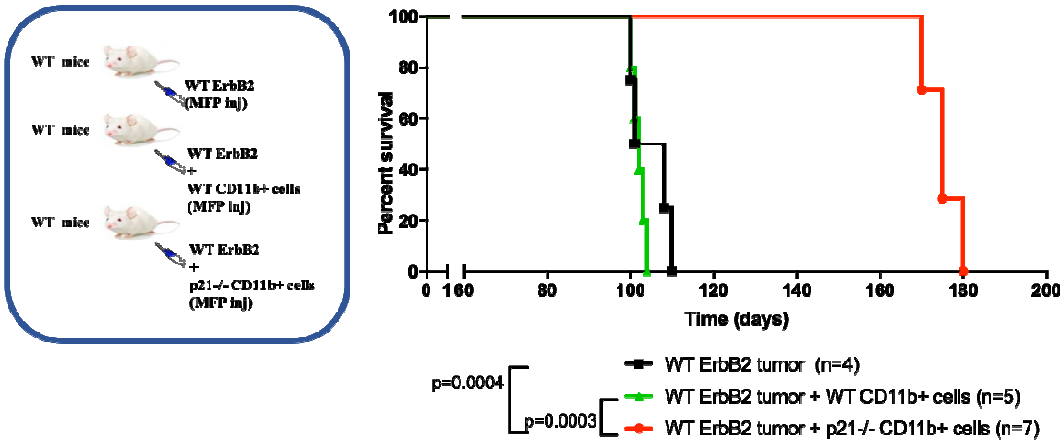

Fig.18 Survival curves of WT sygeneic mice after transplantation of WT ErbB2-tumors along with WT or p21-/- CD11b+ cells.
WT ErbB2 tumor cells and purified CD11b+ cells were co-transplanted into the mammary fat pad of WT syngeneic mice, and mice sacrificed when tumors reached an overall diameter of 1cm. Statistical analysis was performed using log-rank (Mantel-Cox test). CD11b+ cells were obtained from spleen by sorting technique.

4.3. p21-/- CD11b+ cells induce proliferationand differentiation of CD4+T cells towards an effector-memory phenotype

4.3.1 p21-/- CD11b+ cells induce antigen-independent and MHC-II - dependent proliferation of CD4+ T cells *in vitro*

We next tried to reconstitute *in vitro* the anti-tumor immune response mediated by p21-/- CD11b+ cells, by analyses of their capacity to induce proliferation of naïve, WT CD4+ or CD8+ T-lymphocytes. T-cell proliferation was monitored by staining with carboxyfluorescein succinimidyl ester (CFSE), a label which penetrates the cell membrane and allows monitoring of cell proliferation and estimation of times of cell division (CFSE dilution assay)[134]. CD4+ or CD8+ lymphocytes were purified from the WT mice using FACS-sorting from suspensions of spleen cells. CD11b+ cells were purified from WT or p21-/- spleens, as described above. WT CD4+ or CD8+ T-lymphocytes were co-cultured in complete RPMI-1640 medium for 4 days (500ml RPMI-1640 Sigma Aldrich, 10% North America Fetal Bovine Serum, 2.5ml no essential amino acids, 2.5ml Sodium Pyruvate, 5% Penicillin/Streptavidin 5% L-Glutamine, 200µl B-Mercapto ethanol). As expected[135], WT CD11b+ cells induced modest proliferation of CD4+ or CD8+ T-lymphocytes (8%+/-3.4 and 4%+/-2.12, respectively) (**Fig.19).** Strikingly, p21-/- CD11b+ cells induced instead massive proliferation of CD4+ T cells (49%+/-2.12; p=0.005) and, to a significantly lesser extent, of CD8+ T cells (20%+/-4.24; p=0.04) (**Fig.19 p=0.01).** We next characterized the type of proliferation of T-lymphocytes induced by p21-/- CD11b+ cells, focusing on CD4+ cells. MHC-II molecules on APCs form a complex with the expressed antigenic peptide and engage the TCR on antigen-specific CD4 T cells, a process that results in the proliferation and activation of specific CD4+ T-lymphocytes[47,48]. To test the role of MHC-II – antigen expression, we exposed the co-cultures of CD11b+ and CD4+ cells to ErbB2-tumor cells or ErbB2 tumor cell-lysates (as source of tumor-specific antigens), or antibodies against mouse MHC Class II haplotypes that are known to inhibit the T-cell response[136].The proliferation of CD4+ lymphocytes induced by p21-/- CD11b+ cells was tumor-cell (not shown) and tumor-lysate independent **(Fig.20).** Strikingly, addition of the anti-MHC-II antibody reduced

proliferation of CD4+ lymphocytes of about 95% (**Fig.20**, p=0.0021). Thus, p21-/- CD11b+ cells induce massive proliferation of CD4+ T-lymphocytes, which is independent of the presence of tumor cells or lysates, yet markedly dependent on the expression of MHC-II molecules.

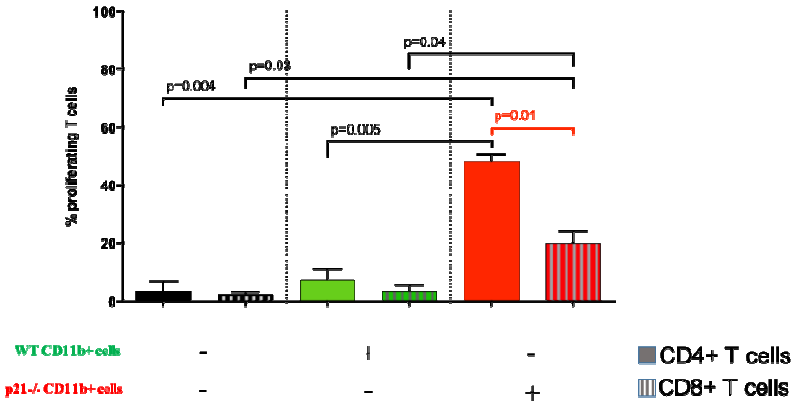

Fig.19 *In vitro* proliferation of CD4+ or CD8+ T-lymphocytes primed with WT or p21-/- CD11b+ cells. CFSE-labelled naïve CD4+ or CD8+ lymphocytes from WT mice were co-incubated with WT or p21-/- CD11b+ cells (purified from spleen cell-suspensions) at 4:1 ratio. After 4 days of coculture, T-cell CFSE-signal was determined by FACS analyses. Histogram plots show the percentages of proliferating CD4+ or CD8+ T-lymphocytes as mean +/- s.d. of 2 independent experiments (the two experiments were analyzed together using the unpaired *t* test).

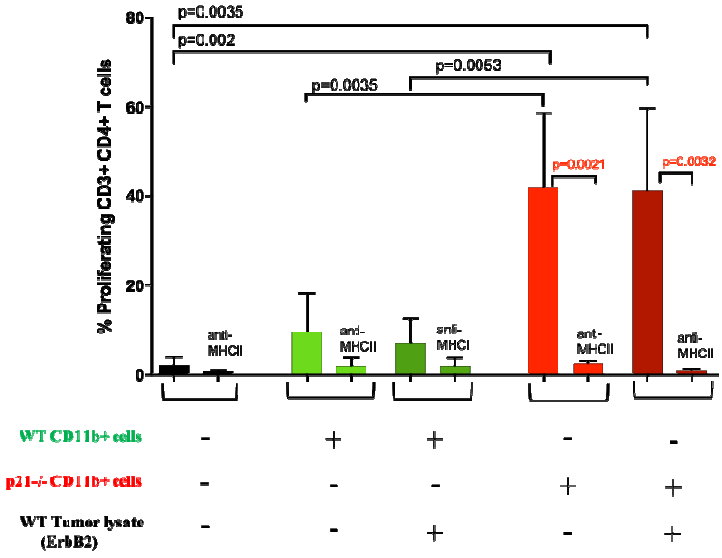

Fig.20 Effects of antigen-loading and MHC-II expression on the *in vitro* proliferation of CD4+ T-lymphocytes after priming with WT or p21-/- CD11b+ cells. CFSE-labelled naïve CD4+ lymphocytes from WT mice were co-incubated with WT or p21-/- CD11b+ cells (purified from spleen cell-suspensions) at 4:1 ratio in the presence, or not, of tumor lysates from ErbB2 tumors, or inhibitory anti-MHC-II antibodies, as indicated. After 4 days of co-culture, T-cell CFSE-signal was determined by FACS analyses. Histogram plots show the percentages of proliferating CD4+ T-lymphocytes as mean +/- s.d. of 6 independent experiments (addition of anti-MHCII were repeated twice). All experiments were analyzed together using the unpaired *t* test.

4.3.2 p21-/- CD11b+ cells induce differentiation of CD4+T cells towards an effector/memory function.

We then analyzed the effects of CD11b+ cells on the phenotype of CD4+ T-lymphocytes. Naïve, effector or memory are the three main phenotypic states of T lymphocytes[137]. Naïve T-lymphocytes are considered immature since, unlike activated effector or memory T cells, they have not yet encountered their cognate antigen [137]. Indeed, antigen-naïve T cells can expand and differentiate into memory and effector T cells after encountering their related antigen loaded on MHC molecules on the surface of professional APCs. Appropriate co-stimulation must be present at the time of antigen encounter for this process to occur[63]; for example CD80, often in tandem with CD86, plays a large and diverse role in activation and regulation of T cells. Activation occurs through stimulatory interaction with CD28 on the surface of all naive T cells, which can enhance cytokine production, and cell proliferation and differentiation.These costimulatory signals are necessary to prevent anergy and also essential for T lymphocytes to receive the full activation signal, which in turn leads to T cell differentiation and division[63]and consequently influence the abiliy of APCs to induce T cell proliferation and differentiation.Naïve, effector and memory T-lymphocytes can be recognized by staining with antibody against specific surface molecules, including CD44- and CD62L+ for naïve T-lymphocytes, CD44+ and CD62L- for effector T-lymphocytes and CD44+ and CD62L+ for memory T-lymphocytes[138].

Purified CD4+ T-lymphocytes were co-cultured with WT or p21-/- CD11b+ cells, as described above, and analyzed for surface marker expression after 4 days. Notably, CD4+ T-lymphocytes primed with WT CD11b+ cells maintained their naïve phenotype (**Figure 21**). Priming with p21-/- CD11b+ cells, instead, increased the percentage of both effector (from 11% to 31%; p=0.005) and memory (from 4 to 9%; p=0.04) CD4+ T-lymphocytes. Most notably, the acquisition of the effector and memory phenotypes was MHCII-dependent, as shown by dramatic inhibitory effect exerted by the addition of antibodies against MHC-II molecules **(Fig.21).**

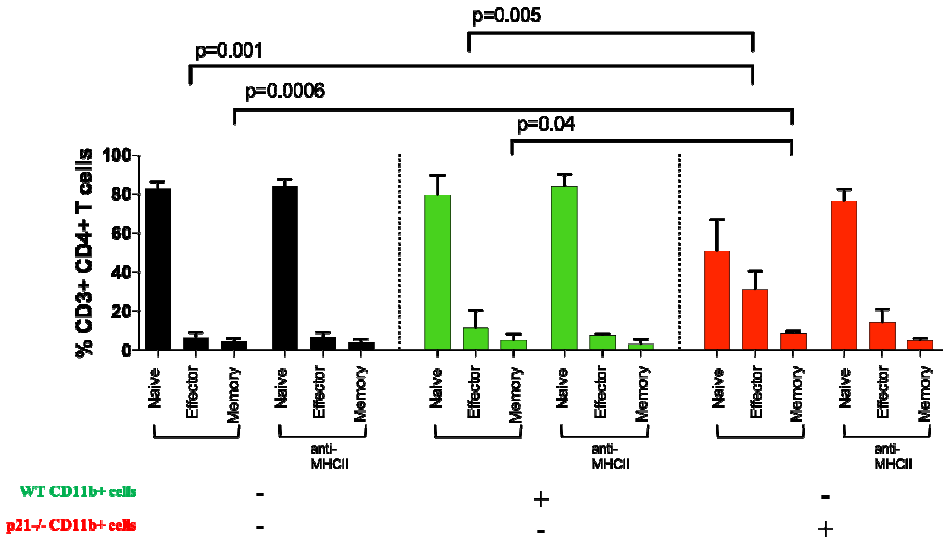

Fig.21 Effects of WT or p21-/- CD11b+ cells on the phenotype of CD4+ T cells upon *in vitro* priming with WT or p21-/- CD11b+ cells.
CSFE-stained naïve CD4+ T-lymphocytes from WT mice were co-incubated with WT or p21-/- CD11b+ cells (purified from spleen cell-suspensions) at 4:1 ratio in the presence, or not, of anti-MHC-II antibodies. After 4 days of coculture, T-cells were analyzed by FACS analyses and expression of CD44 and CD62L (NAÏVE: CD44- CD62L+, EFFECTOR: CD44+ CD62L-, MEMORY: CD44+ CD62L+) using specific antibodies. Results of CSFE dilution confirmed the strong and MHC-II – dependent proliferation of CD4+ T-lymphocyte induced by p21-/- CD11b and are not reported here. Histogram plots show the percentages of Naïve, Effector and Memory CD4+ T-lymphocytes as mean +/- s.d.of 6 independent experiments (anti-MHCII addition in all conditions was repeated three times). All experiments were analyzed together using the unpaired *t* test.

4.4. CD4+T cells primed by p21-/- CD11b+ cells display a polyclonal TCR repertoire and no enrichment of specific V-beta chains.

The results described above showed that p21-/- CD11b+ cells induce a potent, MHCII-dependent and antigen-independent T-cell proliferation. This response is reminiscent of the ability of superantigens, such as staphylococcal enteroxins, to stimulate large numbers of T-cells *in vitro* and *in vivo*[49,50]. In fact, at variance with conventional immune responses where only a few clones of T-lymphocytes proliferate in response to a foreign antigen presented by MHC-II,superantigens short-circuit the immune system and result in massive and polyclonal activation of T-cells[50]. They simultaneously bind MHC-II molecules, directly, and specific variable regions of the beta-chain of the T-cell receptor (V-beta), outside the normal antigen-binding interface [50]. Thus, we tested the

hypothesis that CD4+ T-lymphocytes are induced to hyper-proliferate by a MHC-superantigen complex exposed on the surface p21-/- CD11b+ cells, by analyses of the TCR repertoire of CD4+ T cells primed *in vitro* with WT or p21-/- CD11b+. CSFE-stained CD4+ T-lymphocytes were purified from the peripheral blood of WT mice and cultured with CD11b+ purified from WT or p21-/- spleens. As control of polyclonal proliferation, CD4+ lymphocytes were activated by CD3/CD28 co-stimulation using Dynabeads™ Mouse T-Activator CD3/CD28 for T-Cell Expansion and Activation (Thermofisher).After 4 days, the CD4+ T-lymphocytes that had proliferated were isolated by FACS sorting, as $CFSE^{med\text{-}low}$ cells, and subjected to DNA sequence of VDJ regions. Briefly, we extracted DNA from CD4+ lymphocytes, generated libraries of the TCR VDJ-recombination regions and sequenced the CD3 variable chains by NGS, according to established procedures (ImmunoSeq assay Adaptive Biotechnology). Analyses of the sum of the unique productive rearrangements (expressed as Productive Clonality; see Methods 2.5.1) showed the presence of a polyclonal TCR V-beta repertoire in CD4+ T-lymphocytes primed with either WT or p21-/- CD11b+ cells, to an extent that was comparable with that of CD3/CD28-activated CD4+ lymphocytes (**Figure 22A**). Most notably, we observed no significant enrichment for a specific V beta chain (**Figure 22B),** arguing against the involvement of a superantigen in the hyper-proliferation of CD4 T-lymphocytes induced by p21-/- CD11b+ cells.

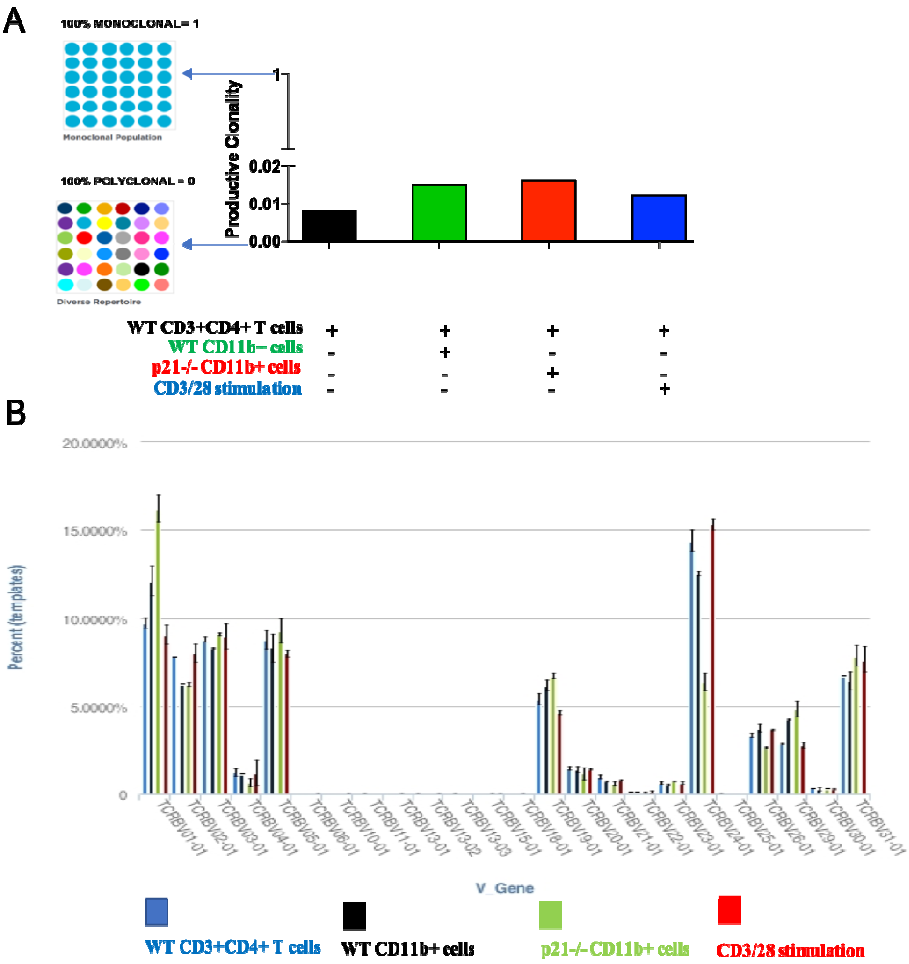

Fig.22 Productive Clonality and V beta-chain enrichment of CD4+ lymphocytes primed *in vitro* by WT or p21-/- CD11b+ cells.

CSFE-stained naïve CD4+ lymphocytes from WT mice were co-incubated with WT or p21-/- CD11b+ cells (purified from spleen cell-suspensions) at ratio 4:1. As control, CD4+ T-lymphocytes were treated with Dynabeads™ Mouse T-Activator CD3/CD28 for T-Cell Expansion and Activation (Thermofisher). After 4 days of coculture, $CFSE^{med\text{-}low}$CD4+ T lymphocytes were isolated by FACS-sorting and VDJ regions sequenced by NGS.

A. Histogram plots show the level of productive Clonality of the *in vitro* primed CD4+ T-lymphocytes. The squares on the left represent a schematic representation of the two extreme situations of clonality: monoclonality, where each spot represents the same productive rearrangement shown with the same color (upper square), or polyclonality, where each spot represents a different productive rearrangement shown with different colors(lower square). The graph on the right represents the level of productive clonality of TCR of CD4+ T cells after *in vitro* priming with WT p21-/- CD11b+ cells or CD3/28 stimulation. B. Histogram plots show the level of enrichment of V beta chains, as indicated in the horizontal axis. The vertical axis indicates the percent of templates (template is a single input molecule that is the input template for PCR. When starting with gDNA this is one rearranged chromosome from a T or B cell). Results are the average +/- SD of two independent experiments.

4.5. p21-/- CD11b+ cells potentiate the fast homeostatic proliferation of CD4+ T cells

4.5.1 CD4+T cells primed *in vitro* with p21-/- CD11b+ cells undergo fast proliferation

As an alternative explanation for the hyper-proliferation of CD4+ T-lymphocytes, we tested the hypothesis that p21-/- CD11b+ cells induce homeostatic proliferation of CD4+ T cells, a condition that is also associated with MHCII-dependent polyclonal proliferation of T-lymphocytes. Homeostatic proliferation (HP) is a physiological process that maintains size and diversity of T-lymphocytes and involves clonal expansion of T-lymphocytes[42]. Most notably, HP strictly depends on the interaction of the TCR on T-lymphocytes with MHC: peptide complexes on APCs, and the presence of specific cytokines[39]. Two types of HP have been described, based on the extent of T-lymphocytes proliferation, effects on T-cell phenotypes and requirement of cytokines: i) fast HP, characterized by rapid cell divisions of naïve T-lymphocytes, generation of effector/memory cells and no requirement of specific cytokines, and ii) slow HP, characterized by a slower proliferation of naïve T cells, in the absence of associated phenotypic changes and driven by the IL7cytokine [135,42].

HP of human T-lymphocytes can be evaluated *in vitro* by co-cultures of human purified CD4+ T-lymphocytes and APCs obtained from peripheral blood mononuclear cells after depletion of T-cells (CD3+) and NK cells (CD56+), in the presence (slow HP) or absence (fast HP) of IL7 [135]. Under these experimental conditions, both fast and slow HP appear after 10-15 days of culture [135]. Thus, we adapted our *in vitro*CD4+-lymphocytes – CD11b+ cells co-culture assay to analyze HP. WT or p21-/- CD11b+ cells were co-cultured with purified naïve CD4+ T-lymphocytes (1/4 ratio) and kept in culture for 15 days. Proliferation of CD4+ T-lymphocytes was measured using the CFSE assay. As reported for the human CD4+ T-lymphocytes [135], fast HP of mouse CD4+ T-lymphocytes primed with WT CD11b+ cells was almost negligible at day 4 (6% CFSE-low/negative cells) and became evident after 10 (55% CFSE-low/negative cells) and 15 (55% CFSE-low/negative cells) days ofculture (**Fig.23).** Upon stimulation with p21-/- CD11b+ cells, instead, CD4+ T-lymphocytes

showed a strong homeostatic proliferation already at 4 days (~50% of proliferating CFSE low/neg cells), which further increased after 15 days and reached levels significantly higher than in control cultures (90% vs 55% of proliferating CFSE low/neg in CD4+ T-lymphocytes co-cultured with p21-/- vs WT CD11b+ cells; **Fig.23**). The presence of non-cycling CD4 cells by stimulation with WT - but not p21-/- APCs- at day 4 could be due to heterogeneity of WT versus p21-/- APCs, for example differences in M1/M2 macrophage proportions.M1 macrophages are classically activated macrophages, typically by IFN-γ or lipopolysaccharide (LPS), and produce proinflammatory cytokines, phagocytize microbes, and initiate an immune response. M1 macrophages produce nitric oxide (NO) or reactive oxygen intermediates (ROI) to protect against bacteria and viruses, while M2 macrophages are alternatively activated macrophages by exposure to certain cytokines such as IL-4, IL-10, or IL-13. These macrophages are associated with wound healing and tissue repair; moreover M2 macrophages also contribute to the formation of extracellular matrix and do not produce nitric oxide or present antigen to T cells[223].Gorjana Racckov et al.[224] showed thatp21 regulates macrophage reprogramming. p21 deficiency impairs macrophages ability to attenuate IFN-β production and acquire an M2-like hyporesponsive status. Their findings were complemented by data showing that monocytes from sepsis patients had high p21 levels that correlated with low IFN-β expression and a hyporesponsive phenotype.[224]. Thus, the presence of non-cycling CD4 cells by stimulation with WT - but not p21-/- APCs- at day 4 could be due to a reduced proportionof M1 macrophages, key effector cells for immune response initiation, antigenpresentation and T cellactivation.

These data, together with the finding that CD4+ T-lymphocytes stimulated with p21-/- CD11b+ undergo effector/memory maturation (**Fig.21**), suggest that p21-/- CD11b+ cells induce fast HP of CD4+-lymphocytes.

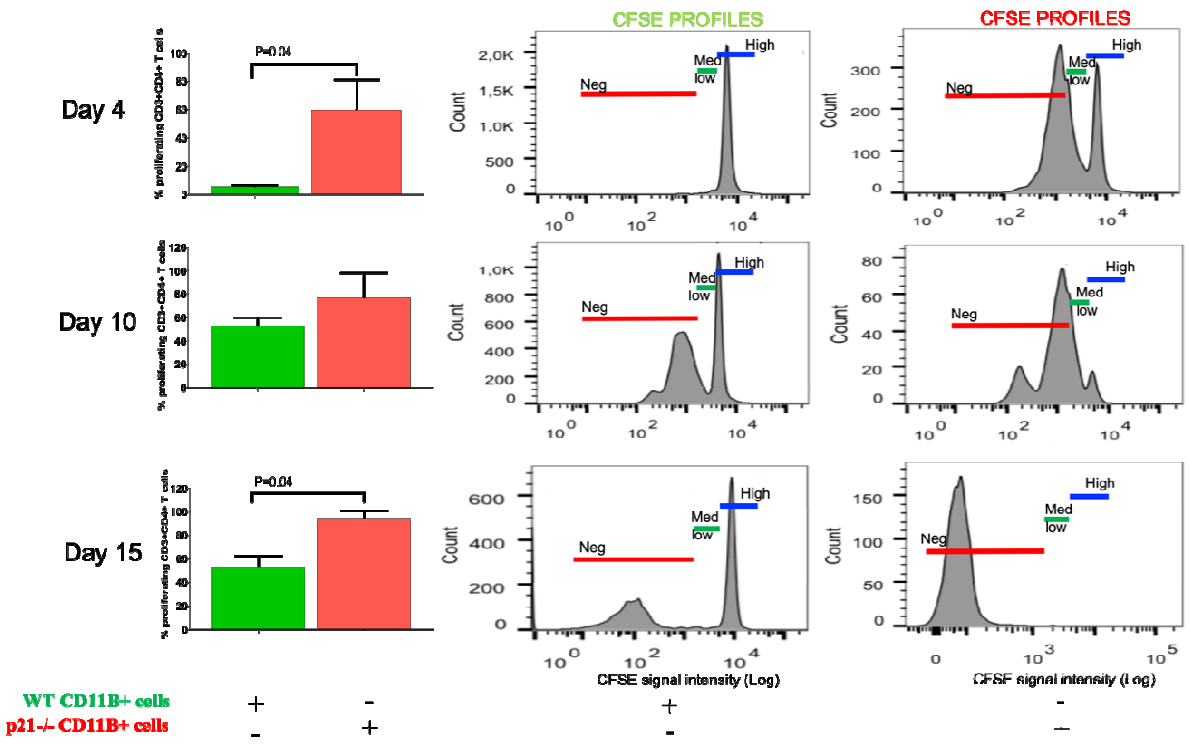

Fig.23 Short- (4 days) and long- (15 days) term proliferation of CD4+ T-lymphocytes after *in vitro*co-culture with WT or p21-/- CD11b+ cells.CSFE-stained naïve CD4+ lymphocytes from WT mice were co-incubated with WT or p21-/- CD11b+ cells (purified from spleen cell-suspensions) at ratio 4:1. Fresh sorted CD11b+ cells were re-added after 4 and 10 days of incubation (see material and methods 2.3.1.1). After 4, 10 and 15 days of co-culture, T-cell CFSE-signal was determined by FACS analyses. Histogram plots on the left show the percentages of proliferating CD4+ T lymphocytes as mean +/- s.d. of 2 independent experiments (the two experiments were analyzed together using the unpaired *t* test). The images on the right show representative FACS profiles of CD4+-lymphocytes co-cultures with WT (green) or p21-/- (red) CD11b+ cells. Neg: CD4+ T cells with negative CFSE signal (below 10^3) represent the T cells that already have a massive proliferation; Med low:CD4+ T cells with low-medium CFSE signal (between 10^3 and the first signal peak of CFSE (usually at 10^4) represent the T cells that have just begun to proliferate; High: CD4+ T cells with positive signal of CFSE (usually positionated at 10^4/10^5) represent the no proliferating T cells.Fast-, slow- and non-proliferating CD4+-lymphocytes are highlighted in the FACS-profile panels using blue, green orred bars, respectively.

4.5.2 Proliferation of CD4+T-lymphocytes upon priming with p21-/- CD11b+ cells is IL7 independent.

We next characterized the role of IL7 on the HP of CD4+ T-lymphocytes. To this aim, co-culture of WT or p21-/- CD11b+ cells were treated for 4 days with different concentrations of IL7 (5 or 10 ng/ml) or with IL7-blocking antibodies (anti-IL7 Abs)[135]. As expected[135], proliferation of CD4+ T-lymphocytes primed with WT CD11b+ cells was increased by IL7 (from 3% to 13% of $CSFE^{low/negative}$ cells; p=0.03). IL7 addition, instead, had no effects on the proliferation of CD4+

lymphocytes primed with p21-/- CD11b+ cells, nor their proliferation was affected by addition of the IL7-blocking antibodies (**Figure 24**), thus suggesting that p21-/- CD11b+ cells do not activate slow HP of CD4+ T-lymphocytes.

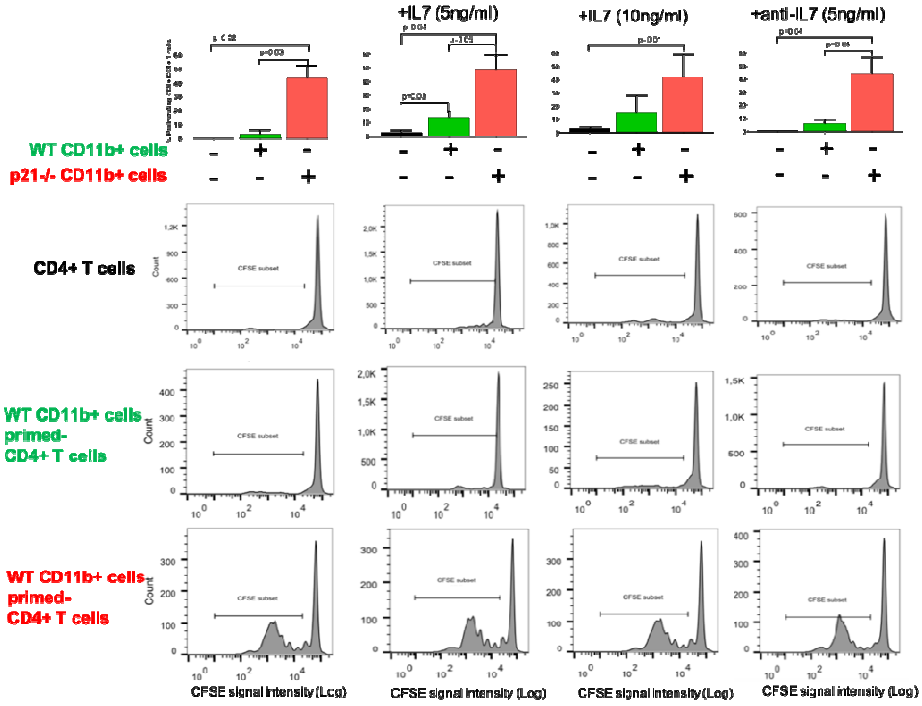

Fig.24 Effect of IL7 on the proliferation of CD4+ T-lymphocytes after *in vitro*co-culture with WT or p21-/- CD11b+ cells.CSFE-stained naïve CD4+ lymphocytes from WT mice were co-incubated with WT or p21-/- CD11b+ cells (purified from spleen cell-suspensions), at ratio 4:1, in the absence or presence of IL7(5 or 10ng/ml) or anti-IL7 antibodies (5ng/ml). Histogram plots on the top show the percentages of proliferating CD4+ T cells as mean +/- s.d of 2 independent experiments (the two experiments were analyzed together using the unpaired *t* test). The images below show representative FACS profiles of CD4+-lymphocyte co-cultures with WT (green) or p21-/- (red) CD11b+ cells, as indicated. CSFE subset representthe CFSE dilution signal due to the proliferating CD4+ T cells. In the histograms, black bar represents the % of proliferating CD4+ T cells not primed (alone), green bar represents the % of proliferating CD4+ T cellsprimed in *vitro* with WT CD11b+ cell ,while red bar represents the % of proliferating CD4+ T cellsprimed *in vitro* with p21-/- CD11b+ cells

4.5.3 CD4+ T cells proliferation depends on the APCs/T cells ratio.

We then investigated the effect of decreasing amounts of CD11b+ cells and IL7 on the fast and slow HP of CD4+ T-lymphocytes primed with WT or p21-/- CD11b+ cells, by using different ratio CD4+/CD11b+ cells in the co-culture experiments (4:1, as used in the previously shown experiments, 4:0.1, 4:0.05) and different concentrations of rIL7 (5 and 10 ng/ml). As shown in **Figure 25**, proliferation CD4+ T-lymphocytes induced by WT CD11b+ cells was not detected after 4 days of culture, as already shown in **Fig.24**, and was increased significantly (~5 folds) by 5ng/ml

rIL7, with small or no differences when using 10ng/ml rIL7 concentrations (~5 fold increase). This is consistent with the reported effects of rIL7 on the slow proliferation of human CD4+-lymphocytes induced by APCs[135]. Fast proliferation CD4+ T-lymphocytesin the co-cultures withp21-/- CD11b+ cells decreased progressively at ratios of 4:0.1 (2 fold decrease) and 4:0.05 (4 fold decrease).Thedimishing effect of decreasing amounts of p21-/- CD11b+ cells on the fast HP proliferation of CD4+ T-lymphocytes, however, was completely abrogated by the addition of rIL7, which supported proliferation of CD4+-lymphocytes even at the lowest concentrations of CD11b+ cells (**Figure 25).**Treatment with anti-IL7 antibodies did not affect proliferation of CD4+ T-lymphocytes, at any of the concentrations of p21-/- CDC11b+ cells used (**Figure 25**). Thus, as observed for the human CD4+-lymphocytes and WT APCs[135], the fast hyper-proliferation of mouse CD4+ T-lymphocytes induced by p21-/- CD11b+ cells is dependent on concentrations of the antigen-presenting cells and is IL7-independent, yet it can be enhanced by addition of exongenous rIL7.

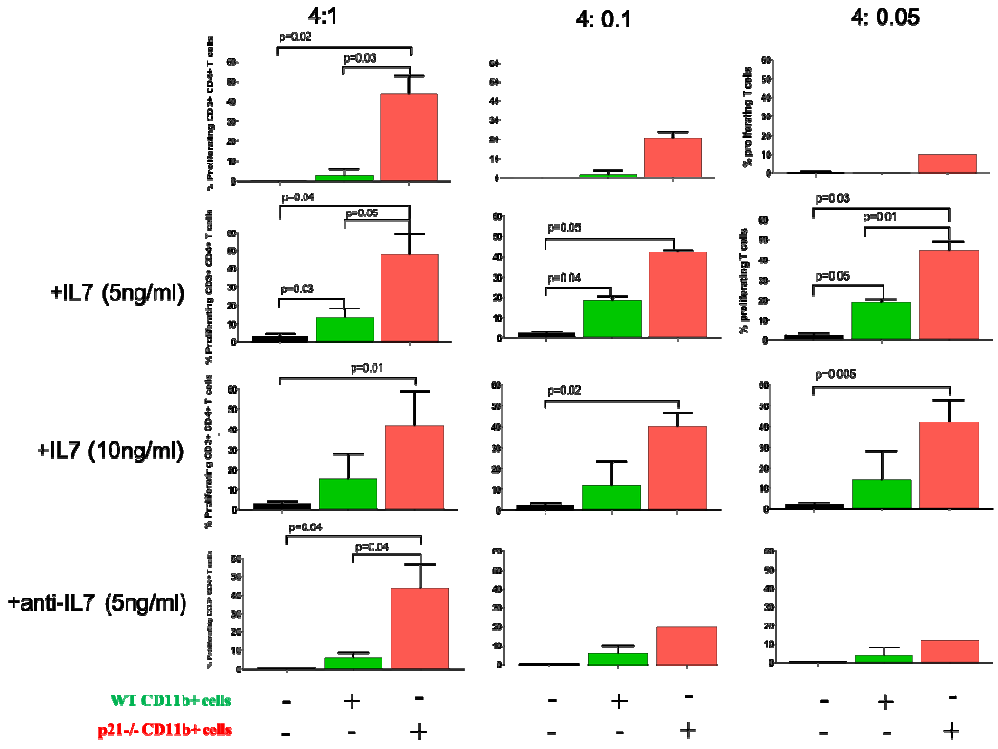

Fig.25 Effect of IL7 and different ratios of CD4+-lymphocytes/CD11b+ cellson*in vitro* proliferationCD4+ T cells co-cultured with WT or p21-/- CD11b+ cells.

CSFE-stained naïve CD4+ lymphocytes from WT mice were co-incubated with WT or p21-/- CD11b+ cells (purified from spleen cell-suspensions) at decreasing ratios(4:1, 4:0,1 and 4:0,05) in the absence or presence of rIL7(5 or 10ng/ml) or anti-IL7 antibodies (5ng/ml). After 4 days incubation, the CFSE signal of CD4+ T-lymphocytes was determined by FACS analyses. Histogram plots show the percentages of proliferating CD4+ T-lymphocytes as mean +/- s.d of 2 independent experiments. anti-IL7 addition on T cells primed with p21-/-CD11b+ at ratio 4:0.1 and 4:0.05 and standard condition of T cells primed with WT and p21-/- CD11b+ cells at ratio 1:0.005 were performed once.The two experiments were analyzed together using the unpaired *t* test.

4.5.4 p21-/- CD11b+ cells induce a general cytokine response

Activated CD4+ T cells produce a variety of different cytokines that are critical for their clonal expansion and differentiation [139]. Thus, we analyzed the spectrum of secreted cytokines by CD4+ T-lymphocytes primed with WT or p21-/- CD11b+ cells, using a multiplexed flow cytometric assay (BD™ CBA assay) for the simultaneous detection of 7 soluble cytokines (IL10, IL4, IL6, IL17A, INFY, TNFα, IL2) that characterize the three main effector phenotypes of activated CD4+ T-lymphocytes, e.g. T helper type 1 (Th1), T helper type 2 (Th2) or T helper type 17 (Th17) [139,140]. Naïve T helper cells (Th) are activated by recognition of a peptide antigen-MHCII complex presented on APCs. Through the interaction with the TCR, Th cells begin to divide and give rise to a clone of effector cells, each specific for the same antigen-MHCII complex [141]. These CD4+ effector Th cells are distinct in three main types, each characterized for cytokine-secretion phenotypes and functional characteristics: Th1 cells secrete interferon IFNγ, IL2 and TNFα, which allow these cells to be particularly effective in protecting against intracellular infections by viruses and bacteria and micro-organisms that grow in macrophages, as well as eliminating cancerous cells[142]. Th2 cells secrete interleukin IL-4, -6, -10 and -13, which up-regulate antibody production and target parasitic organisms; Th17 cells secrete IL-17, IL-17F, IL-22 and appear to play an integral role tissue inflammation and neutrophils activation against extracellular bacteria.

As shown in **Figure 26**, co-cultures of naïve CD4+ T cells and p21-/- CD11b+ cells produced increased amounts of INFγ, TNFα and IL2 (cytokines released by Th1 cells), IL10, IL4 and IL6 (cytokines released by Th2), and IL17A (cytokine released by Th17), as compared to co-cultures of naïve CD4+ T cells and WT CD11b+ cells, suggesting p21-/- CD11b+ cells induce maturation toward all three CD4+ effector T-cell subpopulations (Th1, Th2, Th17).

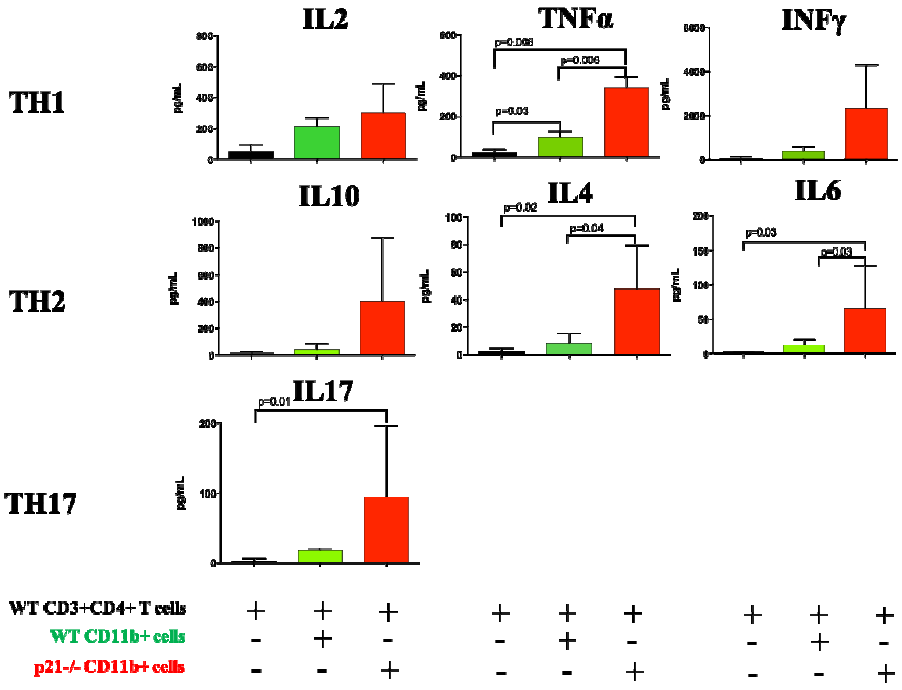

Fig.26 Characterization of the effector CD4+T-lymphocyte cell sub-populations after *in vitro*priming with WT or p21-/- CD11b+ cells.
Naïve CD4+ lymphocytes from WT mice were co-incubated with WT or p21-/- CD11b+ cells (purified from spleen cell-suspensions) at 4:1 ratio. After 4 days incubation, cytokine production in the supernatants was measured using the BD^{TM} Cytometric Beads Array System (CBA). Histogram plots show concentrations of cytokines in the supernatants (pg/ml) of the different co-cultures, as indicated, as mean +/- s.d. of 3 independent experiments (IL10 and InterferonY were quantified twice).All experiments were analyzed together using the unpaired *t* test.

Together, these data demonstrate the proliferation of naïve CD4+ T-lymphocytes induced by p21-/- CD11b+ cells resembles the HP proliferation induced by WT APCs, in terms of numbers of timing of the cell divisions, maturation toward memory and effector cells, yet it is more rapid and significantly more potent, suggesting that p21-/- CD11b+ cells potentiate the fast homeostatic proliferation of CD4+ T-lymphocytes.

4.6 CD4+T-lymphocytes activated by p21-/- CD11b+ cells induce anti-tumor response *in vivo*

We next investigated whether the CD4+ T-lymphocytes activated by p21-/- CD11b+ cells *in vitro* posses *in vivo* anti-tumor activity, by adoptive transfer of *in vitro* primed- CD4+ T cells in tumor-bearing mice. CD4+ T-lymphocytes were co-cultured with WT or p21-/- CD11b+, as described above, and injected in the tail vein of recipient syngeneic mice one day before transplantation of ErbB2 tumor cells in the Mammary Fat Pad of immunodeficient recipients, which were then monitored for tumor growth. CD4+ T-lymphocytes activated by WT CD11b+ cells exerted no effect on growth of ErbB2 tumors (**Figure 27**).CD4+ T cells primed *in vitro* with p21-/- CD11b+ cells, instead, delayed significantly tumor growth (mean survival from 144 to 176 days ; p=0.0038; **Fig.27**).

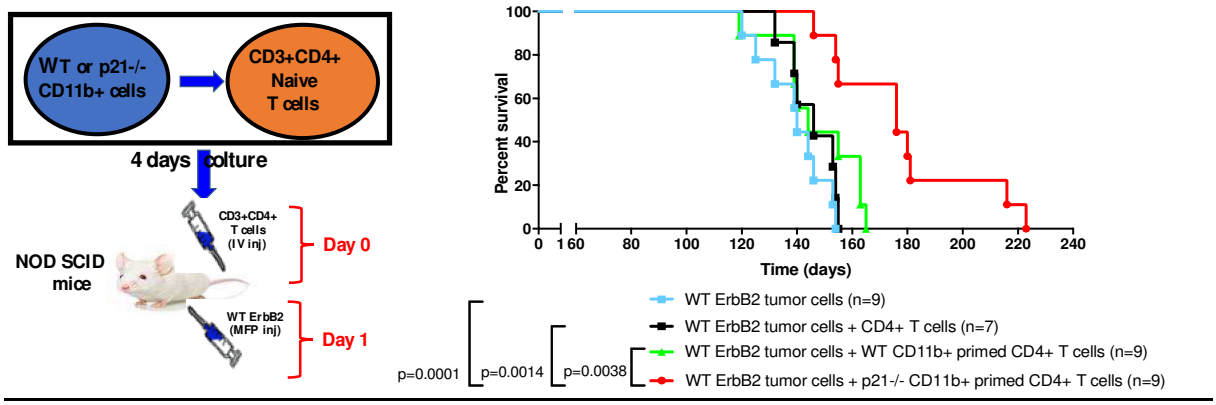

Fig.27 Survival curves of NOD-scid immunodeficient mice injected with a single boost of CD4+ T cellsprimed *in vitro* with WT or p21-/- CD11b+ cells and then transplanted with WT ErbB2 tumors. CD4+ T cells were obtained by 4-days co-cultures with WT or p21-/- CD11b+ cells and then injected in the tail vein of NOD-scid immunodeficient mice (day 0; d0).Cell suspensions from ErbB2-tumors (300,000 cells/mouse)were injected in the in mammary fat pad at day 1 (d1), as shown in scheme above. The ratio CD4+ T-lymphocytes: ErbB2 cells was 4:1. Mice were sacrificed when tumors reached an overall diameter of 1cm. The survival curves shown above are derived from three independent experiments that were analyzed together using the log-rank (Mantel-Cox) statistical test. Injection of CD4+ T cells primed with WT CD11b+ cells was performed once.

4.7 CD11b+c+ myeloid cells are essential to induce homeostatic proliferation of CD4+ T cells

To investigate mechanisms underlying the effects of p21 depletion on the APC function of CD11b+ cells, we first tried to identify the specific cell-type responsible for the observed CD4+ - mediated anti-tumor response. Data presented above suggest that the critical CD11b+ sub-population is present in the seemingly normal spleen of p21-/- mice (**Fig.12),**expresses MHCII molecules (**Fig.13**)and infiltrates p21-/- erbB2-tumors (**Fig.16)**. To characterize CD11b+ cells in the WT and p21-/- spleens we used a recently published combination of cell surface markers that allow identification of splenic APCs (dendritic and myeloid cell-subsets) (CD11b, CD11c, MHCII, CD8, Ly6c and Ly6g)[76,77]. As reported[76,77], we identified 4 cell sub-populations expressing the CD11b antigen: Monocyte/Macrophages (Resident Monocyte; Migrant Monocyte; Inflammatory Monocytes; Active Macrophages; Inactive Macrophages), polymorphonuclear cells (Eosinophil; Neutrophil; Neutrophils with APC function), Dendritic cells (Dendritic like cells, Activated Dendritic Like cells; CD8- conventional DC) and lymphocytes (T and B cells). These sub-populations were similarly distributed within the whole CD11b+ population of WT and p21-/- spleens (**Table 1A**) or the whole spleen of WT and p21-/- mice (**Table 1B).** Notably, only a few of them express MHCII molecules and has been reported to activate CD4+ T-cells*in vitro*[76], including macrophages (~1% of the all CD11b+ population) and CD8a- conventional dendritic cells (~9%). CD8a- is a subtype of conventional DCs (cDCs), mainly localized in the marginal zone of spleen [76], and distinguished by the expression of the CD11c integrin[76]. Together, these results suggest that expression of MHCII molecules in WT or p21-/- splenocytes correlates with expression of CD11b on monocytes/macrophages and both CD11b and CD11c on dendritic cells. Thus, we investigated the correlation between CD11b+/CD11c+ expression and the capacity to activate HP of T-lymphocytes. We first analysed the biological effects of CD11c+ cells. CD11c+ cells were purified from WT and p21-/- spleens by FACS-sorting technique. WT CD11c+ cells induced a modest proliferation of CD4+ and CD8+ T-lymphocytes (10.5%+/-0.71 and 3.5%+/-0.71; **Figure 28**).As previously shown for the CD11b+ subset,p21-/- CD11c+ cells induced instead a potent proliferation of CD4+ T cells (53%+/-0.71; p=0.0003), and, to a lesser extent, of CD8+ T cells (37%+/-2.83; p=0.02) (**Fig.28**). Proliferation of CD4+ lymphocytes induced by p21-/- CD11b+ cells was tumor-cell (not shown) and tumor-lysate independent (**Fig.29**), but MHCII dependent (reduction of about 91%; **Fig.29**, p=0.0002). Analyses of the degree of differentiation of CD4+ T-lymphocytes (**Fig.30**) showed increased percentages of both effector (from 16 to 34%; p=0.04) and memory (from 6.5 to 14%;

p=0.04) cells upon priming with p21-/- CD11b+ cells. As for the CD11b+ cells (**Fig.21**), the acquisition of the effector and memory phenotypes was MHC-II-dependent (**Figure 30**).

A

CD11b+ sub-populations	CD11b	CD11c	CD8	Ly6c	Ly6g	MHCII	WT (%)		p21-/- (%)	
Monocytes								SUM		SUM
Resident Monocyte	high	low	neg	low/high	neg	neg	2,6		3,2	
Migrant Monocytes	high	low	neg	low/high	neg	high	1	7,9	0,93	10,13
Inflammatory Monocytes	high	neg	neg	low/high	neg	neg	4,4		6	
Macrophages										
Active Macrophages	high	neg	neg	neg	neg	high	0,4	0,9	0,75	2,15
Inactive Macrophages	high	neg	neg	low	neg	neg	0,5		1,4	
Polymorphonuclear cells										
Eosinophils	high	neg	neg	low	neg	neg	0,5		1,4	
Neutrophils	high	neg	neg	low/high	high	neg	17,6	23,2	19	24
neutrophils with APC function	high	neg	neg	low/high	high	high	5,1		3,6	
Dendritic cells										
Dendritic like cells	high	low	neg	neg	neg	neg	16,3		13,1	
Activated Dendritic like cells	high	low	neg	neg	neg	high	15,1	40,7	17,3	41,4
CD8-cDC	high	high	neg	neg	neg	high	9,4		11	
Lymphocytes										
T lymph	high		high			neg	7,2	18,1	4	16
B cells	high		high			high	10,8		12	

B

Spleen sub-populations	CD11b	CD11c	CD8	Ly6c	Ly6g	MHCII	WT (%)		p21-/- (%)	
Monocytes								SUM		SUM
Resident Monocyte	high	low	neg	low/high	neg	neg	0,1		0,1	
Migrant Monocytes	high	low	neg	low/high	neg	high	0,1	0,7	1,25	1,15
Inflammatory Monocytes	high	neg	neg	low/high	neg	neg	0,5		0,8	
Macrophages										
Active Macrophages	high	neg	neg	neg	neg	high	0	0,1	0,1	0,3
Inactive Macrophages	high	neg	neg	low	neg	neg	0,1		0,2	
Polymorphonuclear cells										
Eosinophils	high	neg	neg	low	neg	neg	0,1		0,5	
Neutrophils	high	neg	neg	low/high	high	neg	1,5	1,8	0,5	2,16
neutrophils with APC function	high	neg	neg	low/high	high	high	0,2		1,15	
Dendritic cells										
Dendritic like cells	high	low	neg	neg	neg	neg	1,3		1,5	
Activated Dendritic like cells	high	low	neg	neg	neg	high	1,3	3,2	1	3,5
CD8-cDC	high	high	neg	neg	neg	high	0,6		1	
Lymphocytes										
T lymph	high		high			neg	0,6	1,7	0,38	1,08
B cells	high		high			high	1,1		0,7	

Tab.1 Characterization of WT and p21-/- CD11b+ cell sub-populations.
FACS analysis and characterization of APC sub-populations in the whole splenic CD11b+_ subset or in the whole spleen from WT and p21-/- mice (3 biological replicas). Cells were analysed by FACS using the antibodies indicated in the Tables(CD11b, CD11c, MHCII, CD8, Ly6c and Ly6g). Percentage +/- SD were calculated on 100% CD11b+ cells (A) or 100% spleen cells (B).

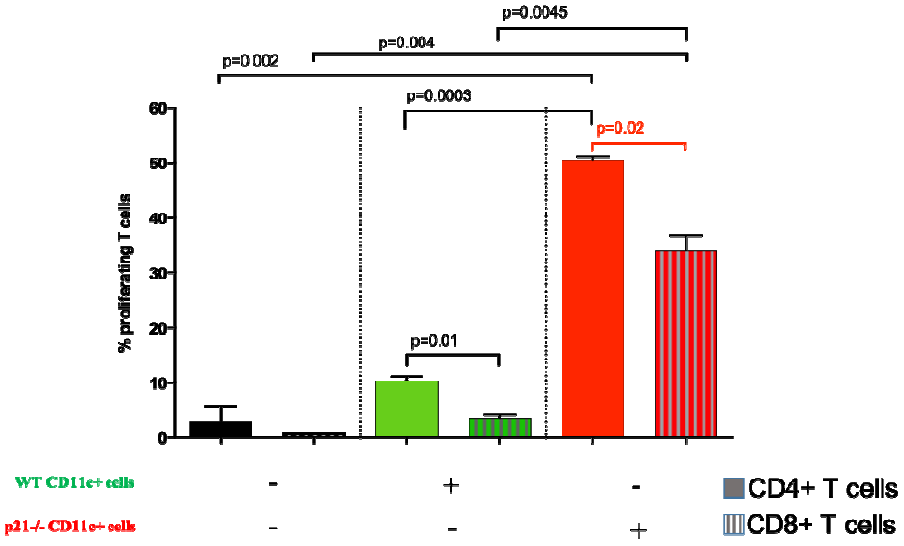

Fig.28 *In vitro* proliferation of CD4+ or CD8+ T-lymphocytes primed with WT or p21-/- CD11c+ cells. CFSE-labelled naïve CD4+ or CD8+ lymphocytes from WT mice were co-incubated with WT or p21-/- CD11c+ cells (purified from spleen cell-suspensions) at 4:1 ratio. After 4 days of coculture, T-cell CFSE-signal was determined by FACS analyses. Histogram plots show the percentages of proliferating CD4+ or CD8+ T-lymphocytes as mean +/- s.d. of 2 independent experiments (the two experiments were analyzed together using the unpaired *t* test).

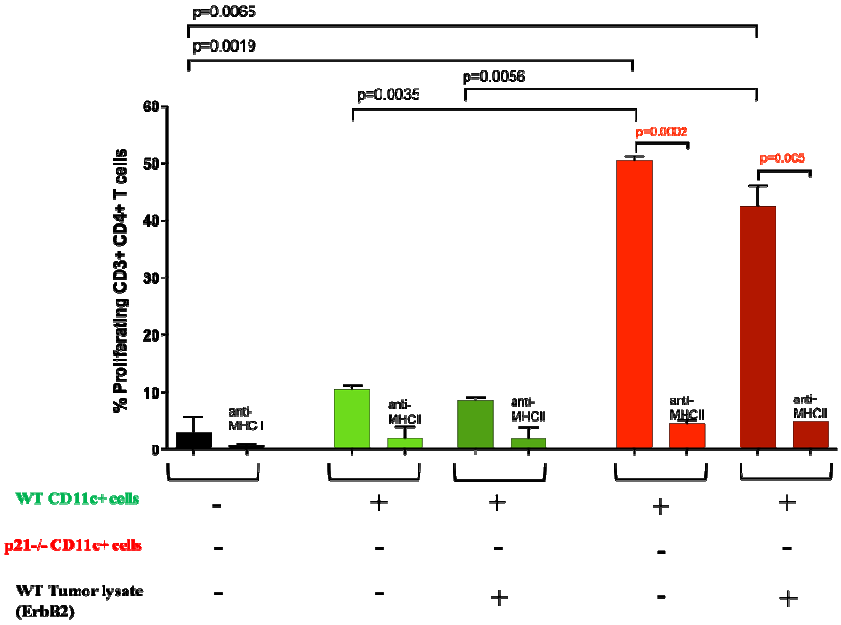

Fig.29 Effect of antigen-loading and MHC-II expression on the *in vitro* proliferation of CD4+ T-lymphocytes after priming with WT or p21-/- CD11c+ cells. CFSE-labelled naïve CD4+ T-lymphocytes from WT mice were co-incubated with WT or p21-/- CD11c+ cells (purified from spleen cell-suspensions) at 4:1 ratio in the presence, or not, of tumor lysates from ErbB2, or inhibitory anti-MHC-II antibodies, as indicated. After 4 days of co-culture, T-cell CFSE-signal was determined by FACS analyses. Histogram plots show the percentages of proliferating CD4+ T-lymphocytes as mean +/- s.d of 3 independent experiments, which were analyzed together using the unpaired *t* test.

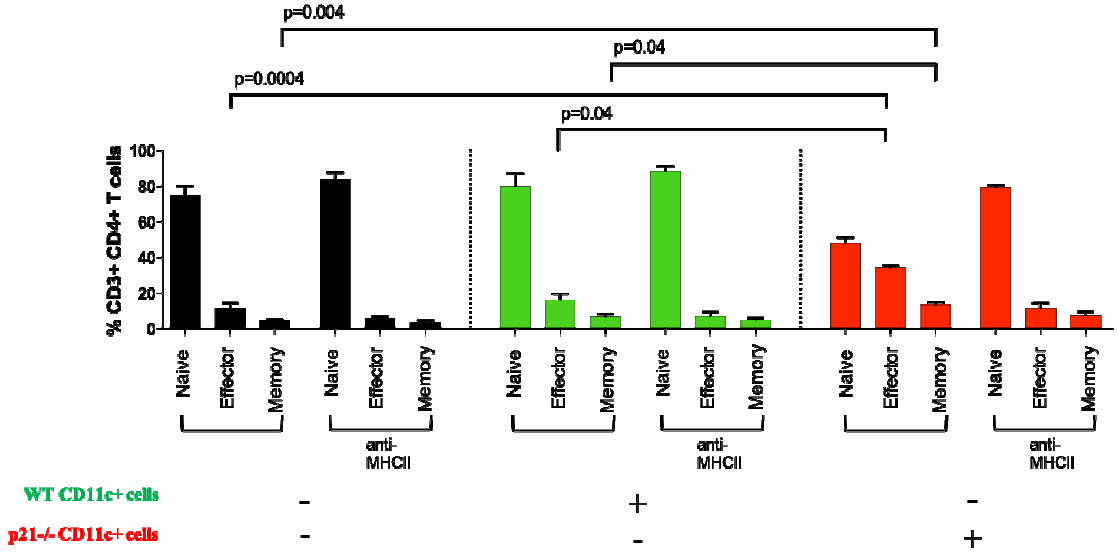

Fig.30 Effect of WT or p21-/- CD11c+ cells on the phenotype of CD4+ T cells upon *in vitro* priming with WT or p21-/- CD11c+ cells.
CSFE-stained naïve CD4+ lymphocytes from WT mice were co-incubated with WT or p21-/- CD11c+ cells (purified from spleen cell-suspensions) at 4:1 ratio in the presence, or not, of anti-MHC-II antibodies. After 4 days of coculture, T-cells were analyzed by FACS analyses and expression of CD44 and CD62L (NAÏVE: CD44- CD62L+, EFFECTOR: CD44+ CD62L-, MEMORY: CD44+ CD62L+) using specific antibodies. Results of CSFE dilution confirmed the strong and MHC-II – dependent proliferation of CD4+ T-lymphocyte induced by p21-/- CD11b and are not reported here. Histogram plots show the percentages of Naïve, Effector and Memory CD4+ T-lymphocytes as mean +/- s.d.of 3 independent experiments that were analyzed together using the unpaired *t* test.

Finally, we investigate whether the capacity of activating HP of CD4+ lymphocytes is shared by both CD11b+ or CD11c+ cells, or is restricted to cells co-expressing CD11b+ and CD11c+. To this end, we purified CD11b+/CD11c+ double-positive cells from WT or p21-/- spleens, by FACS-sorting and analysed their capacity to induce proliferation of naïve CD4+ T-lymphocytes. As controls, we used CD11b-/CD11c+ and CD11b+/c- cell sub-fractions. Strikingly, only p21-/- CD11b+c+ cells were able to induce massive proliferation of CD4+ T cells (40%+/-8.48; **Figure 31**) and their differentiation towards the effector/memory phenotype (**Figure 32**) (considering also the preexisting effector and memory T cells), as compared to either CD11b-/CD11c+ and CD11b+/c-. Notably, the extent of induced proliferation or differentiation were comparable to that observed using CD11b+ or CD11c+ (**Figures 31 and 32).** As observed for CD11b+ and CD11c+, both the proliferative and differentiative effects of p21-/- CD11b+c+ cells were MHC-II - dependent (**Figure 31 and 32**). Taken together, these data suggest that the cell type responsible for the activation of HP in the absence of p21 expression is a rare splenic population (~1%; **Table 1B**) that co-expresses MHC-II, CD11b and CD11c molecules.

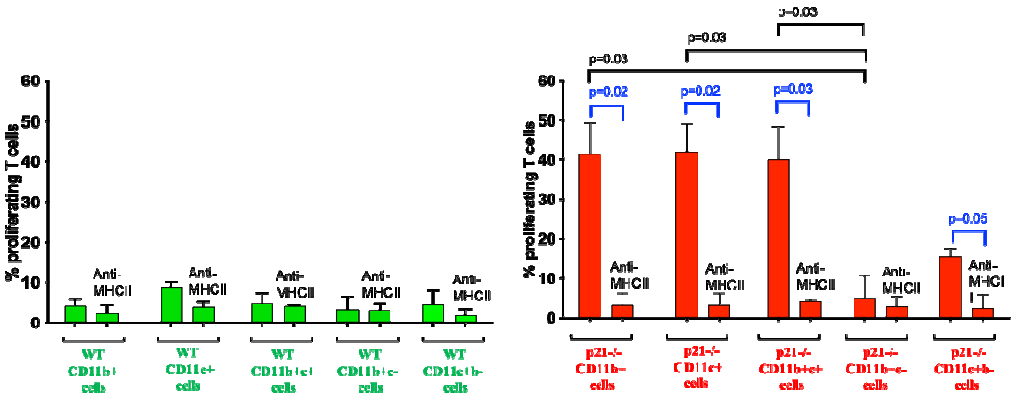

Fig.31 Effect of different WT or p21-/- CD11b+ and/or CD11c+ sub-population on the *in vitro* proliferation of CD4+ T-lymphocytes.CFSE-labelled naïve CD4+ T-lymphocytes from WT mice were co-incubated with different WT or p21-/- CD11b+ and/or CD11c+ subsets (CD11b+; CD11c+; CD11b+c+; CD11b+c-; CD11c+b- cells purified from spleen cell-suspensions) at 4:1 ratio in the presence, or not, of inhibitory anti-MHC-II antibodies, as indicated. After 4 days of co-culture, T-cell CFSE-signal was determined by FACS analyses. Histogram plots show the percentages of proliferating CD4+ T-lymphocytes as mean +/- s.d. of 2 independent experiments, which were analyzed together using the unpaired *t* test.

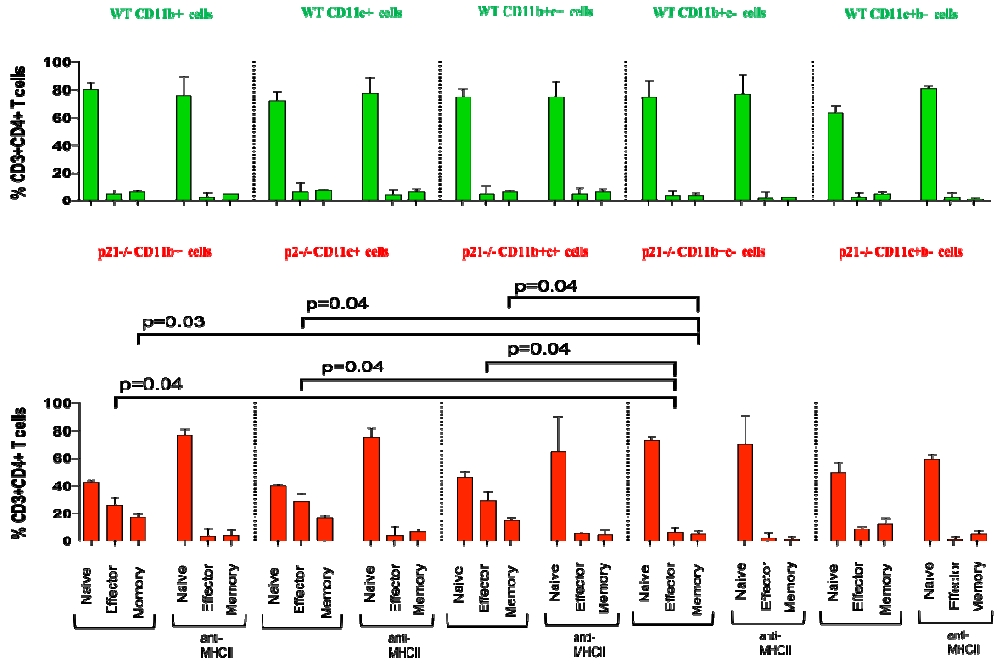

Fig.32 Effect of different WT or p21-/- CD11b+ and/or CD11c+ sub-populations on the phenotype of CD4+ T-lymphocytes upon *in vitro* priming with WT or p21-/- CD11b+ and or CD11c+ cells.CSFE-stained naïve CD4+ lymphocytes from WT mice were co-incubated with different WT or p21-/- CD11b+ and/or CD11c+ subsets (CD11b+; CD11c+; CD11b+c+; CD11b+c-; Cd11c+b- cells purified from spleen cell-suspensions) at 4:1 ratio, as indicated. After 4 days of coculture, T-cells were analyzed by FACS analyses and expression of CD44 and CD62L (NAÏVE: CD44- CD62L+, EFFECTOR: CD44+ CD62L-, MEMORY: CD44+ CD62L+) using specific antibodies. Results of CSFE dilution confirmed the strong and MHC-II –dependent proliferation of CD4+ T-lymphocyte induced by p21-/- CD11b and are not reported here. Histogram plots show the percentages of Naïve, Effector and Memory CD4+ T-lymphocytes as mean +/- s.d.of 2 independent experiments that were analyzed together using the unpaired *t* test.

4.8 CD11b+c+ myeloid cells are characterized by differential expression of genes encoding for antigen-processing and -presentation proteins

4.8.1 scRNAseq analyses of WT and p21-/- CD11b+ cells allowed identification of 9 major cell-types

To investigate molecular mechanisms underlying the potent anti-tumor response induced by the p21-/- APC, we performed single-cell RNA sequencing (SC-RNAseq) of WT and p21-/- CD11b+ cells. CD11b+ cells were purified from cell-suspensionsof WT or p21-/- spleens by FACS-sorting, using anti-CD11b antibodies, as described before (section 4.7).We performed three biological replicas for each condition (WT and p21-/-).~5,000 cells *per* sample were processed for library preparation, using the 10x Chromium technology and sequenced on NovaSeq 6000 Sequencing System (Illumina) with an asymmetric paired-end strategy with a coverage of about 75,000 reads/cell (Methods 2.5.2).Demultiplexing, barcode processing and single-cell 3' gene counting separately for each sample were obtained using Cell Ranger v3.0.2. Gene-by-cell matrices (also called, in bioinformatic jargon,'feature-barcode matrices") were obtained using confidently mapped, non-PCR duplicates with valid barcodes and unique molecular identifiers. Further analysis—including quality filtering, identification of highly variable genes, dimensionality reduction, standard unsupervised clustering algorithms and cluster markers identification— was performed using the Seurat R package[182]analyzing "merged samples". The MergeSeurat function of Seurat, that we have used, simply allows to analyze the data of all the cells, from the 6 samples, all together, instead of sample-by-sample separately. It permits, after a proper normalization step, a direct comparison of cells at several levels: between samples replicates, among different experimental conditions or just between groups of cells which are sharing particular transcriptional profiles, even independently of the sample they belonged to (i.e. clusters or predicted cell-type subpopulations).

After removing cells that had more than 10% of the transcripts coming from mitochondrial genes, to further exclude those cells that were outliers in terms of library complexity and that might possibly include multiple cells or doublets, we calculated the distribution of genes detected *per* cell *per* each

sample and removed any cells in the top 2% quantile. To exclude low-quality cells, we also removed cells that had fewer than 500 detected genes. After filtering of unwanted cells from the dataset, as described above, 14,640and 17,548total cells remained for the WT and p21-/- CD11b+ samples, respectively. After quality filtering, the mean and median numbers of detected genes-per-cell were 1,716.0and 1,616in WT, and 1,823.8and 1,666.9 in the p21-/- samples, respectively. After the preprocessing steps described above, we then normalized the raw data by the total expression of each cell and multiplied by a scale factor of 10,000.The last step was introduced, as is the case in other published procedures, for convenience, only to obtain normalized expression levels in, roughly, the same order as the pre-normalized ones.

To identify cellular states characteristics of the p21-/- APCs, we first tried to deconvolve the heterogeneity of the WT and p21-/- CD11b+ subsets using a computational approach based on the assignment of cellular identity for single-cell transcriptomes through their comparison to reference-datasets of purified cell types.To this end, we compared our sc-RNAseq datasets with the Immunological Genome Project (ImmGen) database[143], using the SingleR (single cell recognition)computational tool [144]. This analysis allowed the identification of 19 specific cell-types within the whole WT and p21-/- CD11b+ subsets (**Table 2**).

cell_type_singleR	total_cell_count	#WT	#P21	%WT	%P21	Average%WT_P21
Neutrophils	10,747	3,588	7,159	24.51	40.80	32.65
DC	8,785	4,796	3,989	32.76	22.73	27.75
Monocytes	5,617	2,949	2,668	20.14	15.20	17.67
B cells	3,789	1,863	1,926	12.73	10.98	11.85
NK cells	922	307	615	2.10	3.50	2.80
Macrophages	628	334	294	2.28	1.68	1.98
Basophils	529	267	262	1.82	1.49	1.66
T cells	463	285	178	1.95	1.01	1.48
Stem cells	202	28	174	0.19	0.99	0.59
ILC	175	28	147	0.19	0.84	0.51
B cells pro	91	32	59	0.22	0.34	0.28
Tgd	86	63	23	0.43	0.13	0.28
NKT	56	29	27	0.20	0.15	0.18
Eosinophils (*)	48	39	9	0.27	0.05	0.16
Microglia	42	25	17	0.17	0.10	0.13
Epithelial cells	3	3	0	0.02	0.00	0.01
Fibroblasts	2	2	0	0.01	0.00	0.01
Mast cells	2	1	1	0.01	0.01	0.01
Stromal cells	1	1	0	0.01	0.00	0.00
TOT	32,188	14,640	17,548	100.0	100	100.0

Table.2 Deconvolution of the cell-type composition of the WT and p21-/- CD11b+ subsets by analyses of scRNA-seq data.Sc-RNAseq data of WT and p21-/- CD11b+ subsets were compared to the ImmGen database using the SingleR computational tool.The table shows the list of all identified "cell-types" and their absolute (#) and relative (%) abundance in WT and p21-/- CD11b+ samples (3 biological replicas for each condition) and the average (between WT and p21-/- samples) of the relative abundance. Cell-types with a <1% representation are colored in light blue. (*) As an exception, also Eosinophils have been considered in the further analyses, together with the first 8 cellular subtypes.

8 cell-types (neutrophils, dendritic cells, monocytes, T and B lymphocytes, basophils, NK cells, and macrophages) were present at a relative frequency >~1% and accounted for ~98% of the total CD11b+ population in both WT and p21-/- cells. For the subsequent analyses,together with the 8 subtypes listed above, we also included eosinophils, as they were among the subtypes identified by FACS analyses (**Table 1**). Data were visualized using the UMAP algorithm (uniform manifold approximation and projection) [145].The UMAP analyses of cells of the 9 sub-types (total of

31,528cells) is shown in **Figure 33**, where UMAP maps are shown separately for the integrated WT and p21-/- (panel A), WT (panel B) or p21-/- (panel C) samples. Cells are coloured by subtype.

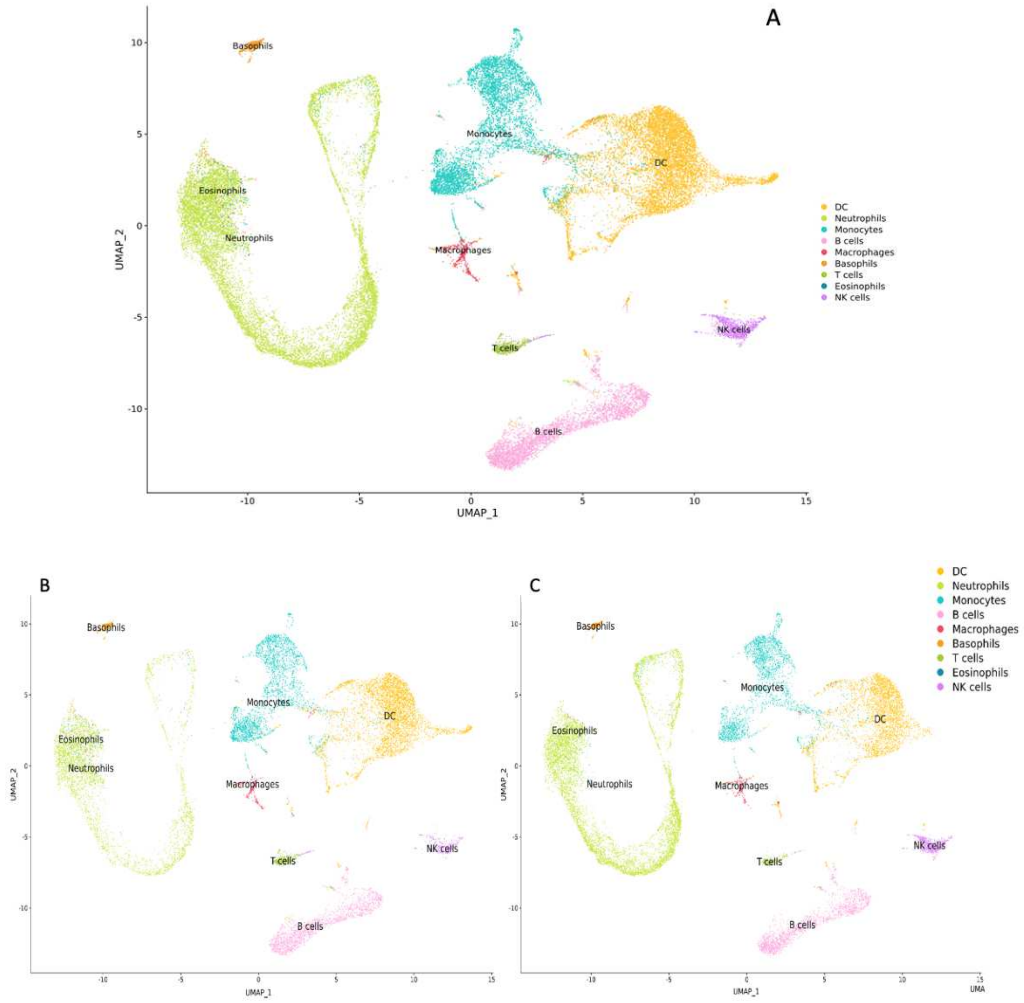

Fig.33 UMAP analyses and visualization of 9 selected cell-types in WT and p21-/- CD11b+ cells.scRNAseq dataset of WT and p21-/- CD11b+ subsets were analysed by SingleR tocharacterize their "cell-type" composition. Data of 9 selected cell-types were analysed and visualized using the UMAP algorithm. A: integrated WT and p21-/- CD11b+ cells; B: WT CD11b+ cells; C: p21-/- CD11b+ cells. Cells are colored by "cell type", as described in the inlet of each panel.

The selected 9 cell-types showed an overall consistency with the subtypes identified by FACS analyses: i) 7/9 (with the exceptions of basophils and NK cells) were also identified by FACS-analyses; and ii) all major subtypes identified by FACS-analyses were also identified by our *in silico* analyses (compare **Tables 1 and 2**). **Table 3** shows the relative frequencies of the 9 subtypes identified in silico in the WT and p21-/- samples. Overall, their distribution is comparable

betweenWT and p21-/- CD11b+ subsets, with the exception of neutrophils, that were more abundant in the p21-/- samples and dendritic cells and monocytes that were more represented in the WT samples (**Figure 33**).

	FACS-analyses		SC-RNAseq	
CD11b+ sub-populations:	**WT**	**p21-/-**	**WT**	**p21-/-**
Dendritic cells	40,7	41,4	32,76	22,73
Polymorphonuclear cells	23,2	24	24,77	40,85
Eosinophil	0,5	1,4	0,27	0,05
Neutrophil	22,7	19	24,5	40,8
Basophil			1,82	1,49
Lymphocytes	18,1	16	16,8	16,2
T lymph	7,2	4	1,95	1,71
B cells	10,8	12	12,73	10,98
NK			2,1	3,5
Monocytes	7,9	10,13	20,14	15,2
Macrophages	0,9	2.15	2,28	1,68
Total	**90,9**	**93,68**	**96,7**	**96,7**

Table 3 Comparison of the relative frequency in the WT and p21-/- CD11b+ subset of the major cell-types identified by FACS-analyses or SingleR analyses of sc-RNAseq data. Data are derived from those shown in Tables 1 and 2. Discrepancy between values obtained in Flow Cytometry and RNAseq could be due to the variability among the samples:we used differentspleen samples: three different spleens/replicates per group (both WT and p21-/- group)for Flow Cytometry analysis and three different spleens/replicates (both WT and p21-/- group) for RNAseq analysis.

4.8.2 scRNAseq analyses of WT and p21-/- CD11b+ cells allowed identification of CD11b+c+ double-positive cells within neutrophils, dendritic cells and monocytes/macrophages.

We next tried to map the CD11b+/CD11c+ APC cell-type within our UMAP of WT and p21-/- cells. First, we analyzed the patterns of CD11b (Itgam gene) or CD11c (Itgax gene) RNA-expression within WT and p21-/- cells. Notably, we observed no significant differences in terms of expression levels and cell distribution Itgam/CD11b and Itgax/CD11c gene transcripts between p21-/- and WT CD11b+ cells(**Figure 34**), suggesting that these two genes are not regulated by p21 expression in the

CD11b+ cell subset, and can be effectively used as lineage markers to map subpopulations in WT and p21-/- samples.

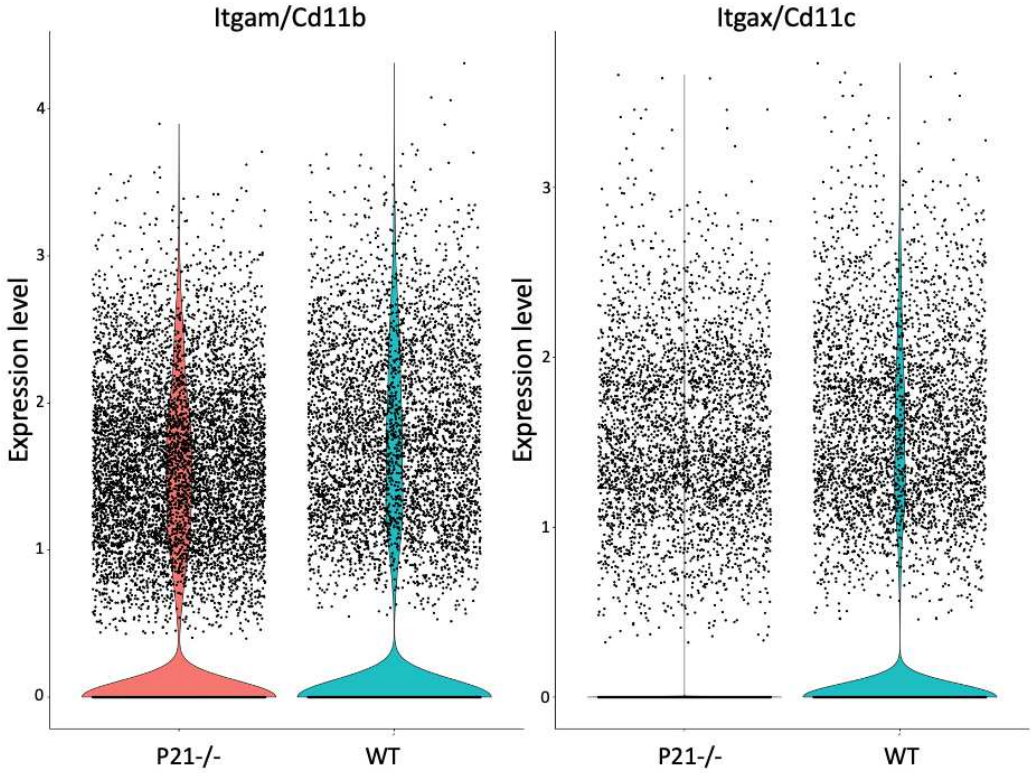

Figure 34 Expression levels of Itgam/CD11b and Itgax/CD11c in WT and p21-/- CD11b+ cells. The distributions of Itgam/CD11b and Itgax/CD11c expression level (left and right plot, respectively) in each cell are shown as super-imposed violin- and scatter-plots for WT and p21-/- CD11b+ samples.The absence of dots, in the lower part of the combined scatter/violin plots, used to describe the distribution of the expression levels of Itgam and Itgax genes, should not surprise (Fig. 34): the same is often observed in this kind of plots, when low expressed genes are depicted. Indeed, this is the result of a graphic artifact, due to the fact that most of the cells are not expressing that genes, therefore most of the black dots of the scatter plot coincide with the x-axis. On closer examination, they could be even distinguished from the x-axis, which is gray. Instead, the apparent incoherent shape of the violin plots in the dot-free area of the plot, is the result of the smoothing process used to produce the violin profiles.

We then tried to identify cells co-expressing CD11b and CD11c transcripts within the 32,188 cells identified by scRNAseq experiments. Based on the distributions of the expression levels of CD11b or CD11c transcripts (**Figure 34**), we set an arbitrary threshold to define, respectively,*bona fide* high CD11b or CD11c expressing cells (above their respective first-quartile).The majority of cells did not express CD11b (n=25,913) or CD11c (n=25,968) transcripts and were classified as CD11b- or

CD11c- cells, respectively. The thresholds allowed identification of 4 cell sub-populations, based on expression levels of CD11b and CD11c genes: CD11b-c+ (17,1%), CD11b-c- (61,2%), CD11b+c+(3,0%), CD11b+c- (18,7%) (**Figure 35**). Notably, the CD11b+CD11c+ subpopulation (3,0%) corresponds to the CD8-cDC sub-population identified by FACS analysis (9% and 11% of the WT and p21-/- CD11b+ population, respectively).

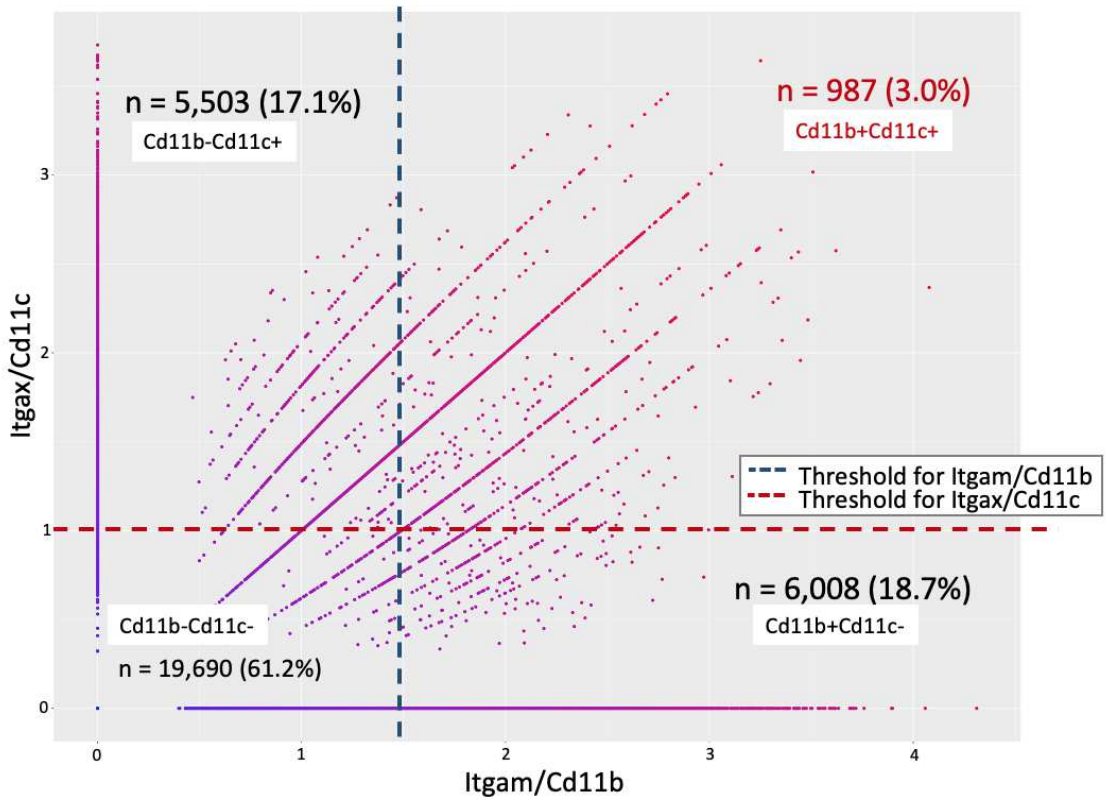

Fig.35 Identification of cells sub-populations expressing Itgam/CD11b and/or Itgax/CD11c transcripts.The scatterplot reports the position of each of the 32,188 WT or p21-/- cells identified by scRNAseq, based on their expression of Itgam/CD11b (x axis) or Itgax/CD11c (y axis). Horizontal or vertical broken lines indicate the threshold of positivity for Itgam/CD11b or Itgax/CD11c expression (set at the first quartile; see **Figure 34**). Numbers and relative frequency of the 4 identified populations are indicated (CD11b-c+, CD11b-c-, CD11b+c+, CD11b+c-.

We then analysed the distribution of the CD11b+c+ double-positive subpopulation (and the CD11b+c-subpopulation) in the 9 cell-types of the UMAP ad between the WT vs p21-/- samples. Three specific cell-types (DC, Neutrophils andMonocytes/Macrophages) contain 98.0 and 93.6% of all CD11b+c+ and CD11b+c- cells, respectively (**Table 4** and **Fig.36**). Notably, the relative distribution of CD11b+c+ and CD11b+c- cells between WT and p21-/- was very similar, confirming

that p21 expression does not regulate significally expression of CD11b/Itgam and CD11c/Itgax genes. Importantly, the percentage of the CD11b+c+ sub-population identified *in silico* matches the percentage of the CD8-cDC sub-population identified by FACS analysis (14% vs 9% in WT CD11b+ samples and 12% vs 11% in p21-/- CD11b+ samples; **Table 1 and 4**).

	DC			Neutrophils			Monocytes			Macrophages			DC/Neutrophils/ Monocytes/Macrophages	Others cell types	ALL cells in subsets
	WT	P21	TOT	WT	P21	TOT	WT	P21	TOT	WT	P21	TOT	TOT	TOT	TOT
Cd11b+/Cd11c+	134 *(13.6)*	118 *(12.0)*	252 *(25.5)*	152 *(15.4)*	232 *(23.5)*	384 *(38.9)*	149 *(15.1)*	156 *(15.8)*	305 *(30.9)*	13 *(1.3)*	13 *(1.3)*	26 (2.6)	967 *(98.0)*	20 *(2.0)*	987 *(100.0)*
Cd11b+/Cd11c-	147 *(2.4)*	122 *(2.0)*	269 *(4.5)*	1,521 *(25.3)*	2,482 *(41.3)*	4,003 *(66.6)*	681 *(11.3)*	605 *(10.1)*	1,286 *(21.4)*	26 *(0.7)*	40 *(0.4)*	66 *(1.1)*	5,624 *(93.6)*	384 *(6.4)*	6,008 *(100.0)*

Tab.4 Distribution of CD11b+c+ and CD11b+c- cells in the*in-silico* predicted cell-type subgroups.
The table shows numbers and percentage of cells of the WT and p21-/- datasets of CD11b+c+ and CD11b+c- cells and their distribution by cell types. Only 4 of the 9 identified cell-types are reported since they represent the 98.0 and 93.6% of allCD11b+c+ and CD11b+c- cells, respectively. Number notation: count *(percentage).*

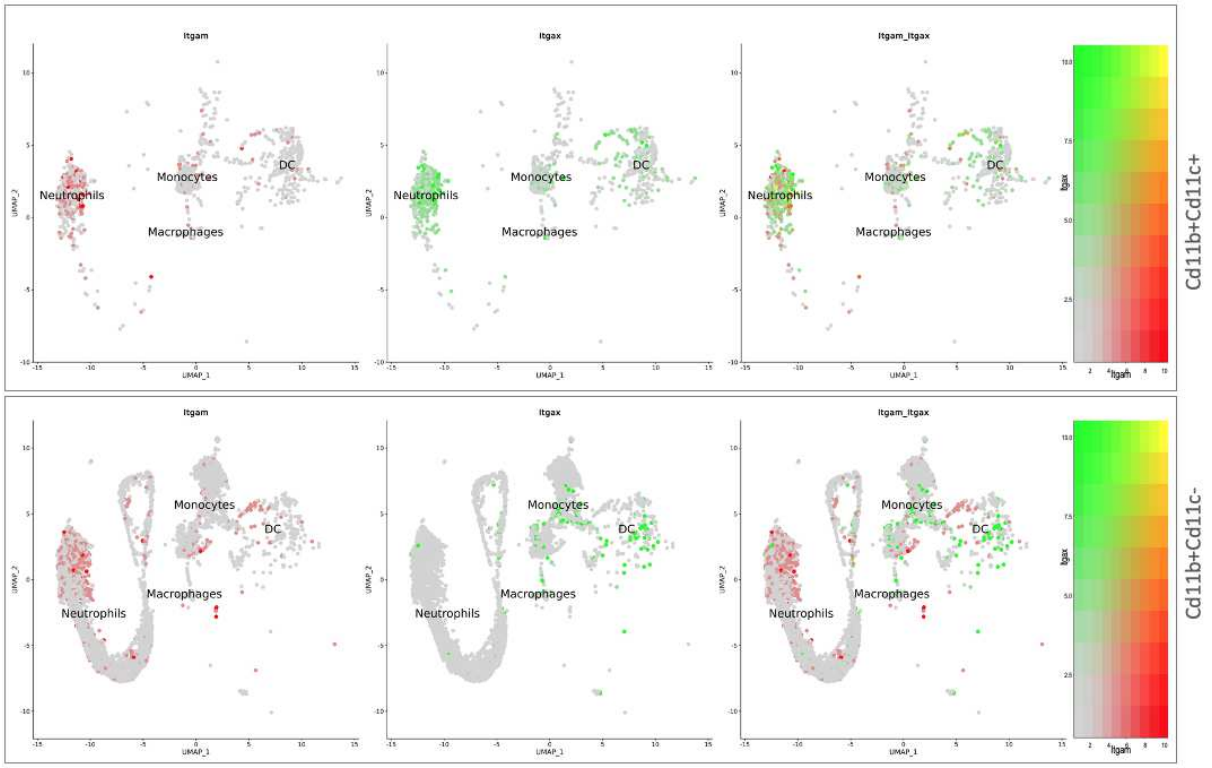

Figure 36 UMAP visualization of Itgam/CD11band Itgax/CD11c expression.
UMAP visualization of co-expression of Itgam/CD11band Itgax/CD11ctranscripts plotted by Seurat FeaturePlot using blend functionin CD11b+c+ (upper panel) and CD11b+c- (lower panel) cells. Cell-types localization, as predicted by SingleR analyses, are also reported.Cells are colored based on the expressionlevel of Itgam/CD11b and Itgax/CD11c. The gradient of colors, from full green to full red, as reported in the color grid on the right, indicates various levels of expression and co-expression of the two genes:red dots denote cells expressing only Itgam/CD11b; green dotscells

expressing only Itgax/CD11c; yellow dots cells where both genes have their maximum expression level

UMAP plots in **Figure 36** show that the CD11b+c+ double-positive cells are mainly found in neutrophils, dendritic cells and monocytes/macrophages, suggesting that CD11b+c+ cells are not cell-type specific.

4.8.3 p21 depletion de-regulates genes involved in antigen presentation in the CD11b+c+ double-positive cells

Finally, we searched for distinguishing gene-expression patterns of the WT and p21-/- CD11b+c+ cell sub-populations. Absolute and relative numbers of CD11b+c+ cells and control subpopulations (CD11b+c-, CD11b-c+, CD11b-c-) are reported in the Table below (**Table 5**).

		number of cells			% of cells	
Subgroup_Symb	Subgroup	ALL	WT	P21-/-	WT	P21-/-
AA	CD11b+Cd11c+	987	461	526	46.7	53.3
BB	CD11b+Cd11c-	6,008	2,550	3,458	42.4	57.6
CC	CD11b-Cd11c+	5,503	2,977	2,526	54.1	45.9
DD	CD11b-Cd11c-	19,690	8,652	11,038	43.9	56.1

Table 5. Absolute and relative numbers of cells forCD11b+c+, CD11b+c-, CD11b-c+ and CD11b-c- subpopulations. The four subpopulations were identified using two arbitrary thresholds, as shown in figure 35. Data are shown for "all cells" as well as separately for WTand p21-/- samples.

We first compared WT and p21-/- CD11b+c+ cells (considered together), with all other subpopulations (WT or p21-/- CD11b+c-, CD11b-c+ and CD11b-c- cells), using the "FindConservedMarker" function of the Seurat package. This analysis allows identification of genes that are conserved in the query populations (WT and p21-/- CD11b+c+ cells), as compared to all other samples. Results revealed 727 marker genes, that represent the distinguishing expression-pattern of the CD11b+c+ sub-population, irrespective of the differences between WT and p21-/- genetic context.

We then directly compared p21-/- vs WT CD11b+c+ cells, using “FindMarkers”, a further function of Seurat, which allows identification of differences in gene markers between two specific populations, and found 151 gene markers.

To characterize the 727 marker-gene list that, *bona fide,* identifies the distinguishing expression-pattern of the CD11b+c+ sub-population regardless of differences between the WT and p21-/- genetic background, we performed a functional analysis using the integrated software suites MetaCore (https://portal.genego.com/) and IPA (https://apps.ingenuity.com/). Among the multiple function/role of p21 in terms of cell cycle, DNA replication, tissue differentiation, senescence, cell migration, tumor growth, and immunity, the top 20 pathways found enriched in MetaCore (listed in **Table 6)** are those linked to immune response, cytokine production, chemotaxis and various types of cell signalling (i.e. M-CSF-receptor signaling pathway, Il-5, IL3- and IL4 signaling, B cell antigen receptor pathway) suggesting and strengthening the involvement of immune system pathways in this mechanism.Then, to identify genes that were specifically modified by the p21 knockdown, we intersected the two 727 and 151 gene-lists (see **Fig.37**) and found that nearly half of the 151 genes (78/151, 51.7%) are shared with the 727 gene-list. Among these, 30 were upregulated (38.5%) and 48 (61.5%) were downregulated in the p21-/- CD11b+c+ subpopulation, as compared to the WT counterpart.

			AA_Conserv_727			
#	Maps	Total	p-value	FDR	In Data	Network Objects from Active Data
1	Immune response_IL-3 signaling via ERK and PI3K	102	6.816E-14	3.083E-11	24	alpha-4/beta-1 integrin, Syk, Talin, R-Ras, ITGB1, EGR1, PDE4, p27KIP1, CSF2RB, Mcl-1, Lyn, RPS6, PI3K cat class IA, c-Raf 1, 14-3-3 zeta/delta, Calmodulin, PI3K cat class IA (p110-delta), Paxillin, Slp76, LPCAT2, GRB2, AKT(PKB), c-Fos, PREL1
2	Signal transduction_Calcium-mediated signaling	72	2.912E-13	7.903E-11	20	COX-2 (PTGS2), p300, RhoA, MLCP (reg), I-kB, EGR1, ACTA2, ROCK, p38 MAPK, HDAC4, MMP-9, NF-AT2(NFATC1), MEF2 MEK3(MAP2K3), Calmodulin, HDAC5, NUR77, AKT(PKB), c-Fos, 14-3-3
3	Immune response_M-CSF-receptor signaling pathway	79	1.972E-12	3.824E-10	20	PU.1, STAT3, Syk, RhoA, Pyk2(FAK2), ETS2, Beta-catenin, Fyn, PI3K cat class IA, CRK, AP-1, c-Raf-1, DAP12, M-CSF receptor, Hck, Calmodulin, GRB2, AKT(PKB), CSF1, c-Fos
4	CHDI_Correlations from Replication data_Causal network (positive correlations)	79	1.972E-12	3.824E-10	20	CD44, RhoA, HSP70, Pyk2(FAK2), I-kB, PI3K reg class IB (p101), ROCK, HIP1, MHC class II, PI3K cat class IA, p38 MAPK, MEF2, CXCR4, MEK3(MAP2K3), CD45, Calmodulin, TLR2, Slp76, AKT(PKB), VIL2 (ezrin)
5	CHDI_Correlations from Replication data_Cytoskeleton and adhesion module	64	3.624E-12	6.148E-10	18	RASSF5, ITGB2, Talin, RhoA, MLCP (reg), alpha-L/beta-2 integrin, Cytohesin1, MyHC, PI3K reg class IB (p101), ROCK, Fyn, MHC class II, CXCR4, MRLC, Paxillin, Slp76, GRB2, AKT(PKB)
6	TNF-alpha and IL-1 beta-mediated regulation of contraction and secretion of inflammatory factors in normal and asthmatic airway smooth muscle	65	4.853E-12	7.317E-10	18	CCL5, COX-2 (PTGS2), PLA2, p300, GRO-2, RhoA, IL-1 beta, p38alpha (MAPK14), TNF-R1, GRO-3, p38 MAPK, HDAC4, MMP-9, NFKBIA, Calmodulin, Histone H3, AKT(PKB), c-Fos
7	Immune response_IL-3 signaling via JAK/STAT, p38, JNK and NF-kB	93	6.040E-12	8.196E-10	21	PU.1, STAT3, Oncostatin M, Bcl-6, I-kB, ITGB1, C/EBPbeta, CSF2RB, Mcl-1, Lyn, MHC class II, PI3K cat class IA, p38 MAPK, Pim-1, SOCS3, MEK3(MAP2K3), MKP-1, RARalpha, AKT(PKB), NOTCH1 precursor, c-Fos
8	Signal transduction_MIF signaling pathway	61	1.712E-11	1.937E-09	17	PU.1, Syk, COX-2 (PTGS2), CD44, NRF2, SFK, PI3K reg class IB (p101), Lyn, PI3K cat class IA, AP-1, c-Raf-1, G-protein alpha i family, CXCR4, CD74, AKT(PKB), IL8RB, SPPL2a
9	Chemotaxis_SDF-1/ CXCR4-induced chemotaxis of immune cells	79	1.899E-11	1.982E-09	19	RASSF5, ITGB2, alpha-4/beta-1 integrin, Talin, RhoA, Pyk2(FAK2), alpha-L/beta-2 integrin, ITGB1, SFK, PI3K reg class IB (p101), Fyn, PI3K cat class IA, CRK, G-protein alpha-i family, CXCR4, CD45, ROCK1, Paxillin, AKT(PKB)
10	Reproduction_Gonadotropin-releasing hormone (GnRH) signaling	73	4.136E-11	3.742E-09	18	JunB, p38alpha (MAPK14), Pyk2(FAK2), ATF-3, EGR1, MEF2D, AP-1, PER1, c-Raf-1, HDAC4, MEK3(MAP2K3), Calmodulin, MKP-1, HDAC5, GRB2, NUR77, c-Fos, G-protein alpha-q/11
11	Glucocorticoids-mediated inhibition of pro-constrictory and pro-inflammatory signaling in airway smooth muscle cells	49	6.092E-11	5.167E-09	15	IRF1, COX-2 (PTGS2), PLA2, GCR, p300, RhoA, IL-1 beta, MLCP (reg), p38 MAPK, NFKBIA, Beta-2 adrenergic receptor, GRK2, MRLC, MKP-1, c-Fos
12	Immune response_B cell antigen receptor (BCR) pathway	110	1.774E-10	1.342E-08	21	alpha-4/beta-1 integrin, Syk, K-RAS, c-Rel (NF-kB subunit), EGR1, Lyn, ORAI1, CD79 complex, p38 MAPK, c-Raf-1, NF-AT2(NFATC1), NFKBIA, PP2A catalytic, MEK3(MAP2K3), CD79B, Calmodulin, PI3K cat class IA (p110-delta), GRB2, CD79A, AKT(PKB), c-Fos
13	Immune response_Fc epsilon RI pathway: signaling through Fyn and PI3K	61	1.858E-10	1.342E-08	16	Syk, I-kB, SGK1, SNAP-23, Fyn, Lyn, AP-1, ZFP36(Tristetraprolin), NF-AT, Fc epsilon RI beta, PI3K cat class IA (p110-delta), FYB1, GRB2, FGR, AKT(PKB), PAG
14	Stellate cells activation and liver fibrosis	70	1.879E-10	1.342E-08	17	GRO-2, IL-1 beta, TNF-R1, Beta-catenin, I-kB, ACTA2, TNF-R2, SARA, PI3K cat class IA, c-Raf-1, SMAD4, IL1RAP, KLF6, TLR2, GRB2, AKT(PKB), c-Fos
15	Immune response_IL-5 signaling via JAK/STAT	56	5.017E-10	3.242E-08	15	STAT3, JunB, PRG2, IL-1 beta, Bcl-6, CSF2RB, Mcl-1, Pim-1, DUSP5, NFKBIA, IL-5, Slp76, Syntenin 1, MKP-1, c-Fos
16	Immune response_Antigen presentation by MHC class II	118	6.928E-10	4.246E-08	21	MHC class II alpha chain, Syk, MHC class II beta chain, R-Ras, RhoA, Dectin-1, Dynamin-2, FCGR3A, MHC class II, CD79 complex, PI3K cat class IA, p38 MAPK, AKT1, LRP1, CD74, LAMP2, CD79B, TLR2, CD79A, MAP1LC3B, SPPL2a
17	Pro-tumoral TNF-alpha signaling in melanoma	41	7.196E-10	4.246E-08	13	ITGA4, alpha-4/beta-1 integrin, TNF-R1, ITGB1, TNF-R2, RhoGDI beta, PI3K cat class IA, MMP-9, AKT1, NFKBIA, Filamin-A (CTF), AKT(PKB), IL8RB
18	Inflammatory mechanisms of pancreatic cancerogenesis	67	8.486E-10	4.674E-08	16	CCL5, STAT3, IRF1, COX-2 (PTGS2), IL-1 beta, C/EBP, TNF-R1, TNF-R2, Mcl-1, AP-1, MMP-9, G-protein alpha-i family, NFKBIA, CXCR4, IL8RB, c-Fos
19	Immune response_CCR5 signaling in macrophages and T lymphocytes	58	8.611E-10	4.674E-08	15	CCL5, STAT3, Pyk2(FAK2), PI3K reg class IB (p101), ORAI1, G-protein alpha-q, p38 MAPK, G-protein alpha-i family, MAPKAPK2, NF-AT2(NFATC1), MEK3(MAP2K3), Calmodulin, Paxillin, AKT(PKB), c-Fos
20	Immune response_Fc epsilon RI pathway: Lyn-mediated cytokine production	87	9.204E-10	4.692E-08	18	Syk, IL-1 beta, EGR1, Lyn, AP-1, p38 MAPK, c-Raf-1, NF-AT2(NFATC1), NFKBIA, NF-AT, Fc epsilon RI beta, IL-5, MEK3(MAP2K3), Calmodulin, Slp76, FYB1, GRB2, c-Fos

Tab.6 Enrichment analysis by MetaCore. List of Pathway Maps obtained from the enrichment analysis performed with default parameters using the Conserved Markers list of 727 genes, which, *bona fide,* identify the distinguishing expression-pattern of the CD11b+c+ sub-population, regardless of differences between the WT or p21-/- genetic background. Column legend: # - map ID; Maps - pathway name; Total - total number of genes in pathway; pvalue - statistical significance of the enrichment, FDR – corrected statistical significance of the enrichment; In Data - number of genes in dataset; Network Objects from Active Data – as described.

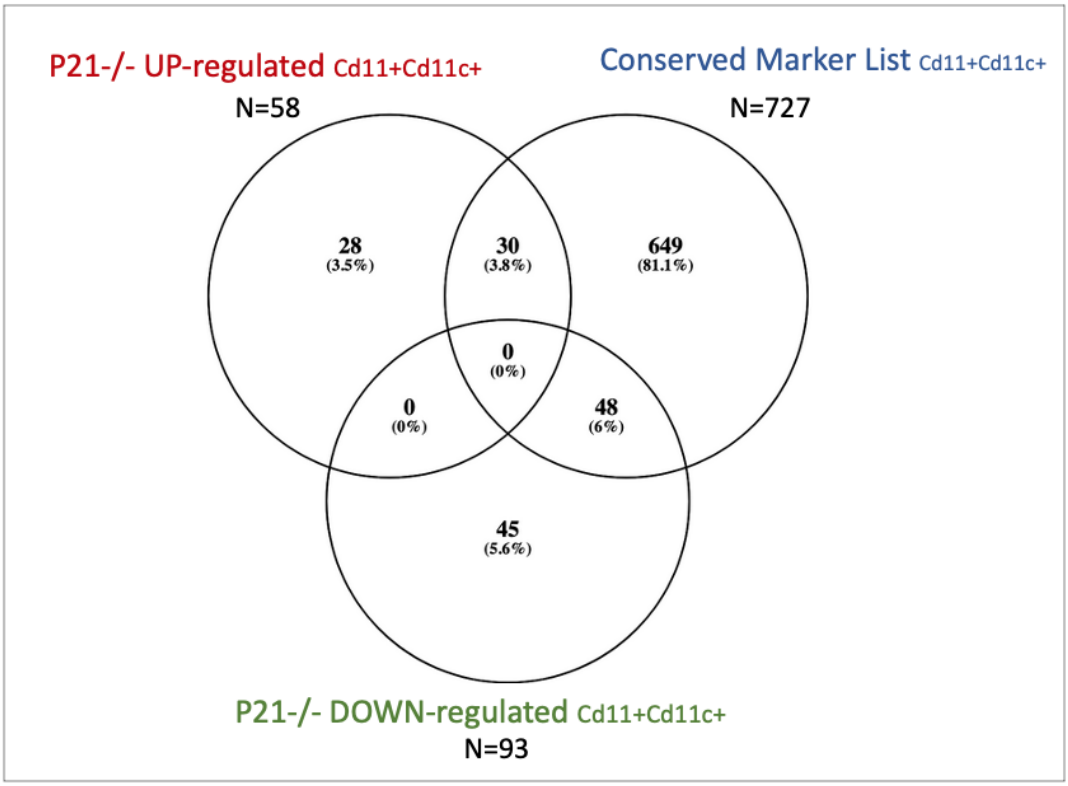

Fig.37 Overlap of P21 upregulated and downregulated specific markers lists with the catalog of 'Conserved markers' of Cd11b+Cd11c+ cell subsets.

To study similarities and differences between the two lists, we next performed the 'Core analysis' in IPA, the QIAGEN Ingenuity Pathway Analysis, using the 727 and 151 gene lists. **Figure 38** shows the 'Graphical Summary' outputs of these analyses. This representation is a special type of network produced by machine learning algorithms. It brings together 'entities' such ascanonical pathways, upstream regulators, diseases, most activated or inhibited regulators, biological functions and pathways from the analysis and allows visualization with reduced redundancy of predictions and minimal number of connections. This representation provides, therefore, a schematic readout of the major biological pathways scored by the analysis and their interconnections. Importantly, the summary analysis of the 727 gene-set (**Fig38 A**) reveals a central role for the Cd11b+Cd11c+ subpopulation in functions such as antigen presentation and cell-to-cell interaction between players of cellular-mediated defense, and highlights a potential crucial role of NFKB, IFNG and IL genes in these pathways. Strikingly, the graphic summary of the p21 specific markers (**Fig38 B**) highlights

the effect of p21 depletion in the CD11b+c+ sub-population toward and 'cell-activation status', in agreement with my biological data. Further studies are needed to deeply characterize each of these pathways and to specifically dissect the molecular mechanisms which govern them. Notably, our functional analysis represents a relevant starting point and a fruitful source of hypotheses for experimental validation.

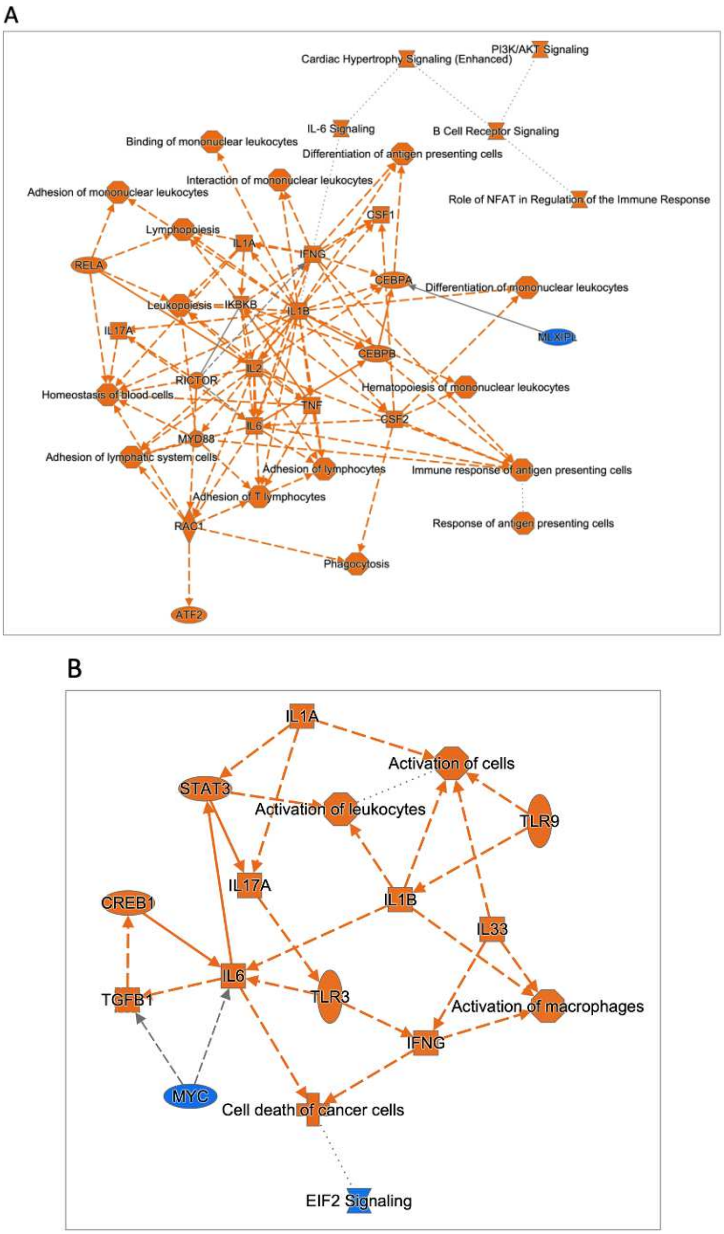

Fig.38.Graphical summaries of IPA functional analysis of Marker genes (using different functions of Seurat R package) which correspond to (A) the list of 727 genes identified as Conserved Markers of the Cd11b+Cd11c+ subpopulation, irrespective of the genetic background conditions, by the corresponding bioinformatic analysis and (B) the list of 151 genes specifically regulated in the p21-/- cells as compared to WT cells, identified by the pairwise FindMarker analysis.

5. Discussion

Several years ago, my host-labshowed that myeloid leukemias expressing the AML1-ETO fusion protein do not develop in mice deficient for the cell-cycle inhibitor p21 (p21-/- mice), while leukemias expressing the PML-RAR fusion protein develop at first, but do not transplant in secondary syngeneic recipients[127]. The effects of loss of p21 on leukemia initiation and maintenance were interpreted with a model whereby expression of p21 is indispensable for maintaining self-renewal of leukemia stem cells. Indeed, expression of leukemia-associated fusion proteins in HSCs induces DD, triggers p21-dependent cell-cycle arrest and DNA repair. In the absence of p21, DD accrual leads to functional exhaustion of LSCs[127].

I report here that, strikingly, primary p21-/- MMTV-ErbB2 breast cancers (and PML-RAR leukemias) re-acquire the ability to grow when transplanted into sublethally irradiated or immune-deficient recipients, revealing a role for the host immune-system in the defective phenotype of p21-/- tumors.Notably, the same ErbB2 breast tumorsorleukemias - as well as MMTV-Wnt and -PyMT breast tumors- obtained in WT mice (herein called “WT” tumors) are nottransplantable in non-irradiated p21-/- syngeneic recipients thus demonstrating that a component of the p21-/- microenvironment is responsible for the cell-extrinsic anti-tumor immune response elicited by p21-/- ErbB2 tumors. This novel role for the cell-cycle inhibitor p21 in the microenvironment adds up to the previously identified function of p21 in cancer SCs and ensures breast tumors (and leukemia) maintenance[127].

To identify the cellular component(s) of the p21-/- environment that mediates the observed potent anti-tumor effect *in vivo*, I performed transplantation experiments of cell suspensions from bulk p21-/- ErbB2 breast tumors, after depletion of specific subpopulations of the p21-/- “micro-environment”. First, I depleted MHCII+ antigen-presenting cells (APCs) and, among those, CD11b+ APCs. The CD11b surface marker is an integrin family member that is expressed on different immune-

competent cells, including dendritic cells and monocyte/macrophages[133].Strikingly, depletion of MHCII+ or CD11b+ APCs rescued the growth potential of p21-/- breast cancersin syngeneic FVB WT mice, demonstrating a key role for this immune cell population in the p21-dependent anti-tumor immune response (***Fig. 16***).Interestingly, also PML-RAR leukemias depleted of MHCII+ or CD11b+ APCs reacquired transplantability, demonstrating that the anti-tumor effect of MHCII+ CD11b+ APCs is not tumor-specific. Notably, injection of p21-/- spleen or, outstandingly, of p21-/-CD11b+ APCs together with WT breast tumors significantly delayed tumor growth.

To analyze the effects of the identified immune cell populations on the proliferation of naïve CD4+ or CD8+ T-cells, I set-up an *in vitro* culture of T cells, labelled them with a cell membrane dye that allows monitoring of cell proliferation and estimation of times of cell division (carboxyfluorescein succinimidyl ester [CFSE] dilution assay)[134], and exposed them to a WT or p21-/- CD11b+ subpopulation purified to near homogeneity from spleens of syngeneic WT or p21-/- mice, respectively. Purified CD11b+ APC cells were also loaded with ErbB2 tumor cell lysates or left unloaded; co-cultures of T cells and APCs were performed in transwell chambers to study cell to cell contact.Strikingly in this model, p21-/- CD11b+ cells - but not WT cells - induced massive proliferation of CD4+ T cells, which was independent of the presence of tumor cell lysates, but strongly dependent on expression of MHCII antigens (as revealed by MHCII blocking antibodies), and on the direct contact between APCs and T cells (***Fig. 20).***The maturational profile of the CD4+ T cellsprimed with WT CD11b+ cells was mainly naïve, whereas cells primed with p21ko CD11b+ APCs acquired mostly effector and memory phenotypes.The mechanism of T cell differentiation was also MHCII-dependent.I performed preliminary experiments using CD8+ T-lymphocytes (not presented in the Results section) showing that *in vitro* the proliferation effect of p21-/- CD11b+ cellswas reduced, as compared to CD4+ T cells, and MHCII independent, as expected. Overall, this *in vitro* system is a powerful tool to characterize the molecular mechanisms underlying the anti-tumor immune response mediated by p21-/- CD11b+ cells *in vivo*.

The potent, MHCII-dependent T-cell proliferation elicited by p21-/- CD11b+ cells *in vitro* is reminiscent of the ability of superantigens (SAgs), such as microbial enterotoxins, to trigger excessive and aberrant activation of T-cells *in vitro* and *in vivo*[49,50]. These family of proteins simultaneously directly bind MHC-II molecules and specific variable regions of the T-cell receptor beta-chain (V-beta), outside the normal antigen-binding interface[50]. Thus, SAgs are powerful but selective stimulators of T cells expressing a specific V beta chain. However, when I analyzed the TCR repertoire of *in vitro* CD11b+ activated CD4+ T cellsI did not observe enrichment for a specific V beta chain. Thus, my data rule out the involvement of a SAg in the hyper-proliferation of CD4 T-lymphocytes induced by p21-/- CD11b+ cells.

My data, instead, suggest thatthe *in vitro* CD11b+ cell-induced hyper-proliferation of CD4+ T-lymphocytes is closely reminiscent of so called homeostatic proliferation (HP) of T-cells, as observed experimentally in lymphopenic mice[39]. HP consists of a peripheral clonal expansion of T-cells in response to homeostatic stimuli like self- or commensal-antigens and cytokines, and includes fast proliferation, mediated by low avidity TCR-contact and capable of generating memory T-cells, and slow proliferation, driven by IL7 and not associated with changes of the T cell-phenotype[135,42]. An *in vitro* system of autologous lymphocytes was set up by Rosado-Sanchez[135] and colleagues to study HP mechanisms in human naïve T cells. In this assay, naïve T-lymphocytes (from peripheral blood) are stained with CFSE and exposed to homeostatic stimuli, recombinant IL7 and/or autologous APCs (purified from peripheral blood and sublethally irradiated to prevent their response to homeostatic stimuli and their potential interference on T-cell proliferation), allowing for simultaneous characterization of both types of HP, i.e. fast and slow HP. Proliferation of CFSE stained T cells was evaluated after 5, 10 and 15 days culture (with new supplementation of APCs and IL7 after each 5-day culture). Under these experimental conditions, when naïve T cells were stimulated only with APCs, fast HP appeared at days 10-15, generating memory/effector T cells; addition of IL7 to the culture system resulted in both, fast and slow HP at 10-15 days of culture.

Thus, I adapted my *in vitro* T cell-APC co-culture system to study HP. I co-cultured WT or p21-/- CD11b+ cells with purified naïve CD4+ T-lymphocytes using different Naïve : APC ratios in the presence or absence of IL7, for 5-10-15 days. My data demonstrate that the *in vitro*CD11b+ cell-induced hyper-proliferation of CD4+ T-lymphocytes can be classified as fast HP since: i) T cell proliferation requires engagement of the T cells' TCR with the MHC complex on APCs; ii) T cell proliferation is independent of exogenous antigens (interaction of TCR occurs with self-pepMHC complexes); iii) T cells differentiate towards an effector/memory phenotype; iv) T cell proliferation is IL7 independent; v) T cell division number is more than a cell division per day (compare to slow HP where CD4+ T cells undergo a cell division every 3-4 days).Importantly, the proliferation of naïve CD4+ T-lymphocytes induced by p21-/- CD11b+ cells resembles the HP proliferation of human T lymphocytes observed by Rosado-Sanchez and colleagues, yet it is more rapid (it occurs at day 5 instead of day 10-15) and significantly more potent (it occurs at a Naïve:APC ratio of 1:4 instead of 1:1), suggesting that p21-/- CD11b+ cells potentiate the fast homeostatic proliferation of CD4+ T-lymphocytes.

Previous papers associated p21 deficiency in T cells of mixed 129/Sv x C57BL/6 background to enhanced T cell activation *in vitro* (following stimulation with anti-CD3 antibodies)[147] and *in vivo* (following BrdU staining and transplantation, though only under certain conditions), to homeostatic proliferation and to mild autoimmune manifestations[147]. Background 129/SvXC57BL/6 mice, Santiago-Rauber and colleauges showed that *in vivo* homeostatic anti-self MHC/peptide ligand-induced proliferation of p21-deficient T cells (detected on day 7 post-transplantation in lymphopenic syngenic hosts) was enhanced as compared to WT T cells. I preliminary tested activation of T cells derived from spleens of our pure FVBp21-/- mice in my *in vitro* system by stimulation with anti-CD3 and anti-CD28 antibodies but did not observe an enhanced activation of p21-/- T cells (the experiment has been performed only once and is not reported in the Results Section of my thesis). This difference, however, might be due to the different genetic background of the mice.

Conceptually, the strong proliferative effect of p21-/- APCs on WT T cells could be (partly or completely) the consequence of an alloreactive reaction rather than homeostatic proliferation. Alloreactivity is a strong primary T cell response against MHC molecules in the species. FVB mice display an MHC (class I and II) "*q*" haplotype, while C57/Bl6 mice (the original p21-/- background) possess a "*b*" allele at each MHC locus. Importantly, our p21-/- FVB mice were extensively backcrossed (for about 12 generations) from a pure C57/BL6 background. However, our extensive backcross might have been "inefficient (or insufficient)" at the MHC locus for two main reasons: i) they are haplotypes, i.e. sets of genes that are inherited together from a single parent; ii) the p21 gene is close to the MHC locus on mouse chromosome 17. Though unlikely, the same might have happened during the C57/BL6 backcross from a mixed Sv129 x C57BL/6 background, where, asmentioned earlier, we also observed a potent antitumor effect mediated by p21-/- APCs (the original experiments using leukemias were performed in the C57/BL6 genetic background). The role of alloreactivity in CD11b+ induced T cell proliferation is currently under investigation. Importantly, however, my data show for the first time that p21 deficiency selectively in CD11b+ APC cells is able to induce extensive proliferation of naïve (WT) T cells.

Interestingly, both homeostatic proliferated T cells and alloreactive T cells have been linked to beneficial antitumor immune responses *in vivo*. In particular, several reports link lymphopenia-induced HP to an effective prevention and reversal of tumor-induced T cell anergy *in vivo*, and thereby to tumor rejection[148,149]. Alloreactive CD4+ T cells have been shown to act as strong mediators of anti-tumor immunity *per se* in NOD-SCID mice engrafted with acute lymphoblastic leukemia[210] or when genetically modified to express a chimeric receptor recognizing an ovarian cancer-associated antigen [211.]

To evaluate whether CD4+ T-lymphocytes activated by p21-/- CD11b+ cells possess antitumor activity *in vitro* and *in vivo*, I performed *in vitro* killing assays or adoptively transferred *in vitro* primed- CD4+ T cells in immunedeficient mice and challenged these mice with ErbB2 tumor cells.

Strikingly, CD4+ T cells primed *in vitro* with p21-/- CD11b+ - but not WT - APCs displayed anti-tumor activities *in vitro* and *in vivo*, upon their adoptive transfer into immunodeficient mice (***Fig. 27***). The same *in vitro* anti-tumor effect of primed CD4+ T-cells was also observed in my host-lab with primary leukemia cells, while their *in vivo* anti-leukemia activity is still under investigation. Similar experiments were performed using CD8+ T-cells primed *in vitro* with p21-/- CD11b+ cells (not presented in the Results section), which showed a significantly milder anti-tumor effect, as compared to CD4+ T-cells, in agreement with the *in vitro* reduced proliferation effect of p21-/- CD11b+ on CD8+ T cells.

Notably, I did not observe significant toxicity in mice injected with the *in vitro* generated CD4+ T-cells.The antitumor effect is, however, not complete as mammary tumors grow at late time points(around day 176; 32 days after the ctrls). Importantly, the life span of T cells transplanted in immunedeficient mice was reported to be about 15 days[146].To test the hypothesis that multiple boosts/injections of p21-/- CD11b+ primed CD4+ T cells could improve the delay of tumor formation, I injected i*n vitro* primed-CD4+ T cells on day 0 and 7, 14 and 21 post tumor cell transplantation (4 total boosts, one boost/week). I did not observe any further delay in tumor outgrowth.However, I obtained preliminary data revealing that the number of injected T cells is extremely reduced already at day4 post-transplantation (these experiments are not shown in the Results Section). Further experiments with *in vitro* primed CD4+ T cell populations are needed to evaluate survival and functionality of the injected T cells in immunedeficient recipients.

To investigate molecular mechanisms underlying the effects of p21 depletion on the function of CD11b+(MHCII+)APCs, I first identified the specific cell subpopulation responsible for the observed CD4+ - mediated anti-tumor response.Taking advantage of the published data on splenic APCs and of the requirement for MHCII expression[76,77], I identified monocytes/macrophages anddendritic cells as possible candidates. Strikingly, I report here that only the rare splenic population that co-expresses MHC-II, CD11b and CD11c molecules (~1% of total spleenand ~10%

of the CD11b+ splenic cells; Table 1B) was able to induce the strong *in vitro* CD4+ T cell proliferation that I previously observed with bulk CD11b+ splenic cells.

Next, I performed scRNAseq analyses of WT and p21-/- CD11b+ cells from spleen (using three biological replicas for each condition) and identified *in silico*8 major cell-types (relative frequency >~1%) that together represent more than ~98% of the CD11b+ population: neutrophils, dendritic cells, monocytes, T and B lymphocytes, basophils, NK cells, and macrophages.Importantly, I found a complete overall consistency with the subtypes and distributions identified by FACS analyses of mouse WT and p21-/- spleen cells (with the exception of eosinophils, that were only among the subtypes identified by FACS analyses), demonstrating a perfect cross-talk between *in silico* and wet data. Likely, when I analysed the the CD11b+c+ sub-population *in silico,*I found that its abundance (in both WT and p21-/- samples) matched the percentage identified by FACS analysis. I next searched for distinguishing gene-expression patterns of WT and p21-/- CD11b+c+ cell sub-populations. First, I found marker genes of the CD11b+c+ sub-population (as compared to CD11b+c-, CD11b-c+, CD11b-c- control subpopulations), irrespective of the differences between WT and p21-/- genetic context. Then, I identified gene marker differences between the two specific populations, namely WT and p21-/- CD11b+c+ cells. Importantly, a functional analysis of the identified genes focusing on biological functions and interconnecting pathways (using MetaCore) revealed a central role for the Cd11b+Cd11c+ subpopulation in antigen presentation and cell-to-cell interaction between players of cellular-mediated defense, and highlighted a potential central role for genes like NFKB, IFNG and IL3 in these pathways. Remarkably, the p21 specific markers in the CD11b+c+ sub-population revealed a role for p21 depletion in the ‘cell-activation status’ function, in agreement with the biological data presented in this thesis. My analysis sets the basis for further studies aimed at dissectingthe molecular mechanisms which govern the identified pathways.

Collectively, myresults in the mouse reveal that p21-/- CD11b+ APC cells can be used *in vitro* to generate T cells with potent anti-cancer effect *in vivo*and that thespecific

cellsubpopulationresponsible for the strong activationof the anti-tumor CD4+ T cells is the rare CD11b+CD11c+ APC subpopulation. We nowplan to transfer our solid results to human cells to set-up an innovative immunotherapy approach.Indeed, despite the tremendous advances of cancer immunotherapy in the past decade, which include the development of cellular-, cytokine-, immune checkpoint blockade- based therapies, and anti-cancer vaccines, generation of new, more efficient approaches is imperative, due both to their associated toxicity as well as lack of efficacy in a large fraction of cancer patients. My datain the mouse pave the way toan innovative and potentially efficient immunotherapy approach based on the exploitation of engineered human APCs lacking p21 (or expressing low level) to potentiate the immune response against tumor cells.

6. References

1. Bartek, J.; Lukas, J. DNA damage checkpoints: From initiation to recovery or adaptation. *Curr. Opin. Cell Biol.* 2007, *19*, 238–245.
2. Nakanishi, M.; Shimada, M.; Niida, H. Genetic instability in cancer cells by impaired cell cycle checkpoints. Cancer Sci. 2006, 97, 984–989.
3. Eastman, A. Cell cycle checkpoints and their impact on anticancer therapeutic strategies. J. Cell Biochem. 2004, 91, 223–231.
4. Karimian, A.; Ahmadi, Y.; Yousefi, B. Multiple functions of p21 in cell cycle, apoptosis and transcriptional regulation after DNA damage. DNA Repair (Amst.) 2016, 42, 63–71.
5. Malumbres, M.; Barbacid, M. To cycle or not to cycle: A critical decision in cancer. Nat. Rev. Cancer 2001, 1, 222–231.
6. Gartel, A.L. Is p21 an oncogene? Mol. Cancer Ther. 2006, 5, 1385–1386.
7. Bertoli, C.; Skotheim, J.M.; de Bruin, R.A. Control of cell cycle transcription during G1 and S phases. Nat. Rev. Mol. Cell Biol. 2013, 14, 518–528.
8. Georgakilas, A.G.; Martin, O.A.; Bonner, W.M. p21: A Two-Faced Genome Guardian. Trends Mol. Med. 2017, 23, 310–319.
9. Niculescu, A.B., 3rd; Chen, X.; Smeets, M.; Hengst, L.; Prives, C.; Reed, S.I. Effects of p21(Cip1/Waf1) at both the G1/S and the G2/M cell cycle transitions: pRb is a critical determinant in blocking DNA replication and in preventing endoreduplication. Mol. Cell Biol. 1998, 18, 629–643.
10. Bunz, F.; Dutriaux, A.; Lengauer, C.; Waldman, T.; Zhou, S.; Brown, J.P.; Sedivy, J.M.; Kinzler, K.W.; Vogelstein, B. Requirement for p53 and p21 to sustain G2 arrest after DNA damage. Science 1998, 282, 1497–1501.
11. LaBaer, J.; Garrett, M.D.; Stevenson, L.F.; Slingerland, J.M.; Sandhu, C.; Chou, H.S.; Fattaey, A.; Harlow, E. New functional activities for the p21 family of CDK inhibitors. Genes Dev. 1997, 11, 847–862.
12. Chang, B.D.; Watanabe, K.; Broude, E.V.; Fang, J.; Poole, J.C.; Kalinichenko, T.V.; Roninson, I.B. Effects of p21Waf1/Cip1/Sdi1 on cellular gene expression: Implications for carcinogenesis, senescence, and age-related diseases. Proc. Natl. Acad. Sci. USA 2000, 97, 4291–4296.

13. Parveen, A.; Akash, M.S.; Rehman, K.; Kyunn, W.W. Dual Role of p21 in the Progression of Cancer and Its Treatment. Crit. Rev. Eukaryot. Gene Expr. 2016, 26, 49–62.
14. Abbas, T.; Dutta, A. p21 in cancer: Intricate networks and multiple activities. Nat. Rev. Cancer 2009, 9, 400–414
15. Bhatia, K.; Fan, S.; Spangler, G.; Weintraub, M.; O'Connor, P.M.; Judde, J.G.; Magrath, I. A mutant p21 cyclin-dependent kinase inhibitor isolated from a Burkitt's lymphoma. Cancer Res. 1995, 55, 1431–1435.
16. Vidal, M.J.; Loganzo, F., Jr.; de Oliveira, A.R.; Hayward, N.K.; Albino, A.P. Mutations and defective expression of the WAF1 p21 tumour-suppressor gene in malignant melanomas. Melanoma Res. 1995, 5, 243–250.
17. Weiss, R.H. p21Waf1/Cip1 as a therapeutic target in breast and other cancers. Cancer Cell 2003, 4, 425–429.
18. Akhter, N.; Akhtar, M.S.; Ahmad, M.M.; Haque, S.; Siddiqui, S.; Hasan, S.I.; Shukla, N.K.; Husain, S.A. Association of mutation and hypermethylation of p21 gene with susceptibility to breast cancer: A study from north India. Mol. Biol. Rep. 2014, 41, 2999–3007.
19. Jung, Y.S.; Qian, Y.; Chen, X. Examination of the expanding pathways for the regulation of p21 expression and activity. Cell Signal. 2010, 22, 1003–1012.
20. Gartel, A.L.; Shchors, K. Mechanisms of c-myc-mediated transcriptional repression of growth arrest genes. Exp. Cell Res. 2003, 283, 17–21.
21. J Philipp-Staheli et al. Distinct roles for p53, p27Kip1, and p21Cip1 during tumor development.*Oncogene* volume **23**, pages905–913(2004)
22. W S el-Deiry et al. WAF1, a potential mediator of p53 tumor suppression. 1993 Nov 19;75(4):817-25
23. J W Harper et al. The p21 Cdk-interacting protein Cip1 is a potent inhibitor of G1 cyclin-dependent kinases. Cell 1993 Nov 19;75(4):805-16.
24. Romanov, V.S.; Rudolph, K.L. p21 shapes cancer evolution. Nat. Cell Biol. 2016, 18, 722–724.
25. Gawriluk, T.R.; Simkin, J.; Thompson, K.L.; Biswas, S.K.; Clare-Salzler, Z.; Kimani, J.M.; Kiama, S.G.; Smith, J.J.; Ezenwa, V.O.; Seifert, A.W. Comparative analysis of ear-hole closure identifies epimorphic regeneration as a discrete trait in mammals. Nat. Commun. 2016, 7, 11164.

26. Winters, Z.E.; Hunt, N.C.; Bradburn, M.J.; Royds, J.A.; Turley, H.; Harris, A.L.; Norbury, C.J. Subcellular localisation of cyclin B, Cdc2 and p21(WAF1/CIP1) in breast cancer. association with prognosis. Eur. J. Cancer 2001, 37, 2405–2412.

27. Ohata, M.; Nakamura, S.; Fujita, H.; Isemura, M. Prognostic implications of p21 (Waf1/Cip1) immunolocalization in multiple myeloma. Biomed. Res. 2005, 26, 91–98.

28. Malumbres, M. (2014). Cyclin-dependent kinases. Genome Biol. 15:122. doi: 10. 1186/gb4184

29. Hydbring, P., Malumbres, M., and Sicinski, P. (2016). Non-canonical functions of cell cycle cyclins and cyclin-dependent kinases. Nat. Rev. Mol. Cell Biol. 17, 280–292. doi: 10.1038/nrm.2016.27

30. Matsushime, H., Roussel, M. F., Ashmun, R. A., and Sherr, C. J. (1991). Colony-stimulating factor 1 regulates novel cyclins during the G1 phase of the cell cycle. Cell 65, 701–713. doi: 10.1016/0092-8674(91)90101-4

31. Cingoz, O., and Goff, S. P. (2018). Cyclin-dependent kinase activity is required for type I interferon production. Proc. Natl. Acad. Sci. U.S.A. 115, E2950–E2959. doi: 10.1073/pnas.1720431115

32. Aderem, A., and Underhill, D. M. (1999). Mechanisms of phagocytosis in macrophages. Ann. Rev. Immunol. 17, 593–623. doi: 10.1146/annurev.immunol.17. 1.593

33. Yoshida, K., Maekawa, T., Zhu, Y., Renard-Guillet, C., Chatton, B., Inoue, K., et al. (2015). The transcription factor ATF7 mediates lipopolysaccharide-induced epigenetic changes in macrophages involved in innate immunological memory. Nat. Immunol. 16, 1034–1043. doi: 10.1038/ni.3257

34. Kapellos, T. S., Taylor, L., Lee, H., Cowley, S. A., James, W. S., Iqbal, A. J., et al. (2016). A novel real time imaging platform to quantify macrophage phagocytosis. Biochem. Pharmacol. 116, 107–119. doi: 10.1016/j.bcp.2016.07.011

35. Kong, E. K., Chong, W. P., Wong, W. H., Lau, C. S., Chan, T. M., Ng, P. K., et al. (2007). p21 gene polymorphisms in systemic lupus erythematosus. Rheumatology 46, 220–226. doi: 10.1093/rheumatology/kel210

36. Scatizzi, J. C., Mavers, M., Hutcheson, J., Young, B., Shi, B., Pope, R. M., et al. (2009). The CDK domain of p21 is a suppressor of IL-1beta-mediated inflammation in activated macrophages. Eur. J. Immunol. 39, 820–825. doi: 10.1002/eji.200838683

37. Trakala, M., Arias, C. F., Garcia, M. I., Moreno-Ortiz, M. C., Tsilingiri, K., Fernandez, P. J., et al. (2009). Regulation of macrophage activation and septic shock susceptibility via p21(WAF1/CIP1). Eur. J. Immunol. 39, 810–819. doi: 10.1002/eji.200838676

38. Surh CD, Sprent J. Homeostatic T cell proliferation: how far can T cells be activated to self-ligands? J Exp Med (2000) 192(4):F9–14. doi:10.1084/jem. 192.4.F9

39. Min B, McHugh R, Sempowski GD, Mackall C, Foucras G, Paul WE. Neonates support lymphopenia-induced proliferation. Immunity (2003) 18(1):131–40. doi:10.1016/S1074-7613(02)00508-3

40. Kuchroo VK, Ohashi PS, Sartor RB, Vinuesa CG. Dysregulation of immune homeostasis in autoimmune diseases. Nat Med (2012) 18(1):42–7. doi:10.1038/ nm.2621

41. Waldburger JM, Masternak K, Muhlethaler-Mottet A, Villard J, Peretti M, Landmann S, et al. Lessons from the bare lymphocyte syndrome: molecular mechanisms regulating MHC class II expression. Immunol Rev (2000) 178:148–65. doi:10.1034/j.1600-065X.2000.17813.x

42. Min B, Yamane H, Hu-Li J, Paul WE. Spontaneous and homeostatic proliferation of CD4 T cells are regulated by different mechanisms. J Immunol (2005) 174(10):6039–44. doi:10.4049/jimmunol.174.10.6039

43. Do JS, Min B. Differential requirements of MHC and of DCs for endogenous proliferation of different T-cell subsets in vivo. Proc Natl Acad Sci U S A (2009) 106(48):20394–8. doi:10.1073/pnas.0909954106

44. Tan JT, Ernst B, Kieper WC, LeRoy E, Sprent J, Surh CD. Interleukin (IL)-15 and IL-7 jointly regulate homeostatic proliferation of memory phenotype CD8+ cells but are not required for memory phenotype CD4+ cells. J Exp Med (2002) 195(12):1523–32. doi:10.1084/jem.20020066

45. Do JS, Visperas A, Oh K, Stohlman SA, Min B. Memory CD4 T cells induce selective expression of IL-27 in CD8+ dendritic cells and regulate homeostatic naive T cell proliferation. J Immunol (2012) 188(1):230–7. doi:10.4049/ jimmunol.1101908

46. Kieper WC, Troy A, Burghardt JT, Ramsey C, Lee JY, Jiang HQ, et al. Recent immune status determines the source of antigens that drive homeostatic T cell

expansion. J Immunol (2005) 174(6):3158–63. doi:10.4049/jimmunol. 174.6.3158

47. Parish WE, Breathnach SM. Clinical Immunology and Allergy.In: Champion Rh, Burton Jl, Burns DA, Breathnach SM, editors. 1998.

48. Janeway CA, Travers P, Walport M, Shlomchik MJ, editors. Antigen recognition by B cell and T-cell receptors. In Immunobiology, The immune system in heakth and disease; 5 th edition. London: Garland Publishing: 2001. p. 93-122.

49. Choi Y, Lafferty JA, Clements JR, Todd JK, Gelfand EW, Kappler J, Marrack P, Kotzin BL. Selective expansion of T cells expressing V beta 2 in toxic shock syndrome. J Exp Med 1990;172:981-4.

50. Llewelyn M, Cohen J. Superantigen: Microbial agents that corrupt immunity.The lancet infectious disease 2002;2:156-62.

51. Speiser DE, Ho PC, Verdeil G. 2016. Regulatory circuits of T cell function in cancer. Nat Rev Immunol 16: 599-611.

52. Clemente CG, Mihm MC Jr, Bufalino R, Zurrida S, Collini P, Cascinelli N. 1996. Prognostic value of tumor infiltrating lymphocytes in the vertical growth phase of primary cutaneous melanoma. Cancer 77: 1303–1310.

53. Oldford SA, Robb JD, Codner D, Gadag V, Watson PH, Drover S. 2006. Tumor cell expression of HLA-DM associates with a Th1 profile and predicts improved survival in breast carcinoma patients. Int Immunol 18: 1591–1602.

54. Hanson HL, Donermeyer DL, Ikeda H, White JM, Shankaran V, Old LJ, Shiku H, Schreiber RD, Allen PM. 2000. Eradication of established tumors by $CD8^+$ T cell adoptive immunothera- py. Immunity 13: 265–276.

55. Matsushita H, Vesely MD, Koboldt DC, Rickert CG, Uppaluri R, Magrini VJ, Arthur CD, White JM, Chen YS, Shea LK, et al. 2012. Cancer exome analysis reveals a T-cell-dependent mechanism of cancer immunoediting. Nature 482: 400–404.

56. Kalams SA, Walker BD. 1998. The critical need for CD4 help in maintaining effective cytotoxic T lymphocyte responses. J Exp Med 188: 2199–2204.

57. Pardoll DM, Topalian SL. 1998. The role of $CD4^+$ T cell responses in antitumor immunity. Curr Opin Immunol 10: 588–594

58. Shankaran V, Ikeda H, Bruce AT, White JM, Swanson PE, Old LJ, Schreiber RD. 2001. IFNγ and lymphocytes prevent primary tumour development and shape tumour immunogenicity. Nature 410: 1107–1111.
59. Fridman WH, Pages F, Sautes-Fridman C, Galon J. 2012. The immune contexture in human tumours: impact on clinical outcome. Nat Rev Cancer 12: 298–306.
60. Grivennikov SI, Greten FR, Karin M. 2010. Immunity, inflammation, and cancer. Cell 140: 883–899.
61. Pardoll DM. 2012. The blockade of immune checkpoints in cancer immunotherapy. Nat Rev Cancer 12: 252–264.
62. Ward-Hartstonge KA, Kemp RA. 2017. Regulatory T-cell heterogeneity and the cancer immune response. Clin Transl Immu- nology 6: e154.
63. Takashi Saito, Facundo D.Batista editors. Immunological Synapse. Current topics in microbiology and immunology. Springers.
64. David Masopust , Kaja Murali-Krishna, Rafi Ahmed. Quantitating the magnitude of the lymphocytic choriomeningitis virus-specific CD8 T-cell response: it is even bigger than we thought. J Virol 2007 Feb;81(4):2002-11
65. Riley RS, June CH, Langer R, et al. Delivery technologies for cancer immunotherapy. Nat. Rev. Drug Discov. 2019;18:175–196.
66. axena M, Bhardwaj N. Re-Emergence of Dendritic Cell Vaccines for Cancer Treatment. Trends in cancer. 2018;4:119–137.
67. van Willigen WW, Bloemendal M, Gerritsen WR, et al. Dendritic Cell Cancer Therapy: Vaccinating the Right Patient at the Right Time. Front. Immunol. 2018;9:2265.
68. Forget M-A, Haymaker C, Hess KR, et al. Prospective Analysis of Adoptive TIL Therapy in Patients with Metastatic Melanoma: Response, Impact of Anti-CTLA4, and Biomarkers to Predict Clinical Outcome. Clin. Cancer Res. 2018;24:4416–4428.
69. Titov A, Petukhov A, Staliarova A, et al. The biological basis and clinical symptoms of CAR-T therapy-associated toxicites. Cell Death Dis. 2018;9:897.
70. Mandy Van Gulijk, Floris Dammeijer, Joachim G.J.V. Aerts nad Heleen Vroman. Combination strategies to optimize efficiacy of dendritic cell-based immunotherapy. Front.immunol. 9:2759.
71. Samar Al Bitar and Hala Gali-Muhtasib. The role of the cyclin dependent kinase inhibitor p21Cip1/waf1 in targeting cancer:molecular mechanism and novel

therapeutics. Cancers (Basel). 2019 Sep 30;11(10):1475. doi: 10.3390/cancers11101475.

72. Phatthamon Laphanuwat and Siwanon Jirawatnotai. (2019). Immunomodulatory roles of cell cycle regulators. Front Cell Dev Biol. 2019 Feb 26;7:23. doi: 10.3389/fcell.2019.00023

73. Booki Min Spontaneous T Cell Proliferation: A Physiologic Process to Create and Maintain Homeostatic Balance and Diversity of the Immune System. Front Immunol. 2018 Mar 19;9:547. doi: 10.3389/fimmu.2018.00547. eCollection 2018.

74. Gonzalez H, Hagerling C, Werb Z. Roles of the immune system in cancer: from tumor initiation to metastatic progression. Genes Dev. 2018 Oct 1;32(19-20):1267-1284. doi: 10.1101/gad.314617.118.

75. Schnell A, Bod L, Madi A, Kuchroo VK. The yin and yang of co-inhibitory receptors: toward anti-tumor immunity without autoimmunity . Cell Res. 2020 Apr;30(4):285-299. doi: 10.1038/s41422-020-0277-x.

76. Hey YY, Quah B, O'Neill HC. Antigen presenting capacity of murine splenic myeloid cells. BMC Immunol. 2017 Jan 11;18(1):4. doi: 10.1186/s12865-016-0186-4.

77. Ying Y Hey 1, Helen C O'Neill. Murine spleen contains a diversity of myeloid and dendritic cells distinct in antigen presenting function. J Cell Mol Med. 2012 Nov;16(11):2611-9. doi: 10.1111/j.1582-4934.2012.01608.x.

78. Cesta MF. Normal structure, function, and histology of the spleen. Toxicol Pathol. 2006;34(5):455–65. 1 90 76

79. Mebius RE, Kraal G. Structure and function of the spleen. Nat Rev Immunol. 2005; 5: 606–16. 3 77 91

80. Nolte MA, Hoen ENM T, Van Stijn A, Kraal G, Mebius RE. Isolation of the intact white pulp. Quantitative and qualitative analysis of the cellular composition of the splenic compartments. Eur J Immunol. 2000;30(2): 626–34. 3 90 76

81. Akashi K, Traver D, Miyamoto T, Weissman IL. A clonogenic common myeloid progenitor that gives rise to all myeloid lineages. Nature. 2000; 404(6774):193–7. 4 90 76

82. Yona S, Kim KW, Wolf Y, Mildner A, Varol D, Breker M, Strauss-Ayali D, Viukov S, Guilliams M, Misharin A, et al. Fate mapping reveals origins and dynamics of monocytes and tissue macrophages under homeostasis. Immunity. 2013; 38:79–91. 5 90 76

83. Geissmann F, Auffray C, Palframan R, Wirrig C, Ciocca A, Campisi L, Narni-Mancinelli E, Lauvau G. Blood monocytes: distinct subsets, how they relate to dendritic cells, and their possible roles in the regulation of T-cell responses. Immunol Cell Biol. 2008;86(5):398–408. 6 90 76

84. Hey YY, Tan JKH, O'Neill HC. Redefining myeloid cell subsets in murine spleen. Front Immunol. 2016. https://doi.org/10.3389/fimmu.2015.00652 10 76 90

85. Geissmann F, Gordon S, Hume DA, Mowat AM, Randolph GJ. Unravelling mononuclear phagocyte heterogeneity. Nat Rev Immunol. 2010;10(6):453–60 11 90 76

86. Serbina NV, Salazar-Mather TP, Biron CA, Kuziel WA, Pamer EG. TNF/iNOS-producing dendritic cells mediate innate immune defense against bacterial infection. Immunity. 2003;19(1):59–70. 12 76 90

87. Geissmann F, Jung S, Littman DR. Blood monocytes consist of two principal subsets with distinct migratory properties. Immunity. 2003;19(1):71–82. 13 76 90

88. Swirski FK, Nahrendorf M, Etzrodt M, Wildgruber M, Cortez-Retamozo V, Panizzi P, Figueiredo JL, Kohler RH, Chudnovskiy A, Waterman P, et al. Identification of splenic reservoir monocytes and their deployment to inflammatory sites. Science. 2009;325(5940):612–6. 14 76 90

89. Fitzgerald-Bocarsly P, Dai J, Singh S. Plas- macytoid dendritic cells and type I IFN: 50 years of convergent history. Cytokine Growth Factor Rev. 2008; 19: 3–19 15 91 77

90. Ronnblom L, Ramstedt U, Alm GV. Prop- erties of human natural interferon-producing cells stimulated by tumor cell lines. Eur J Immunol. 1983; 13: 471–6. 16 91 77

91. Kang YS, Yamazaki S, Iyoda T, Pack M, Bruening SA, Kim JY, Takahara K, Inaba K, Steinman RM, Park CG. SIGN-R1, a novel C-type lectin expressed by marginal zone macrophages in spleen, mediates uptake of the polysaccharide dextran. Int Immunol. 2003;15(2):177–86. 17 90 76

92. Noel G, Guo X, Wang Q, Schwemberger S, Byrum D, Ogle C. Postburn monocytes are the major producers of TNF-alpha in the heterogeneous splenic macrophage population. Shock. 2007;27(3):312–9. 18 90 76

93. Kurotaki D, Uede T, Tamura T. Functions and development of red pulp macrophages. Microbiol Immunol. 2015;59(2):55–62. 2 90 76

94. Italiani P, Boraschi D. From monocytes to M1/M2 macrophages: phenotypical vs. functional differentiation. Front Immunol. 2014;5:514.19 90 76

95. Heath WR, Belz GT, Behrens GMN, et al. Cross-presentation, dendritic cell subsets,and the generation of immunity to cellular antigens. Immunol Rev. 2004; 199: 9–26. 4 91 77

96. Shortman K, Naik SH. Steady-state and inflammatory dendritic-cell development. Nat Rev. 2007; 7: 19–30. 6 91 77

97. Naik SH. Demystifying the development of 17. dendritic cell subtypes, a little. Immunol Cell Biol. 2008; 86: 439–52. 5 91 77

98. Vremec D, Pooley J, Hochrein H, et al. CD4 and CD8 expression by dendritic cell sub- types in mouse thymus and spleen. J Immunol. 2000; 164: 2978–86. 9 77 91

99. Hochrein H, Shortman K, Vremec D, et al. Differential production of IL-12, IFN-a, and 21. IFN-b by mouse dendritic cell subsets. J Immunol. 2001; 166: 5448–55 10 91 77

100. De Smedt T, Pajak B, Muraille E, et al. Regulation of dendritic cell numbers and maturation by lipopolysaccharide in vivo.J Exp Med. 1996; 184: 1413–24. 11 91 77

101. Steinman RM, Pack M, Inaba K. Dendritic cells in the T-cell areas of lymphoid organs. Immunol Rev. 1997; 156: 25–37. 12 91 77

102. Lauterbach H, Bathke B, Gilles S, et al. Mouse CD8alpha+ DCs and human BDCA3+ DCs are major producers of IFN-lambda in response to poly IC. J Exp Med. 2010; 207: 2703–17.

103. Pelayo R, Hirose J, Huang J, et al. Deriva- tion of 2 categories of plasmacytoid dendritic cells in murine bone marrow. Blood. 2005; 105: 4407–15 21 91 77

104. Onai N, Obata-Onai A, Schmid MA, et al. Identification of clonogenic common Flt3 +M-CSFR+ plasmacytoid and conventional dendritic cell progenitors in mouse bone marrow. Nat Immunol. 2007; 8: 1207–16 22 77 91

105. O'Keeffe M, Hochrein H, Vremec D, et al. Mouse plasmacytoid cells: long-lived cells, heterogeneous in surface phenotype and function, that differentiate into CD8- dendritic cells only after microbial stimulus. J Exp Med. 2002; 196: 1307–19. 23 77 91

106. Diebold SS, Montoya M, Unger H, et al. Viral infection switches non-plasmacytoid dendritic cells into high interferon produc- ers. Nature. 2003; 424: 324–8. 24 77 91

107. Petvises S, Talaulikar D, O/'Neill HC. Delineation of a novel dendritic-like subset in human spleen. Cell Mol Immunol. 2015;13:443–50. 29 90 76

108. Tan JKH, Quah BJC, Griffiths KL, Periasamy P, Hey YY, O'Neill HC. Identification of a novel antigen cross-presenting cell type in spleen. J Cell Mol Med. 2011;15(5):1189–99. 30 90 76

109. Borros Arneth . Tumor Microenvironment . Medicina 2020, 56, 15; doi:10.3390/medicina56010015

110. Spill, F.; Reynolds, D.S.; Kamm, R.D.; Zaman, M.H. Impact of the physical microenvironment on tumor progression and metastasis. Curr. Opin. Biotechnol. 2016, 40, 41–48

111. Del Prete, A.; Schioppa, T.; Tiberio, L.; Stabile, H.; Sozzani, S. Leukocyte trafficking in tumor microenvironment. Curr. Opin. Pharmacol. 2017, 35, 40–47.

112. Balkwill, F.R.; Capasso, M.; Hagemann, T. The tumor microenvironment at a glance. J. Cell Sci. 2012, 125, 5591–5596.

113. Hanahan, D.; Coussens, L. Accessories to the crime: Functions of cells recruited to the tumor microenvironment. Cancer Cell. 2012, 21, 309–322.

114. Hanahan, D.; Weinberg, R.A. Hallmarks of cancer: The next generation. Cell 2011, 144, 646–674.

115. Mantovani, A.; Allavena, P.; Sica, A.; Balkwill, F. Cancer-related inflammation. Nature 2008, 454, 436–444.

116. Korneev, K.V.; Atretkhany, K.N.; Drutskaya, M.S.; Grivennikov, S.I.; Kuprash, D.V.; Nedospasov, S.A. TLR-signaling and proinflammatory cytokines as drivers of tumorigenesis. Cytokine 2017, 89, 127–135.

117. Feig, C.; Jones, J.O.; Kraman, M.; Wells, R.J.; Deonarine, A.; Chan, D.S.; Connell, C.M. Targeting CXCL12 from FAP-expressing carcinoma-associated fibroblasts synergizes with anti-PD-L1 immunotherapy in pancreatic cancer. Proc. Natl. Acad. Sci. USA 2013, 110, 20212–20217.

118. Anderson, B.O.; Cazap, E.; El Saghir, N.S.; Yip, C.H.; Khaled, H.M.; Otero, I.V.; Adebamowo, C.A.; Badwe, R.A.; Harford, J.B. Optimisation of breast cancer management in low-resource and middle-resource countries: Executive summary of the Breast Health Global Initiative consensus, 2010. Lancet Oncol. 2011, 12, 387–398.

119. Walker, C.; Mojares, E.; Del Río Hernández, A. Role of extracellular matrix in development and cancer progression. Int. J. Mol. Sci. 2018, 19, 3028.

120. Yan Cui * and Gang Guo . Immunomodulatory Function of the Tumor Suppressor p53 in Host Immune Response and the Tumor Microenvironment . Int. J. Mol. Sci. 2016, 17, 1942; doi:10.3390/ijms17111942

121. Eitan Giat a,⁎, Michael Ehrenfeld a, Yehuda Shoenfeld . Cancer and autoimmune diseases. Autoimmunity Reviews 16 (2017) 1049–1057

122. Qianxia Zhang 1, Dario A A Vignali 2. Co-stimulatory and Co-inhibitory Pathways in Autoimmunity. Immunity. 2016 May 17;44(5):1034-51. doi: 10.1016/j.immuni.2016.04.017.

123. ALEXIS L. FRANKS and JILL E. SLANSKY. Multiple Associations Between a Broad Spectrum of Autoimmune Diseases, Chronic Inflammatory Diseases and Cancer . Anticancer Res. 2012 April ; 32(4): 1119–1136.

124. Kari Hemminki 1, Xiangdong Liu, Jianguang Ji, Asta Försti, Jan Sundquist, Kristina Sundquist. Effect of autoimmune diseases on risk and survival in female cancers. Gynecol Oncol. 2012 Oct;127(1):180-5. doi: 10.1016/j.ygyno.2012.07.100

125. Criscitiello C, Bagnardi V, Esposito A, Gelao L, Santillo B, Viale G, Rotmensz N, Goldhirsch A, Curigliano G. 2016. Impact of autoimmune diseases on outcome of patients with early breast cancer. Oncotarget 7(32):51184–51192.

126. Julio C. Valencia, Nkolika Egbukichi, and Rebecca A. Erwin-Cohen . Autoimmunity and Cancer, the Paradox Comorbidities Challenging Therapy in the Context of Preexisting Autoimmunity . JOURNAL OF INTERFERON & CYTOKINE RESEARCH Volume 39, Number 1, 2019. DOI: 10.1089/jir.2018.0060.

127. Viale A. et al. Cell-cycle restriction limits DNA damage and maintains self-renewal of leukemia stem cells. Nature 2009.Doi:10.1038/nature07618.
128. Elizabeth A. Fry et al. Oncogenic and tumor-suppressive mouse models for breast cancer engaging HER2/neu. Int J Cancer. 2017 February 01; 140(3): 495–503
129. SO-G Pohl et al. Wnt signaling in triple-negative breast cancer. Oncogenesis (2017) 6, e310;
130. Bronte V. et al. The spleen in local and systemic regulation of imunity. Immunity. 2013 November 14; 39(5): 806–818
131. Dingwwll L. et al. B-cell deficiency lowers blood pressure in mice. Hypertension. 2019;73:561-570.
132. Roche Paul.A et al. The ins and out of MHC class II-mediated antigen processing and presentation. Nat Rev Immunol. 2015 April ; 15(4): 203–216.
133. Solovjov Dmitry et al. Distinct roles for the α and β subunits in the functions of integrin αMβ2. THE JOURNAL OF BIOLOGICAL CHEMISTRY . Vol. 280, No. 2, Issue of January 14, pp. 1336–1345, 2005
134. Quah Benjamin J.C.et al.The use of carboxyfluorescein diacetate succinimidyl ester (CFSE) to monitor lymphocyte proliferation. Journal of Visualized Experiments . 2010
135. Isaac Rosado-sanchez et al. An in vitro system of autologous lymphocytes culture that allows the study of homeostatic proliferation mechanism in human naïve CD4 T-cells. Laboratory Investigation 2017. https://doi.org/10.1038/s41374-017-0006-3
136. Kreiter Sebastian et al. Mutant MHC class II epitopes drive therapeutic immune responses to cancer. Nature. 2015 April 30; 520(7549): 692–696. doi:10.1038/nature14426.
137. Golubovskaya Vita et al. Different subsets of T cells, memory, effector functions. and CAR-T immunotherapy. Cancers 2016, 8, 36; doi:10.3390/cancers8030036
138. Sckisel Gail D. et al. Differential phenotypes of memory CD4 nad CD8 T cells in the spleen and peripheral tissues following immunostimulatory therapy.

Journal for ImmunoTherapy of Cancer (2017) 5:33 DOI 10.1186/s40425-017-0235-4

139. Kaiko Gerard E. et al. Immunological decision-making: how does the immune system decide to mount a helper T-cell response?. Immunology, 123, 326–338. 2007

140. Goldsby RA et la. Immunoogy, 5th edn.New York W.H Freeman 2003.

141. Kidd P.et al. Th1/Th2 balance: the hypothesis, its lomitations and implications for health and disease. Altern Med Rev 2003; 8:223-46

142. Roitt IM et la. Roitt's essential immunology, 10th edn. London: Blackwell science 2001

143. Tracy S P Heng et al. The Immunological genome project: networks of gene expression in immune cells. Immunology, 123, 326–338

144. Aran Dvir et al. Reference-based analysis of lung single-cell sequencing reveals a transitional profibrotic macrophage. Nat Immunol. 2019 February ; 20(2): 163–172. doi:10.1038/s41590-018-0276-y.

145. Lin Guo et al. Resolving cell fate decision during somatic cell reprogramming by single-cell RNA-seq. Molecular Cell 73, 815–829 February 21, 2019 a 2019 Elsevier Inc.

146. Nayar S. et al; Extending the lifespan and efficiacies of immune cells used in adoptive transfer for cancer immunotherapies.Oncoimm. 2015.

147. Santiago-Raber M.L et al. Role of cyclin kinase inhibitor p21 in systemic autoimmunity.JImmunol2001;167:4067-4074;doi: 10.4049/jimmunol.167.7.4067

148. Kline J. et al. Homeostatic proliferation plus regulatory T-cell depletion promotes potent rejection of B16 meloanoma. Clin Cancer Res 2008;14(10) May 15, 2008

149. Brown Ian E. et al. Homeostatic proliferations as an isolated variable reverses CD8+ T cell anergy and promotes tumor rejection. J Immunol 2006; 177:4521-4529; ;doi: 10.4049/jimmunol.177.7.4521

150. Kim, K. *et al.* A regulatory SNP at position -899 in CDKN1A is associated with systemic lupus erythematosus and lupus nephritis. *Genes Immun.* **10,** 482-486(2009).

151. Smolen, J. S. et al. HLA-DR antigens in systemic lupus erythematosus: association with specificity of autoantibody responses to nuclear antigens. Ann. Rheum. Dis. 46, 457– 462(1987).

152. Balomenos, D. et al. The cell cycle inhibitor p21 controls T-cell proliferation and sex-linked lupus development. Nat. Med. 6, 171–176 (2000).
153. Martin,M.,Wei,H.&Lu,T.Targetingmicroenvironmentincancertherapeutics.Oncot arget 7, 52575-52583 (2016).
154. Arias, C. F. *et al.* p21CIP1/WAF1 Controls Proliferation of Activated/Memory T CellsandAffectsHomeostasisandMemoryTCellResponses.*J.Immunol.***178**,2296–2306 (2007).
155. Rachel R. Caspi. Immunotherapy of autoimmunity and cancer: the penalty for suc- cess. *Nat. Rev. Immunol.* **8**, 970–976(2008).
156. Giat, E., Ehrenfeld, M. & Shoenfeld, Y. Cancer and autoimmune diseases. *Autoim- mun. Rev.* **16**, 1049–1057(2017).
157. Franks,A.L.MultipleAssociationsBetweenaBroadSpectrumofAutoimmuneDis- eases, Chronic Inflammatory Diseases and Cancer. *Anticancer Res.* **32,** 1119-11136(2012).
158. Simon,T.A.,Thompson,A.,Gandhi,K.K.,Hochberg,M.C.&Suissa,S.Incidence of malignancy in adult patients with rheumatoid arthritis: a meta-analysis. *Arthritis Res. Ther.* **17**, 212(2015).
159. Amos, S. M. *et al.* Autoimmunity associated with immunotherapy of cancer.*Blood***118**, 499–509 (2011).
160. June, C. H., Warshauer, J. T. & Bluestone, J. A. Is autoimmunity the Achilles' heel of cancer immunotherapy? *Nat. Med.* **23**, 540–547(2017).
161. Attia, P. *et al.* Autoimmunity Correlates With Tumor Regression in Patients With Metastatic Melanoma Treated With Anti–Cytotoxic T-Lymphocyte Antigen-4. *J. Clin. On- col.* **23**, 6043–6053 (2005).
162. Beck, K. E. *et al.* Enterocolitis in Patients With Cancer After Antibody Blockade of Cytotoxic T-Lymphocyte–Associated Antigen 4. *J. Clin. Oncol.* **24**, 2283–2289(2006).
163. Whiteside, T. L. The tumor microenvironment and its role in promoting tumor growth. *Oncogene* **27**, 5904–5912(2008).
164. Binnewies, M. *et al.* Understanding the tumor immune microenvironment (TIME) for effective therapy. *Nat. Med.* **24**, 541–550(2018).
165. Wang,M.*etal.*Roleoftumormicroenvironmentintumorigenesis.*J.Cancer***8**,761– 773 (2017).

166. Yang, L. & Zhang, Y. Tumor-associated macrophages: from basic research to clini- cal application. *J. Hematol. Oncol.* **10**, 58(2017).

167. Gabrilovich, D. I., Ostrand-Rosenberg, S. & Bronte, V. Coordinated regulation of myeloid cells by tumours. *Nat. Rev. Immunol.* **12**, 253–268(2012).

168. vonBoehmer,H.&Daniel,C.TherapeuticopportunitiesformanipulatingTRegcells in autoimmunity and cancer. *Nat. Rev. Drug Discov.* **12**, 51–63(2013).

169. Zitvogel, L., Tesniere, A. & Kroemer, G. Cancer despite immunosurveillance: im- munoselection and immunosubversion. Nat. Rev. Immunol. 6, 715(2006).

170. Gajewski, T. F., Schreiber, H. & Fu, Y.-X. Innate and adaptive immune cells in the tumor microenvironment. Nat. Immunol. 14, 1014–1022 (2013).

171. Elpek, K. G. et al. The Tumor Microenvironment Shapes Lineage, Transcriptional, and Functional Diversity of Infiltrating Myeloid Cells. Cancer Immunol. Res. 2, 655–667 (2014).

172. Sinha, P., Clements, V. K. & Ostrand-Rosenberg, S. Reduction of Myeloid-Derived Suppressor Cells and Induction of M1 Macrophages Facilitate the Rejection of Established Metastatic Disease. J. Immunol. 174, 636–645(2005).

173. Liu, C. et al. Expansion of spleen myeloid suppressor cells represses NK cell cyto- toxicity in tumor-bearing host. Blood 109, 4336–4342(2007).

174. Biswas, S. K. & Mantovani, A. Macrophage plasticity and interaction with lympho- cyte subsets: cancer as a paradigm. Nat. Immunol. 11, 889–896(2010).

175. Sica, A. & Mantovani, A. Macrophage plasticity and polarization: in vivo veritas. J. Clin. Invest. 122, 787–795 (2012).

176. Mantovani, A., Sozzani, S., Locati, M., Allavena, P. & Sica, A. Macrophage polari- zation: tumor-associated macrophages as a paradigm for polarized M2 mononuclearphago- cytes. Trends Immunol. 23, 549-555(2002).

177. Laoui,D.etal.TumorHypoxiaDoesNotDriveDifferentiationofTumor-Associated Macrophages but Rather Fine-Tunes the M2-like Macrophage Population. Cancer Res. 74, 24–30 (2014).

178. Petrova, V., Annicchiarico-Petruzzelli, M., Melino, G. & Amelio, I. The hypoxic tumour microenvironment. Oncogenesis 7, 10(2018).

179. Henze, A.-T. & Mazzone, M. The impact of hypoxia on tumor-associated macro- phages. J. Clin. Invest. 126, 3672–3679 (2016).

180.Quail,D.F.&Joyce,J.A.Microenvironmentalregulationoftumorprogressionand metastasis. Nat. Med. 19, 1423–1437(2013).

181. Wyckoff, J. B. et al. Direct Visualization of Macrophage-Assisted Tumor Cell Intravasation in Mammary Tumors. Cancer Res. 67, 2649–2656(2007).

182. Andrew Butler et al. Integrating single-cell transcriptomic data across different conditions, technologies, and species. Nature Biotechnology volume 36, pages411–420(2018)

183. Harper JW. Inhibition of cyclin-dependent kinases by p21. Mol Biol Cell. 1995 Apr;6(4):387-400.

184.Alexis R Barr et al. DNA damage during S-phase mediates the proliferation-quiescence decision in the subsequent G1 via p21 expression. Nat Commun.2017 Mar 20;8:14728.

185.Vanesa Gottifredi et al. The S phase checkpoint: when the crowd meets at the fork. Semin Cell Dev Biol. 2005 Jun;16(3):355-68.

186. Sanbao Ruan et al. Overexpressed WAF1/Cip1 Renders Glioblastoma Cells Resistant to Chemotherapy Agents 1,3-Bis(2-chloroethyl)-1-nitrosourea and Cisplatin. Cancer Research, 1998

187. Insinga A, Cicalese A, Faretta M, Gallo B, Albano L, Ronzoni S, Furia L, Viale A, Pelicci PG.DNA damage in stem cells activates p21, inhibits p53, and induces symmetric self-renewing divisions. Proc Natl Acad Sci U S A. 2013 Mar 5;110(10)

188.Daniel Muñoz-Espín 1, Manuel Serrano 1 .Cellular senescence: from physiology to pathology. Nat Rev Mol Cell Biol. 2014 Jul;15(7):482-96.

189.D A Alcorta ET AL. Involvement of the cyclin-dependent kinase inhibitor p16 (INK4a) in replicative senescence of normal human fibroblasts. Proc Natl Acad Sci U S A. 1996 Nov 26;93(24):13742-7.

190.G H Stein ET AL. Differential roles for cyclin-dependent kinase inhibitors p21 and p16 in the mechanisms of senescence and differentiation in human fibroblasts. Mol Cell Biol. 1999 Mar;19(3):2109-17.

191.M Cheng et al. The p21(Cip1) and p27(Kip1) CDK 'inhibitors' are essential activators of cyclin D-dependent kinases in murine fibroblasts. EMBO J. 1999 Mar 15;18(6):1571-83.

192. Sabrina Florencia Mansilla et al. CDK-Independent and PCNA-Dependent Functions

of p21 in DNA Replication. 10.3390/genes11060593

193. Sabrina F Mansilla et al. Cyclin Kinase-independent role of p21CDKN1A in the promotion of nascent DNA elongation in unstressed cells. eLife. 2016; 5: e18020.

194.Amanda B. Parrish, Christopher D. Freel, and Sally Kornbluth. Cellular Mechanisms Controlling Caspase Activation and Function.Cold Spring Harb Perspect Biol. 2013 Jun; 5(6): a008672.

195.Laura A. Buttitta and Bruce A. Edgar. Mechanisms controlling cell cycle exit upon terminal differentiation. Curr Opin Cell Biol. 2007 Dec; 19(6): 697–704.

196.Pumin Zhang et al. p21CIP1 and p57KIP2 control muscle differentiation at the myogenin step. Genes Dev. 1999 Jan 15; 13(2): 213–224.

197.Nina-Naomi Kreis,* Frank Louwen, and Juping Yuan. Cancers (Basel). The Multifaceted p21 (Cip1/Waf1/CDKN1A) in Cell Differentiation, Migration and Cancer Therapy .2019 Sep; 11(9): 1220

198.Teruhisa Kawamura et al. Linking the p53 tumour suppressor pathway to somatic cell reprogramming. Nature volume 460, pages1140–1144(2009)

199. Cell cycle regulation by the intrinsically disordered proteins p21 and p27 . Mi-Kyung Yoon;Diana M. Mitrea Li Ou;Richard W. Kriwacki. Biochem Soc Trans (2012) 40 (5): 981–988.

200. Emma S. Child David J. Mann. The Intricacies of p21 Phosphorylation Protein/Protein Interactions, Subcellular Localization and Stability. [Cell Cycle 5:12, 1313-1319, 15 June 2006]; ©2006 Landes Bioscience

201.ALGartel , ALTyner. Transcriptional regulation of the p21((WAF1/CIP1)) gene. Exp Cell Res1999 Feb 1;246(2):280-9

202.Andrei L. Gartel, Myc represses the p21(WAF1/CIP1) promoter and interacts with Sp1/Sp3. Proc Natl Acad Sci U S A. 2001 Apr 10; 98(8): 4510–4515.

203.Manpreet Kalkat ET AL. MYC Deregulation in Primary Human Cancers. Genes (Basel). 2017 Jun; 8(6): 151.

204.J. -B. Cazier et al. Whole-genome sequencing of bladder cancers reveals somatic CDKN1A mutations and clinicopathological associations with mutation burden. Nature Communications volume 5, Article number: 3756 (2014)

205.Hiromu Suzuki,* Reo Maruyama, Eiichiro Yamamoto, and Masahiro Kai. Epigenetic alteration and microRNA dysregulation in cancer. Front Genet. 2013; 4: 258.

206. W Xia, ET AL . Phosphorylation/Cytoplasmic Localization of p21Cip1/WAF1 Is Associated with HER2/neuOverexpression and Provides a Novel Combination Predictor for Poor Prognosis in Breast Cancer Patients. Clin Cancer Res. 2004; 10: 3815–3824

207. Wei Zhang,2 S. High Levels of Constitutive WAF1/Cipi Protein Are Associated with Chemoresistance in Acute Myelogenous Leukemia. Clin Cancer Res. 1995; 1: 1051–1057

208. Yefei Huang ET AL. The opposite prognostic significance of nuclear and cytoplasmic p21 expression in resectable gastric cancer patients. J Gastroenterol (2014) 49:1441–1452

209.Shirly Frizinsky et al. The innate immune perspective of autoimmune and autoinflammatory conditions. Rheumatology (Oxford). 2019 Nov; 58(Suppl 6): vi1–vi8.

210. stefanovics et al. Human allo-reactive CD4+ T cells as strong mediators of anti-tumor immunity in NOD/scid mice engrafted with human acute lymphoblastic leukemia. Leukemia 2012 Feb;26(2):312-22.

211. Michael H. Kershaw. Et al. Dual-specific T cells combine proliferation and antitumor activity.Nature Biotechnology 20, 1221-1227 (2002)

212. Asada M., Yamada T., Ichijo H., Delia D., Miyazono K., Fukumuro K., Mizutani S. Apoptosis inhibitory activity of cytoplasmic p21(Cip1/WAF1) in monocytic differentiation. EMBO J. 1999;18:1223–1234. doi: 10.1093/emboj/18.5.1223

213. Tanaka H., Yamashita T., Asada M., Mizutani S., Yoshikawa H., Tohyama M. Cytoplasmic p21(Cip1/WAF1) regulates neurite remodeling by inhibiting Rho-kinase activity. J. Cell. Biol. 2002;158:321–329. doi: 10.1083/jcb.200202071

214. Manapov F., Muller P., Rychly J. Translocation of p21(Cip1/WAF1) from the nucleus to the cytoplasm correlates with pancreatic myofibroblast to fibroblast cell conversion. Gut. 2005;54:814–822. doi: 10.1136/gut.2003.036491

215. Wang J., Walsh K. Resistance to apoptosis conferred by Cdk inhibitors during myocyte differentiation. Science. 1996;273:359–361. doi: 10.1126/science.273.5273.359

216. Mercer S.E., Ewton D.Z., Deng X., Lim S., Mazur T.R., Friedman E. Mirk/Dyrk1B mediates survival during the differentiation of C2C12 myoblasts. J. Biol. Chem. 2005;280:25788–25801. doi: 10.1074/jbc.M413594200

217. Yamamizu K., Schlessinger D., Ko M.S. SOX9 accelerates ESC differentiation to three germ layer lineages by repressing SOX2 expression through P21 (WAF1/CIP1) Development. 2014;141:4254–4266. doi: 10.1242/dev.115436

218. Cheng T., Rodrigues N., Shen H., Yang Y., Dombkowski D., Sykes M., Scadden D.T. Hematopoietic stem cell quiescence maintained by p21cip1/waf1. Science. 2000;287:1804–1808. doi: 10.1126/science.287.5459.1804

219. Topley G.I., Okuyama R., Gonzales J.G., Conti C., Dotto G.P. p21(WAF1/Cip1) functions as a suppressor of malignant skin tumor formation and a determinant of keratinocyte stem-cell potential. Proc. Natl. Acad. Sci. USA. 1999;96:9089–9094. doi: 10.1073/pnas.96.16.9089

220. Kippin T.E., Martens D.J., van der Kooy D. p21 loss compromises the relative quiescence of forebrain stem cell proliferation leading to exhaustion of their proliferation capacity. Genes. Dev. 2005;19:756–767. doi: 10.1101/gad.1272305

221. Ju Z., Choudhury A.R., Rudolph K.L. A dual role of p21 in stem cell aging. Ann. N. Y. Acad. Sci. 2007;1100:333–344. doi: 10.1196/annals.1395.036

222. Vaishali R. Moulton,1,* Abel Suarez-Fueyo,1 Esra Meidan,1,2 Hao Li,1 Masayuki Mizui,3 and George C. Tsokos1,* Pathogenesis of Human Systemic Lupus Erythematosus: A Cellular Perspective. Trends Mol Med. 2017 July ; 23(7): 615–635. doi:10.1016/j.molmed.2017.05.006.

223. Abbas Shapouri-Moghaddam 1, Saeed Mohammadian 2, Hossein Vazini 3, Mahdi Taghadosi 4, Seyed-Alireza Esmaeili 2, Fatemeh Mardani 2, Bita Seifi 5, Asadollah Mohammadi 6, Jalil T Afshari 1, Amirhossein Sahebkar . Macrophage plasticity, polarization, and function in health and disease. J Cell Physiol. 2018 Sep;233(9):6425-6440. doi: 10.1002/jcp.26429

224. Gorjana Rackov,1 Enrique Hernández-Jiménez,2 Rahman Shokri,1 Lorena Carmona-Rodríguez,1 Santos Mañes,1 Melchor Álvarez-Mon,3 Eduardo López-Collazo,2 Carlos Martínez-A,1 and Dimitrios Balomenos1. p21 mediates macrophage reprogramming through regulation of p50-p50 NF-κB and IFN-β. J Clin Invest.2016: 126 (8):3089-3103